Modelling the Spread of Infectious Diseases

Modelling the Spread of Infectious Diseases

By David Champredon, M.Sc

A Thesis submitted to
the School of Graduate Studies in
Partial Fulfilment of the Requirements
for the Degree Doctor of Philosophy

McMaster University

DOCTOR OF PHILOSOPHY (2016) McMaster University
School of Computational Sciences and Engineering Hamilton, Ontario

Title : Modelling the spread of infectious diseases

Author : David Champredon, M.Sc

Supervisors : Prof. Jonathan Dushoff and Prof. David Earn

Number of pages: xiii, 131

Abstract

MATHEMATICAL models applied to epidemiology are useful tools that help understand how infectious diseases spread in populations, and hence support public-health decisions. Over the last 250 years, these modelling tools have have developed at an increasing rate, both on the theoretical and computational sides.

This thesis explores various modelling techniques to address debated or unanswered questions about the transmission dynamics of infectious diseases, in particular sexually transmitted ones.

The role of sero-discordant couples (when only one partner is infected) in the HIV epidemic in Sub-Saharan Africa is controversial. Their importance compared to other sexual transmission routes is critical when designing intervention policies. In chapter 2, I used a compartmental model with an original partnership process to show that infection of uncoupled individuals is usually the predominant route, while transmission within discordant couples is also important, but to a lesser extent.

Despite the availability of inexpensive antimicrobial treatment, syphilis remains prevalent worldwide, affecting millions of individuals. Development of a syphilis vaccine would be a potentially promising step towards control, but the value of dedicating resources to vaccine development should be evaluated in the context of the anticipated benefits. In chapter 3, I explored the potential impact of a hypothetical syphilis vaccine on morbidity from both syphilis and HIV using an agent-based model. My results suggest that an efficacious vaccine has the potential to sharply reduce syphilis under a wide range of scenarios, while expanded treatment interventions are likely to be substantially less effective.

General concepts in epidemic modelling, that could be applied to any disease, are still debated. In particular, a rigorous definition and analysis of the genera-

tion interval – the interval between the time that an individual is infected by an infector and the time this infector was infected – needed clarification. Indeed, the generation interval is a fundamental quantity when modelling and forecasting epidemics. Chapter 4 clarifies its theoretical framework, explains how its distribution changes as an epidemic progresses and discuss how empirical generation-interval data can be used to correctly inform mathematical models.

Acknowledgments

I would like to thank Jonathan Dushoff and David Earn for their open-mindedness when accepting to supervise my endeavour to learn something new. They both provided me with an ideal environment to pursue my PhD: time, moral support and intellectually stimulating discussions have never been in short supply. It was a real pleasure to learn from them. I am also grateful they funded numerous trips to conferences that allowed me to disseminate my research, interact with fellow academics and extend my new professional network. And special thanks to Jonathan, who spent countless hours guiding and feeding my academic apprenticeship.

I would also like to thank Marek Smieja who provided me with invaluable insights on the medical and clinical side of infectious diseases during my PhD studies. I also benefited immensely from numerous discussions with Ben Bolker, who was always available to help.

Lab members and friends were instrumental in shaping a friendly and stimulating environment. Hoping not to forget anyone: Andrei Akhmetzhanov, Akram Alyass, Sigal Balshine, Steve Bellan, Caroline Cameron, Michelle deJonge, Wim Delva, Sarah Drohan, Karsten Hempel, Spencer Hunt, Morgan Kain, Lindsay Keegan, David Leaman, Michael Li, David Meyre, Chai Molina, Irena Papst, Audrey Patocs, Dora Rosati, Jake Szamosi, Steve Walker and Lee Worden. I also thank Guillaume Blanchet and Mounira for proof reading this thesis. And of course, Chyun Shi who made the lab feel like home.

My PhD has been a great experience thanks to everyone.

Finalement, une reconnaissance infinie à ma famille qui m'a soutenu et cru en moi dans cette aventure pour le moins insolite.

Declaration of Academic Achievement

Each chapter of this thesis has been written as a separate manuscript. Chapters 2 and 4 have been published. Chapter 3 has been submitted and is currently under peer-review.

Programming, analysis and manuscript preparation for each chapter was primarily an individual effort, with contributions in programming, analysis and editing from Jonathan Dushoff on chapters 2, 3 and 4. In chapter 2, Steve Bellan contributed to the analysis and editing. In chapter 3, Caroline Cameron and Marek Smieja contributed to the analysis and editing.

Contents

List of Figures

List of Tables

Chapter 1

Introduction

Historical background

THE use of mathematical models to understand, and eventually control, the spread of infectious diseases is more than 250 years old and started with what could be anachronistically labelled a "public health assessment for smallpox vaccination".

Before being eradicated in 1977, smallpox decimated human populations for centuries. As early as the 10^{th} century, the Chinese were aware that smallpox inoculation could protect individuals against a more lethal form of this disease. This technique consisted in exposing intentionally the skin of susceptible (not naturally infected yet) individuals to secretions from naturally infected persons. The inoculated individual was still exposed to the virus, but symptoms would typically be less severe, resulting in a significantly reduced mortality rate (less than 2% versus about 30% when naturally infected). However, there could be cases where inoculation would still trigger severe symptoms that could potentially lead to death.

Smallpox inoculation being the only tool against the disease, it was introduced and promoted in Western Europe by Theodore Tronchin in 1756, a Swiss medical doctor. However, the "variolation", as it was also called, was very controversial and met with resistance. Daniel Bernoulli, a Swiss scientist, laid down in 1760 a mathematical model to assess the potential benefits of vaccinating a population against smallpox on life expectancy [10]. This is considered to be the first documented attempt to address a public health issue using the rigour of mathe-

matics.

Although it is not clear what the impact of this mathematical argument was in introducing variolation to European populations, its goal was the same as what epidemiological modellers do today: short of epidemiological experiments, careful reasoning is used in designing mathematical models representing the real world in order to understand and assess strategies to control the trajectory of an epidemic.

Interestingly, aside from Bernoulli's mathematical model, mathematical epidemiology did not develop further for roughly 150 years. It was only in 1910 that Ronald Ross conceptualized the transmission dynamics of malaria with difference equations ([85, 151-164]). This mathematical model highlighted that malaria could theoretically be eradicated without necessarily eliminating all mosquitos (the vectors transmitting malaria to humans). In other words, Ross' mathematical model enabled to keep the mosquito-control option (that, today, we know is effective) as one of the possible public-health policies, whereas it would probably have been ignored (and hence losing an effective tool) if policy makers believed in the necessity to wipe out entire mosquito populations.

In the 1920s, Kermack and McKendrick formalized the dynamics of infectious diseases transmission with a system of deterministic differential equations [70]. This type of model is still widely used today in mathematical epidemiology.

Epidemics of infectious diseases are based on contacts between individuals, which are essentially random events. Modern probabilistic approaches in demography and bacterial growth were developed from the 1940s, in particular by Kendall [67]. Bartlett and Bailey capitalized on these advances to propose epidemiological models involving stochastic processes (for example [5, 7]). The increasing power and availability of computers encouraged the development of more sophisticated epidemiological models. For example, Bartlett used "the Manchester electronic computer" (at the time, one of the most advanced computers) to simulate a spatial epidemic in a population of about 5,000 individuals dispersed in 36 geographical locations with a stochastic model [7]. So, thanks to this unprecedented computing power, mathematical tractability, although desirable, was not a blocking point any more in the design of models that aimed to better represent real epidemics (or what we think they are).

The technological revolution of personal computers starting in the early 1980s opened a new phase in mathematical epidemiology. Modellers could not only

design ever more sophisticated models, but could also start to embrace epidemiological data and calibrate the values of model parameters to it. For example, Rvachev and Longini [88] built a model to forecast the worldwide spread of pandemic flu across 52 cities, fitting on air transportation data). Another example could be Earn *et al.* who managed to explain the complex and puzzling dynamical transitions of measles epidemics that occurred in the UK and USA during the second half of the twentieth century [40]. Such models would then start to be closer to reality, or at least to the reality represented by the epidemiological data set considered, and potentially give more credibility to the inferences made from these models.

Calibrating models to data can become rapidly challenging numerically because of the high-dimensionality of the epidemiological problem. It certainly became rapidly out of reach for pre-2000 personal computers, so modellers tried to find a balance between analytical and numerical tractability. For example, this is well illustrated by the approach taken in Anderson and May in their landmark book [2] where data is present as long as mathematical tractability is not too compromised. In particular, there is no chapter dedicated to fitting mathematical models to data.

A new era began about 10 years ago with both the affordable access to high performance computers and the harvest of immense amount of data. Sophisticated epidemiological models can now embrace large quantities of data from different fields, such as social media, meteorology and mobile phones ([57, 103, 108]). In order to cope with models' complexity and the quantity of data used to fit them, these mathematical models heavily rely on state-of-the-art statistical methods. Indeed, the non-linearity and high dimensionality of the models involved have promoted the use of techniques that are often used for mathematical models applied to epidemiology, such as Markov chains Monte Carlo, approximate Bayesian computation [97] and iterative filtering [60].

This brief historical review of mathematical models applied to epidemiology shows the tremendous evolution these models have undergone over the past two and a half centuries (Table 1.1). Along with these developments, one important goal has been to better understand the spread of pathogens in human populations in order to support public health decision-makers. The development of a versatile toolbox of models have undoubtedly increased our understanding and ability to respond to epidemics. This toolbox was especially helpful to fight burdensome epidemics like the sexually transmitted ones, and particularly the current HIV

(human immunodeficiency virus) pandemic that started in the early 1980s.

Sexually-transmitted infections

Among all infectious diseases, sexually transmitted ones were studied relatively early with "modern" mathematical models. For example in 1973, Cooke and York [31] considered one of the first mathematical models of gonorrhea transmission.

Today, the burden of sexually transmitted infections (STIs) on humankind is enormous: the World Health Organization (WHO) estimated that nearly 500 million new cases of curable STIs (e.g., chlamydia, gonorrhea, syphilis and trichomoniasis) occurred during 2008 alone [105]. Although there is no more recent study, it is reasonable to think these numbers are still reasonably accurate. Some of these infections can lead to severe outcomes for the infected individuals and, in the case of pregnant women congenital syphilis. Congenital syphilis causes destructive infection in newborns, and can result in long term neurological damage, as well as an unusual appearance. Most curable STIs have a relatively cheap treatment, but depending on the setting, access to care or identifying infected patients may be challenging, hindering the epidemic control. Moreover, these infections are believed to facilitate HIV transmission by increasing both HIV susceptibility and infectiousness [12, 25, 62, 79, 86, 87, 107].

Tremendous efforts have managed to slow down the HIV pandemic using various interventions like "treatment as prevention" (giving antiretrovirals as soon as possible and not only when immuno-competency starts to decay), voluntary male circumcision (which only provides partial protection to the risk of male HIV acquisition), promoting condom use and behavioural campaigns to limit the number of sexual partners. But the HIV pandemic is far from over: approximately 35 million people are living with HIV (and many are not aware of being infected), 2 million new HIV infections and 1.5 million AIDS-related deaths occur every single year [99]. In addition to social and political hurdles there are other practical issues that hamper the control of the HIV pandemic. For example, antiretroviral therapy dramatically reduces the risk of HIV transmission, but only as long as the patient is on treatment, so adherence and availability of the drugs are critical. Availability may be challenging in resource-limited settings. Even in countries with strong financial and public health capabilities, the ratio of HIV-infected patients who are effectively virologically suppressed to the total prevalence (the

"HIV care cascade") is surprisingly low, typically between 30 and 60% [76].

The epidemiological landscape for STIs begs for mathematical modelling. As briefly described above, there is a relatively broad range of possible interventions to control their spread. But given the high prevalences, the resulting large scale of their implementation forces us to carefully assess their effectiveness. Unfortunately, modelling STIs is challenging: partnerships and demographic dynamics, as well as the natural history of the disease can play important epidemiological roles. For example, demographics are important because of long infectiousness period (*e.g.*, HIV, herpes simplex virus type 2) or trans-generational partnership formation. Concurrency – having simultaneous sexual partnerships – can also be critical in the transmission dynamics [78]. Many of these features are potentially important to include in mathematical models of sexually transmitted infections, making its tractability challenging.

About this thesis

This thesis explores practical epidemiological issues in order to incrementally fill some knowledge gaps that would help better understand, and thus better manage epidemics. As such, a variety of modelling tools are used to this end, from relatively simple models (chapter 4) to agent-based models that require high-performance computers (chapter 3).

The HIV pandemic is principally affecting the general population of Sub-Saharan Africa: this region accounts for about three quarters of the worldwide incidence, prevalence and AIDS-related deaths [99]. As outlined earlier in this introduction, various interventions are implemented and others contemplated to control the epidemic trajectory. Serodiscordant couples – when only one partner is infected with HIV – have received particular attention because of their suspected important role in spreading the disease, but previous studies found inconsistent results [28, 39]. Chapter 2 analyzes the importance of serodiscordant couples to the HIV transmission dynamics in the general population. It explored, using a compartmental model with parameters based on estimates from Sub-Saharan Africa, how mechanistic factors – like partnership dynamics and rates of extra-couple transmission – affect various routes of transmission. We found that infection of uncoupled individuals is usually the predominant route while transmission within discordant couples is also important, but rarely represented the majority of transmissions. We also gave some insights regarding correlations between

HIV prevalence, contact rate of uncoupled individuals, within-couple transmission and discordance proportion.

No vaccines exist for most sexually transmitted infections (Human papillomavirus, hepatitis A and B being the only exceptions). However, important advances have been made in basic sciences such that vaccine development for some STIs can be contemplated [14]. In particular, a vaccine against syphilis is especially appealing given the failure of current treatment options to control this epidemic, the existence of a relevant animal model [16] and WHO's goal of eliminating its congenital form [106]. In chapter 3, a mathematical model – that simulates individuals' behaviour and the natural history of STIs – was used to explore the potential impact of rolling out a hypothetical syphilis vaccine on morbidity from both syphilis and HIV. The epidemiological impact from vaccination was compared to the impact of expanded "screen and treat" programs using existing treatments. Our results suggested that an efficacious vaccine has the potential to sharply reduce syphilis under a wide range of scenarios, while expanded treatment interventions are likely to be substantially less effective.

The distribution of the "generation interval" – interval between the time that an individual is infected by an infector and the time this infector was infected – plays a central role in the disease transmission dynamics: its distribution underpins estimates of the reproductive number (number of cases generated on average by a single case over the course of its infectious period, in a fully susceptible population) and hence informs public health strategies. Empirical generation-interval distributions are often derived from contact-tracing data, but linking observed generation intervals to the underlying generation interval required for modeling purposes is surprisingly not straightforward, and misspecifications can lead to incorrect estimates of the reproductive number, with the potential to misguide interventions. Chapter 4 extended previous approaches [66, 81, 89, 95] by clarifying the theoretical framework for three conceptually different generation-interval distributions: the "intrinsic" one typically used in mathematical models and the "forward" and "backward" ones typically observed from contact tracing data, looking respectively forward or backward in time. We explained how the relationship between these distributions changes as an epidemic progresses and discussed how empirical generation-interval data can be used to correctly inform mathematical models.

Table 1.1. *History of mathematical models applied to epidemiology. The remarkable studies are subjectively chosen. The figure in the last row is a stylized representation of the order of magnitude for the maximum size of data handled by epidemiological models.*

Period	**1760-1910**	**1910-1950**	**1950-1980**	**1980-2000**	**2000 onwards**
Remarkable studies	Bernoulli [10]	Ross [85], Kermack and McKendrick [69]	Bartlett [7], Bailey [5]	Anderson and May [2], Diekmann *et al.* [36]	*time will tell*
Epidemic Model	n/a	- Compartmental deterministic - Renewal equation	- Compartmental deterministic and stochastic - Renewal equation	- Complex compartmental - Renewal equation - Agent-based model	- Complex compartmental - Renewal equation - Agent-based model - Statistical models
Mathematical Tools	Arithmetics	- Basic probablities and stats - ODE / Dynamical systems	- Modern probabilities - Dynamical systems - Basic stats	- Modern probabilities - Dynamical systems - Advanced stats	- Modern probabilities - Dynamical systems - Advanced stats - Computer sciences
Computational Tools	Brain	Brain	- Large room computers - Brain	- Personal computer - Brain	- High-performance computers - Personal computer

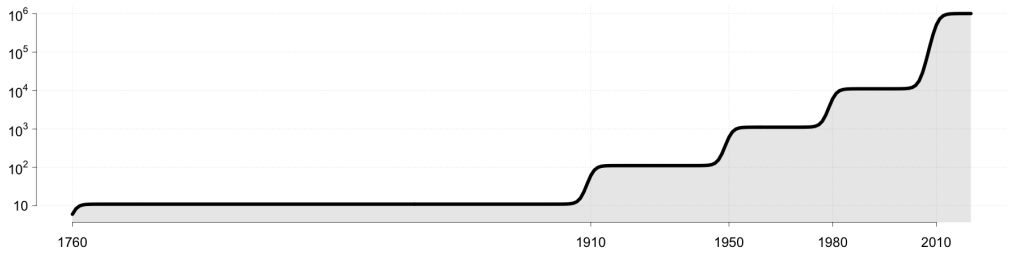

Chapter 2

HIV sexual transmission is predominantly driven by single individuals rather than discordant couples: a model-based approach

Champredon D, Bellan S, Dushoff J. PLoS ONE 2013; 8: e82906.

DOI: 10.1371/journal.pone.0082906

2.1 Abstract

Understanding the relative contribution to HIV transmission from different social groups is important for public-health policy. Information about the importance of stable serodiscordant couples (when one partner is infected but not the other) relative to contacts outside of stable partnerships in spreading disease can aid in designing and targeting interventions. However, the overall importance of within-couple transmission, and the determinants and correlates of this importance, are not well understood. Here, we explore how mechanistic factors – like partnership dynamics and rates of extra-couple transmission – affect various routes of transmission, using a compartmental model with parameters based on estimates from Sub-Saharan Africa. Under our assumptions, when sampling model parameters within a realistic range, we find that infection of uncoupled

individuals is usually the predominant route (median 0.62, 2.5%-97.5% quantiles: 0.26-0.88), while transmission within discordant couples is usually important, but rarely represents the majority of transmissions (median 0.33, 2.5%-97.5% quantiles: 0.10-0.67). We find a strong correlation between long-term HIV prevalence and the contact rate of uncoupled individuals, implying that this rate may be a key driver of HIV prevalence. For a given level of prevalence, we find a negative correlation between the proportion of discordant couples and the within-couple transmission rate, indicating that low discordance in a population may reflect a relatively high rate of within-couple transmission. Transmission within or outside couples and among uncoupled individuals are all likely to be important in sustaining heterosexual HIV transmission in Sub-Saharan Africa. Hence, intervention policies should be broadly targeted when practical.

2.2 Introduction

Diseases spread by sexual intercourse can be transmitted through a wide variety of social routes: within a stable, monogamous relationship; within a stable, non-monogamous relationship; or in casual encounters between people who may or may not also be involved in stable relationships. Understanding the importance of these routes for disease spread is important for making predictions and designing public-health interventions. Recent debates about HIV control have involved discussion of the importance of stable, "serodiscordant" partnerships (partnerships where one partner is infected and the other is not) to disease transmission [8,26,27,29,34,39,61,75,84,92].

Serodiscordant couples can arise from extra-couple transmission, or from new pairings involving a person who was infected either while single, while in a previous relationship or, more rarely in Sub-Saharan Africa, via non-sexual transmission (e.g. injection drug use, blood transfusions, or vertical transmission). Similarly, serodiscordant couples can be "lost" through couple dissolution, infection of the seronegative partner via either within-couple or extra-couple transmission, or the death of a partner via AIDS-related or unrelated causes. Serodiscordant couples represent a clear example of an individual at risk for transmission, and a valuable lens through which to study transmission risk and evaluate interventions [13]. If most transmission occurs within stable, serodiscordant couples, then couple-based intervention is a promising route for cost-effective interventions.

However, if a lot of transmission is occurring outside of couples, population-based interventions will be necessary.

The relationship between the number of serodiscordant couples in a population and their role in transmission is complicated. Looking *forward* in time, the presence of serodiscordant couples implies potential risk of within-couple transmission in those very couples. Conversely, looking *backward* in time, the presence of serodiscordant couples implies that the infected individual was infected by somebody other than the current partner, and thus implies an increased importance of non-couple routes of transmission or of partner switching.

Dunkle *et al.* [39] used a "forward" approach to suggest that transmission between partners in serodiscordant couples contributed to the majority of all new HIV infections. In a follow-up study, Coburn *et al.* [29] used a similar forward approach to argue that transmission within stable serodiscordant couples can be an important driver of the HIV epidemic when the proportion of coupled individuals in a population is large. Importantly, such "forward" modelling directly considers the potential *contributions* of serodiscordant couples to new HIV incidence, but not their *origin*.

In the "backward" approach, inference is based instead on the origin of serodiscordance. A high level of serodiscordance is thus seen as evidence of outside infection. Such studies ([34, 49, 75, 92]) have concluded that within-couple transmission plays a smaller role in contributing to HIV incidence than Dunkle *et al.* [39]. For example, Lurie *et al.* [75] investigated serodiscordance through a specific group of migrant populations in rural South-Africa and estimated that a migrant man living in a stable couple was 26 times more likely to be infected outside this partnership rather than within. More recently, Bellan *et al.* [8] fitted a mechanistic model to Demographic and Health Surveys (DHS) data from several countries in Sub-Saharan Africa that combined both the "forward" and "backward" approaches and concluded that within-couple, pre-couple and extra-couple transmission are all important in most of the countries considered.

Some studies have looked specifically at within- versus extra-couple transmission within serodiscordant couples [26, 34, 47]. For example, Chemaitelly *et al.* [26] concluded that extra-couple infections contribute "minimally" to HIV incidence within serodiscordant couples in Sub-Saharan Africa, especially in countries with low overall HIV prevalence. Extra-couple transmissions has also been suspected to drive the number of serodiscordant couples [34]. Serodiscordant couple cohort

studies have additionally found that 13-32% of seroconversions in seronegative partners were not virologically linked to their partner's virus and thus due to extra-couple infection [23, 38, 41, 80, 98]. However, couples in cohorts may not be representative of the general population, are HIV serostatus-aware, and heavily counselled with resulting effects on their behavior [80].

The epidemiological role of serodiscordant couples changes throughout the course of an epidemic [13, 84, 92], and its evolution over time is complex. Robinson *et al.* [84] used individual-based simulations fitted to data from rural Uganda to conclude that within-couple transmission was the main route of infection once the HIV epidemic reaches an endemic phase. Johnson *et al.* [61], on the other hand, fitted a Bayesian model to prevalence and sexual-behaviour data in South-Africa, and concluded that HIV incidence continues to result predominantly from transmission outside of stable relationships.

The studies discussed above all focus on the amount of transmission that occurs directly through various routes. Direct transmission is clearly relevant, but is not the only factor determining the importance of a route. Some routes of transmission may be disproportionately important in spreading infection throughout the population. To take an extreme example, the amount of direct transmission of immunodeficiency viruses from non-humans to humans is negligible; but without early transmission through that route, there would have been no HIV epidemic. Here we take a complementary approach to earlier studies that focus on routes of transmission by using a simple dynamic model that allows us to ask not only what factors affect the amount of transmission through various routes, but also how changing transmission rates along various routes is expected to affect long-term disease prevalence.

We construct a partnership-based model specifically aimed at comparing the effects of transmission within stable couples, transmission to and from uncoupled individuals, and "extra-couple" transmission to and from coupled individuals. Partnership-based models have previously been used to study various aspects of sexually transmitted infections (STI) (see [17] for a recent review). Many of these trace back to the work of Dietz and Haldeler [37], who used a simple model to gain analytic insight into a model with sequential partnerships. Although previous dynamical models involving pair formation have been used to study various issues associated with the spread of STIs, no dynamical model has focused specifically on the contribution of transmission within serodiscordant couples to HIV incidence and prevalence. We explore the behaviour of our model across a range

of parameters representative of HIV in Sub-Saharan Africa using latin hypercube sampling.

2.3 Materials and Methods

2.3.1 Model formulation

Many of the parameters involved in modelling both couple formation and disease transmission are difficult to estimate, since they relate to private behaviours associated with strong social expectations. We therefore made this model as simple as seemed reasonable in order to disentangle and interpret the fundamental mechanisms involved. Our model explores the role of serodiscordance and within-couple transmission in HIV spread. In particular, we do not model genders separately. Including gender in the model would add a lot of complexity (and parameters), and is not necessary for addressing our question, since evidence suggests that the gender-specific proportion of index cases [8,42] and probabilities of transmission [12] are at least roughly similar. Nor do we account for stages of HIV infectiousness, circumcision, co-infections or condom use.

We do include individual heterogeneous infection risk by phenomenologically reducing the contact rate as disease prevalence increases. This is a common method for introducing heterogeneity into transmission models without substantially increasing model complexity [55]. In particular, it allows the model to capture the early rapid rise in prevalence with realistic parameters and long-term behaviour. While we allow for extra-couple transmission by coupled individuals (i.e. once-off contacts while in a stable relationship), we do not keep track of more than one *stable* partnership per individual – a form of "concurrency" that is potentially important to HIV spread [78].

Model structure

We model uncoupled individuals and couples, classified by HIV status. Uncoupled susceptible individuals are denoted X and uncoupled infectious individuals are denoted Y. Couples are classified as N (concordant **n**egative) when both partners are susceptible; P (concordant **p**ositive) when both partners are infectious; and D (sero**d**iscordant) when only one partner is infectious. The total number of

individuals at any given time is $T = X + Y + 2(N + D + P)$ and the total number of infectious individuals is $I = Y + D + 2P$. See Figure 2.1 for a graphical representation.

We assume that individuals die naturally at rate μ and that new individuals are recruited into the sexually active population as uncoupled susceptibles (compartment X) at rate μT^* (thus, T^* is the equilibrium population size in the absence of disease). Uncoupled individuals form couples at rate m and couples dissolve at rate δ. Infected individuals die of AIDS at rate α. Marital parameters m and δ do not depend on infectious status.

Extra-couple intercourse is modelled by allowing both individuals in stable couples and uncoupled individuals to interact in a general mixing pool. Coupled and uncoupled individuals participate in this abstract pool at different rates, but they mix freely and proportionally in the pool. This allows us to keep the model simple and the number of parameters limited, while allowing for both partnership dynamics and the effects of extra-couple transmission on epidemic dynamics. Note that we formally model the short-term relationships as "one offs", but our interpretation is intended to cover all but the main partnership. This is a substantial simplification, but not at all rare: in fact, many influential models implicitly treat all relationships as one off [17].

Couple formation and dissolution

The size of the uncoupled population is $(X + Y)$, so partnerships are formed at total rate $m(X + Y)$. Since we assume that individual behaviour towards couple formation or dissolution is unaffected by infection status, the proportion of new couples for each type will follow a binomial distribution (see Appendix A for more details):

- $X + X \rightarrow N$: $\frac{X^2}{(X+Y)^2}$
- $X + Y \rightarrow D$: $\frac{2XY}{(X+Y)^2}$
- $Y + Y \rightarrow P$: $\frac{Y^2}{(X+Y)^2}$

Each of these proportions is multiplied by the total rate $m(X + Y)$.

The dissolution dynamics for coupled individuals is straightforward: $N' = -2\delta N$, $P' = -2\delta P$ and $D' = -2\delta D$. After dissolution, only the susceptible partner of D

moves to X and both partners of N moves to X, hence $X' = 2(\delta D + 2\delta N)$. Similarly, only the infected partner of D moves to Y and both partners of P moves to Y: $Y' = 2(\delta D + 2\delta P)$.

Thus, we can write the effects of only couple formation and dissolution on the dynamics:

$$\begin{cases} X' = -2mX + 2(\delta D + 2\delta N) \\ Y' = -2mY + 2(\delta D + 2\delta P) \\ N' = mX^2/(X+Y) - 2\delta N \\ P' = mY^2/(X+Y) - 2\delta P \\ D' = 2mXY/(X+Y) - 2\delta D \\ T' = 0 \end{cases} \tag{2.1}$$

Transmission

Susceptible individuals in serodiscordant couples become infected at the **w**ithin-couple effective mixing rate c_w (individuals in seroconcordant couples are implicitly assumed to experience the same mixing rate, but do not transmit infection to each other). We also assume that coupled individuals mix with individuals outside the relationship with an **e**xtra-couple effective mixing rate c_e, and thus become infected (if susceptible) at rate $c_e\lambda$, where λ is the proportion of their contacts that are infectious. Similarly, **u**ncoupled individuals are exposed at rate c_u and become infected at rate $c_u\lambda$.

The "effective mixing rates" c thus represent the rate at which individuals become infected through various routes, conditional on their partners being infectious. All of our mixing rates are best considered as effective mixing rates that combine frequency of contact and rate of partner change (for c_u and c_e only). They implicitly aggregate all other effects important for transmission (like condom use, circumcision, STI co-infections, etc.)

We also include phenomenological heterogeneity in the effective mixing rates to account for behavioural change as the epidemic progresses. We set $c_u = c'_u e^{-\phi P}$ and $c_e = c'_e e^{-\phi P}$ where c' is the baseline effective mixing rate and ϕ the strength of the behavioural response [50]. The range of values for the phenomenological parameter ϕ (Table 2.1) were chosen after fitting both prevalence trajectories and observed behaviour changes (for the latter, we assumed change in reported con-

dom usage from DHS data was a fair proxy for behaviour change) for sub-Sahara African countries where such data were available.

We assume that individuals mix homogeneously when interacting with individuals other than their stable partners; thus λ is given by the proportion of mixing in the non-couple pool that is accounted for by infectious individuals:

$$\lambda = \frac{c_u Y + c_e(D + 2P)}{c_u(X + Y) + 2c_e(N + D + P)} \tag{2.2}$$

Within-couple transmission also has an implicit prevalence term: within-couple prevalence is 0 for concordant negative couples, and 1 for the susceptible individual in a serodiscordant couple.

The dynamical terms for disease transmission can now be calculated. The flow of singles from X to Y is $\lambda c_u X$. A concordant negative couple (N) moves to D if either partner is infected, so this flow is $2\lambda c_e N$. Couples move from D to P when the susceptible partner is infected from the mixing pool or by the infectious partner, that is a flow of $(\lambda c_e + c_w)D$.

Recruitment and death

A couple is dissolved when either partner dies. This happens at rate μ for susceptible individuals and at rate $\mu + \alpha$ for infectious individuals. Thus, concordant couples are dissolved by death at rate $2\mu N$ and $2(\mu + \alpha)P$, respectively, while serodiscordant are dissolved at rate $(2\mu + \alpha)D$. Surviving individuals are distributed to X and Y. X experiences a recruitment rate of μT^* and a death rate μ. X also increases when either partner of a sero-negative couple dies, or when the infected partner of a serodiscordant couple (D) dies. Hence, $X' = \mu T^* - \mu X + 2\mu N + (\mu + \alpha)D$. Similarly, $Y' = -(\mu + \alpha)Y + \mu D + 2(\mu + \alpha)P$.

Combined dynamics

Adding all the components above, the population dynamics are given by:

$$\begin{cases} X' = \mu T^* - (2m + \lambda c_u + \mu)X + 2(\mu + 2\delta)N + (2\delta + \mu + \alpha)D \\ Y' = -(2m + \mu + \alpha)Y + \lambda c_u X + (2\delta + \mu)D + 2(\mu + \alpha + 2\delta)P \\ N' = mX^2/(X+Y) - 2(\delta + \lambda c_e + \mu)N \\ D' = 2mXY/(X+Y) - (2\delta + 2\mu + \alpha + c_w + \lambda c_e)D + 2\lambda c_e N \\ P' = mY^2/(X+Y) + (\lambda c_e + c_w)D - 2(\mu + \alpha + \delta)P \\ T' = T^* - \mu T - \alpha I. \end{cases} \tag{2.3}$$

The global incidence is $G = c_w D + \lambda(c_u X + c_e(2N + D))$, the first term being the incidence from within serodiscordant couples.

Relative incidences

The main outcomes studied here are the relative contribution of transmission to the global incidence from either uncoupled individuals or serodiscordant couples. We call υ the proportion of global incidence due to transmission to uncoupled individuals and ω the proportion due to within-couple transmission. Hence, using the model notation, we have:

$$\upsilon = \lambda c_u X/G \tag{2.4}$$
$$\omega = c_w D/G \tag{2.5}$$

The importance of within-couple transmission has been measured in several different ways. For example [29, 39] estimated what we call ω – the proportion of *all* infections that are due to within-couple transmission. Another study [8] considered all transmissions *to* couples that were infected by each of the three routes: pre-couple formation and within or outside couple transmission. Here, we use another ratio which is more appropriate to our model and define $\omega_C = c_w D/(c_w D + \lambda c_e(2N + D))$ as the proportion of these infections that are due to within-couple transmission when only coupled individuals are accounted for.

Finally, the model in [26] was restricted to the proportion of infections transmitted within serodiscordant couples only; we call this quantity $\omega_D = c_w/(c_w + \lambda c_e)$. Figure 2.2 illustrates the difference between these ratios.

We measure all ωs and υ at the time horizon of our simulations, set at 40 years. Numerical simulations indicate that results are not sensitive to this choice as these ratios tend to converge quickly to their equilibrium values (see Appendix A).

Serodiscordance statistic

We also create a unitless measure of serodiscordance to compare with the proportion ω. If no transmission happened in couples (or if dissolution dynamics were very fast), we would expect the proportion of all couples that are serodiscordant to be $\hat{d} = 2i_c(1 - i_c)$, where $i_c = (2P + D)/C$ is the proportion of all coupled individuals who are infectious and $C = 2(P + D + N)$ is the number of individuals living in a stable couple. We can then compare this expectation to the observed proportion of serodiscordant couples $d = D/C$, and define a unitless serodiscordance statistic

$$\mathcal{D} = d/\hat{d} \tag{2.6}$$

that measures how serodiscordant the population is compared to this null model.

2.3.2 Numerical Simulations

Unfortunately, even this simplified model does not provide simple analytic insights when both partnership dynamics and HIV-induced mortality are included. We therefore used numerical simulations to explore a broad range of plausible parameters.

Latin hypercube sampling

We perform latin hypercube sampling on the model parameters and examine how measures of prevalence, discordance and within-couple transmission are distributed, and how they are correlated with parameters. Every parameter z was assigned a range between z_{min} and z_{max} and n values are equally spaced on

the log scale from z_{min} to z_{max} (i.e. the *ratio* between successive values is the same, see Appendix A for more details)

Parameter ranges

Table 2.1 summarizes the ranges used for all model parameters. The parameter ranges are chosen to reflect demography and heterosexual HIV transmission in Sub-Saharan Africa; details are described in Appendix A.

The natural death rate μ was chosen to reflect the range of life expectancies found in Sub-Saharan Africa and also the fact we are considering sexually active individuals (assumed over 15 years old, see Appendix A).

The disease-induced death rate is relatively well documented and we chose a range consistent with published studies (see Appendix A).

Couple formation and dissolution rates (m and δ) are uncertain. However, our model gives an analytical relationship between the coupled population at the disease-free equilibrium (DFE) and the parameters μ, δ and m (see Appendix A for details). Hence, we chose to calibrate δ and m to the DHS data of proportion of coupled individuals while also yielding realistic distributions of relationship durations (see Appendix A).

The susceptible groups X_0 and N_0 are set at the DFE of our model. A small amount of infectious individuals is introduced to start the epidemic (see Appendix A for details).

The hazard of within-couple transmission c_w has been estimated by numerous serodiscordant couple cohort studies (see for example [12, 13, 38, 48, 59, 90]) and our range was chosen to reflect these findings. Little information is available about the pool mixing rates, c_u and c_e. We decided to use the same range for c_u as for c_w – in other words, we explore the same ranges of sexual contact rates for uncoupled individuals mixing with uncoupled individuals as for individuals with their stable partners. We assumed the effective extra-couple contact rate c_e is less than the within-couple rate c_w (also recall that effective contact rates are multiplied by prevalence to yield transmission hazards). We therefore allowed the ratio $\rho = c_e/c_w$ to vary between 0.01 and 1.

Sensitivity analysis

In order to conveniently assess the main drivers of HIV incidence as well as discordance in our model, a sensitivity analysis was performed. Details of the methodology are given in Appendix A.

2.4 Results

Simulations shown hereafter were run with 10,000 samples. The time horizon for the simulations was set at 40 years.

2.4.1 Relative incidences

Figure 3 shows various measures of the importance of singles and serodiscordant couples to HIV incidence at the time horizon of our simulations. These quantities come to equilibrium relatively quickly in our model, and so the values here will be very close to equilibrium values.

In the parameter space explored in Table 2.1, Figure 3 panel A shows that at equilibrium HIV incidence is in most cases primarily driven by cases due to transmissions between singles, our simulations giving a median value of υ at 0.62 (95% of all simulations fall between 0.26 and 0.88).

Panel B shows that ω, the equilibrium contribution from transmission within serodiscordant couples at the *whole population* level, is mostly constrained to relatively low levels (median is 0.33 and 95% of all simulations fall between 0.10 and 0.67) as shown in Figure 3 panel B. In other words, it is unlikely for mature epidemics to be driven primarily by transmission within stable couples.

Importantly, low importance of within-couple transmission in the *whole* population (low values of ω) is consistent with high values among *coupled* individuals (ω_C, panel C) and particularly among serodiscordant couples (ω_D, panel D). In particular, our relatively low values for ω are consistent with the country-specific estimates of ω_D from [26].

Table 2.1. Ranges of model parameters. *These ranges, used in the latin hypercube sampling, are to represent realistic values for Sub-Saharan Africa. Unit of all rates is per year.*

Parameter	Range	Source
Death rate μ	$1/60 - 1/40$	UN
Disease-induced death rate α	$1/16 - 1/4$	[3, 96]
Couple formation rate $\mathfrak{m}$	$1/20 - 1/5$	Inferred from DHS
Couple dissolution rate δ	$1/30 - 1/10$	Inferred from DHS
Effective uncoupled contact rate c_u	$0.05 - 0.25$	Assumption
Effective within-couple contact rate within serodiscordant c_w	$0.05 - 0.25$	[12, 13, 38, 48, 59, 90]
Relative contact rate extra-couple c_e/c_w	$0.01 - 1$	Assumption
Phenomenological decay ϕ	$2 - 7$	Inferred from DHS

2.4.2 Long-term Effects of Transmission Routes

We further elucidate the "importance" of different routes of transmission by asking what would happen to long-term (i.e. equilibrium) HIV prevalence if mixing rates were to change. Figure 2.4, panel A shows that a proportional change in the mixing rate of uncoupled individuals c_u is expected to have a much larger effect on the epidemic than the same proportional change in either c_e or c_w.

The reasons why the other two mixing rates have less proportional effect on prevalence are different for c_e and c_w. In the case of extra-couple contact c_e, panel B shows that if we consider *absolute* changes in mixing rate, the effects of changes in c_e and c_u are similar. Thus, the relatively low proportional effect of c_e is due to our assumptions: we always assume that $c_e < c_w$, and over most of our parameter range it is much less, while we let c_w and c_u vary over the same range. When c_e is small, proportional changes in c_e will have relatively little effect.

In contrast, even absolute changes in the within-couple effective contact rate c_w have a relatively small effect on prevalence. This is due to the fact that the serodiscordant population to which c_w applies (D) is much smaller than the uncoupled (X) and coupled (D + 2N) susceptible individuals. Our model initially fits the proportion of coupled individuals (infected or not) to actual demographic data (Appendix A), and the proportion of discordant couples that emerges from our model remains relatively low throughout our simulations. This in turn has two causes: relatively few people are infected with HIV most of the time; and peo-

ple with HIV-infected partners are relatively less likely to be susceptible, because they are likely to have been infected by their partners already.

Hence, our result on the importance of uncoupled mixing rates in driving prevalence is underpinned by uncoupled individuals constituting a large proportion of the sexually active population (fitted to actual data), an extra-couple mixing rate (c_e) up to 2 orders of magnitude lower than the one of uncoupled (c_u) and a proportion of discordant couples that remain low throughout our simulations (Appendix A).

2.4.3 Serodiscordance statistic and backward interpretation

Another interesting result from the model is the negative relationship between the level of serodiscordance in the whole population ($\mathcal{D}$) and the contribution of within-couple transmission to global incidence (ω) as illustrated in Figure 2.5. Hence, at a given prevalence, a high observed discordance is associated with a relatively low contribution of within-couple transmission to the total incidence.

Furthermore, results in Figure 2.6 show this same level of discordance ($\mathcal{D}$) exhibits a strong negative correlation with the within-couple transmission rate (c_w).

These results give more support to the "backward" interpretation, where – for a given prevalence – high observed serodiscordance is likely to be a signature of non-couple routes of transmission and their interactions with the partner switching dynamics.

2.5 Discussion

Identifying the main factors that drive transmission of a sexually transmissible disease is key to designing effective interventions and, in the context presented here, to allocating resources between couple-based and population-based interventions.

The importance of non-couple versus couple-based transmission, and more specifically the role of serodiscordant couples in HIV transmission remains controversial [8, 26, 29, 39, 61, 75, 84, 92]. Using a simple dynamical model, we explored

a plausible parameter space for HIV transmission in Sub-Saharan Africa, and found that prevalence was mainly driven by the mixing rate of uncoupled individuals. Furthermore, within-couple transmission had low to moderate importance at the whole population level in transmitting HIV under all combinations of our parameters (Figure 3). Simultaneously, we found that within-couple transmission contributed to the majority of secondary infections within serodiscordant couples. Thus, estimates of a high importance of within-couple transmission at the level of the sub-population of serodiscordant couples [26] are consistent with estimates of relatively low importance of this route of transmission in the whole population [8, 29, 61, 92].

Our model also sheds light on what inferences can be made from measured levels of serodiscordance. We introduced a unitless index of discordance (the proportion of couples which are discordant, relative to a random expectation), and found negative correlations between discordance and both the within-couple transmission effective mixing rate c_w and the proportion of total HIV incidence due to within-couple transmission, ω. This lends credence to what we have called the "backward" interpretation – that for a given prevalence higher levels of discordance suggest a greater role of non-couple routes of transmission and their interactions with the partner switching dynamics.

To efficiently explore a poorly understood parameter space, our model made a large number of simplifying assumptions. We did not include gender asymmetries – however, there is evidence that these are not very strong [8, 12, 42]. We model a form of concurrency by allowing partners to have outside relationships, but do not explicitly model concurrent, stable relationships, which may also be an important factor.

We also assume that the transmission rate is constant throughout the natural history of disease; in particular, we do not model the acute phase of increased HIV infectiousness 6 to 8 weeks after HIV acquisition [30]. This effect could either increase within-couple transmission (when one member of a susceptible couple is infected via extra-couple contact) or decrease it (when infection occurs well before couple formation). To some extent, these two effects should balance out.

Our model also assumes that all mixing between non-stable partners only occurs as one-off interactions rather than as longer sustained interactions. This simplification is commonly used in models of sexually-transmitted diseases. Allowing non-stable interactions to involve multiple contacts would primarily affect model

dynamics by causing some individuals to spend more time with infected individuals and others to spend more time with uninfected individuals, thereby creating a more heterogeneous distribution of risk.

Future work should investigate the robustness of our conclusions when more types of heterogeneity – such as the greater infectiousness of the acute phase, gender asymmetries, super-spreader groups, etc – are included. We note that our analysis provides a simple framework from which to analyze the fundamental forces driving incidence among coupled and uncoupled individuals, and that analyses of more complex models will require great care in order to clearly disentangle the causal dynamical processes.

In conclusion, our results provide further evidence that transmission within couples, extra-couple transmission and transmission to uncoupled individuals are all likely to be important in sustaining heterosexual HIV transmission in Sub-Saharan Africa. Infections of uncoupled individuals, in particular, were identified in our model as a key driver of long-term HIV prevalence and thus should be appropriately targeted by interventions.

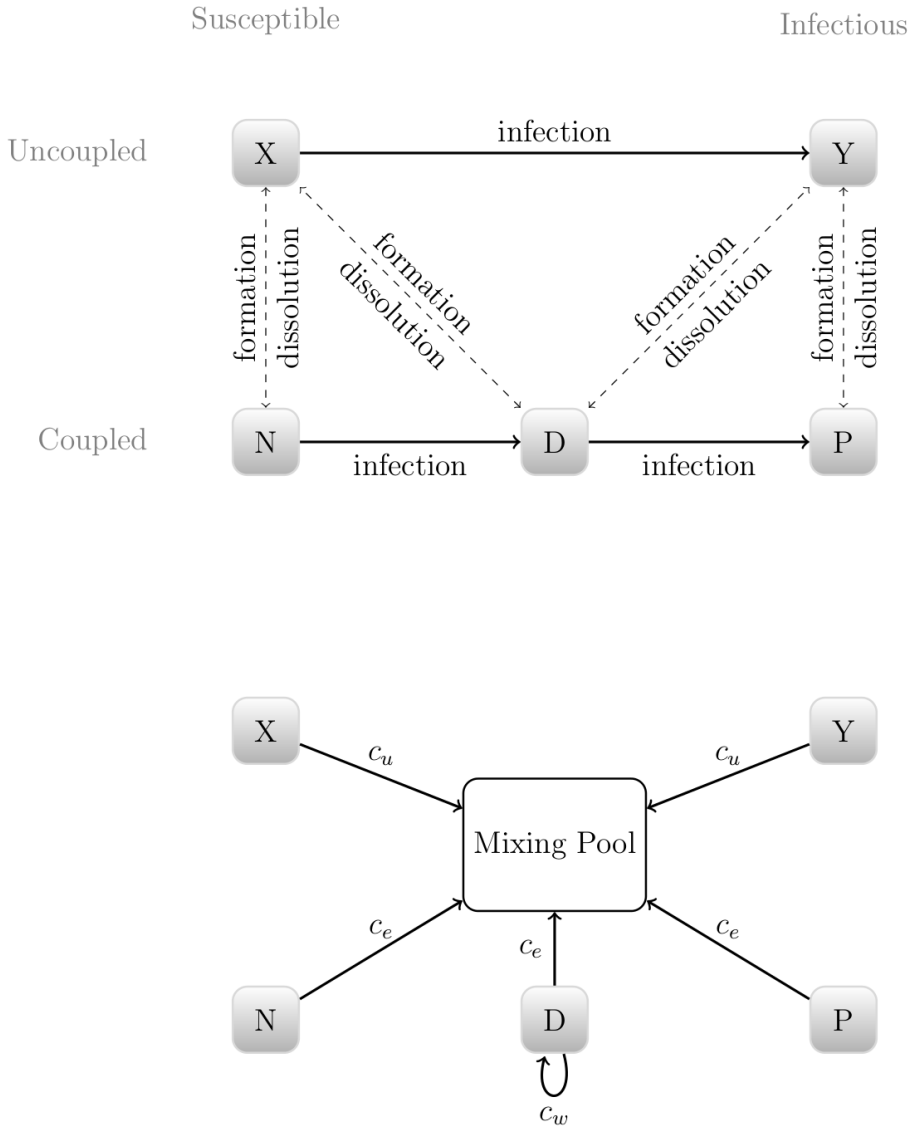

Figure 2.1. Model diagram. *The top panel describes all possible movements between compartments. The bottom panel shows the infection pathways for each group. The mixing pool is an abstract representation of where all extra-couple sexual contacts occur.*

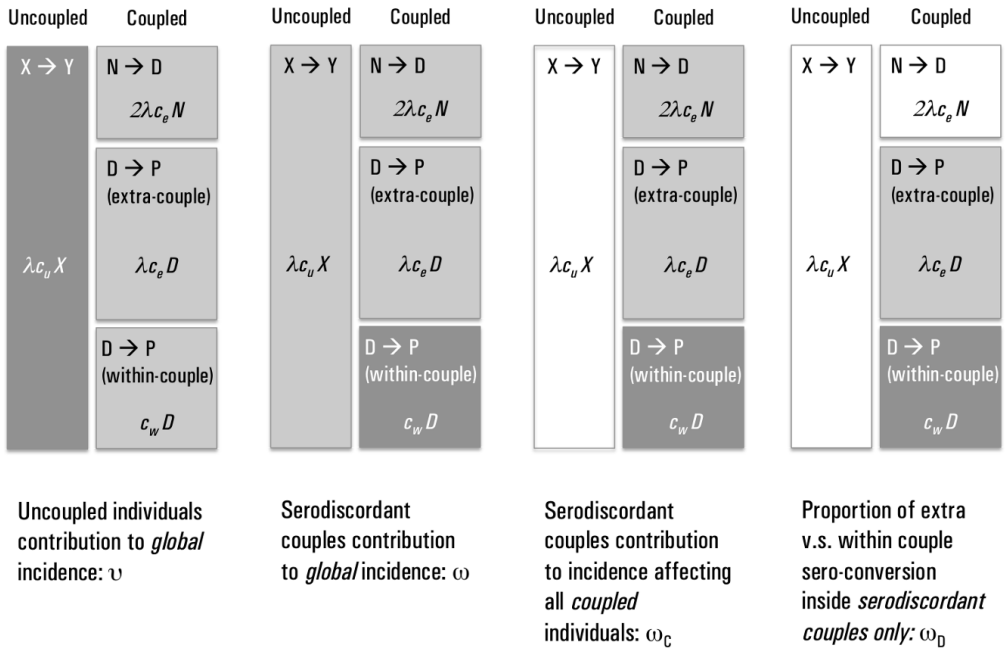

Figure 2.2. Incidence proportions. *Different measures of the proportion of within-couple transmission have been used in the past, this figure illustrates the measures discussed here. Each panel graphically represents how the incidence proportion is calculated: dark shaded compartment divided by all non-white compartments. Each compartment represent a transmission route. The proportion of new HIV infections due to uncoupled individuals (υ) is illustrated in the left panel. The next three panels show the different definitions of the proportion of within-couple transmission calculated as a fraction of other transmission components: global transmission (ω, all compartments, middle left panel); transmission to coupled individuals (ω_C, middle right panel); or transmission within serodiscordant couples, (ω_D, right panel).*

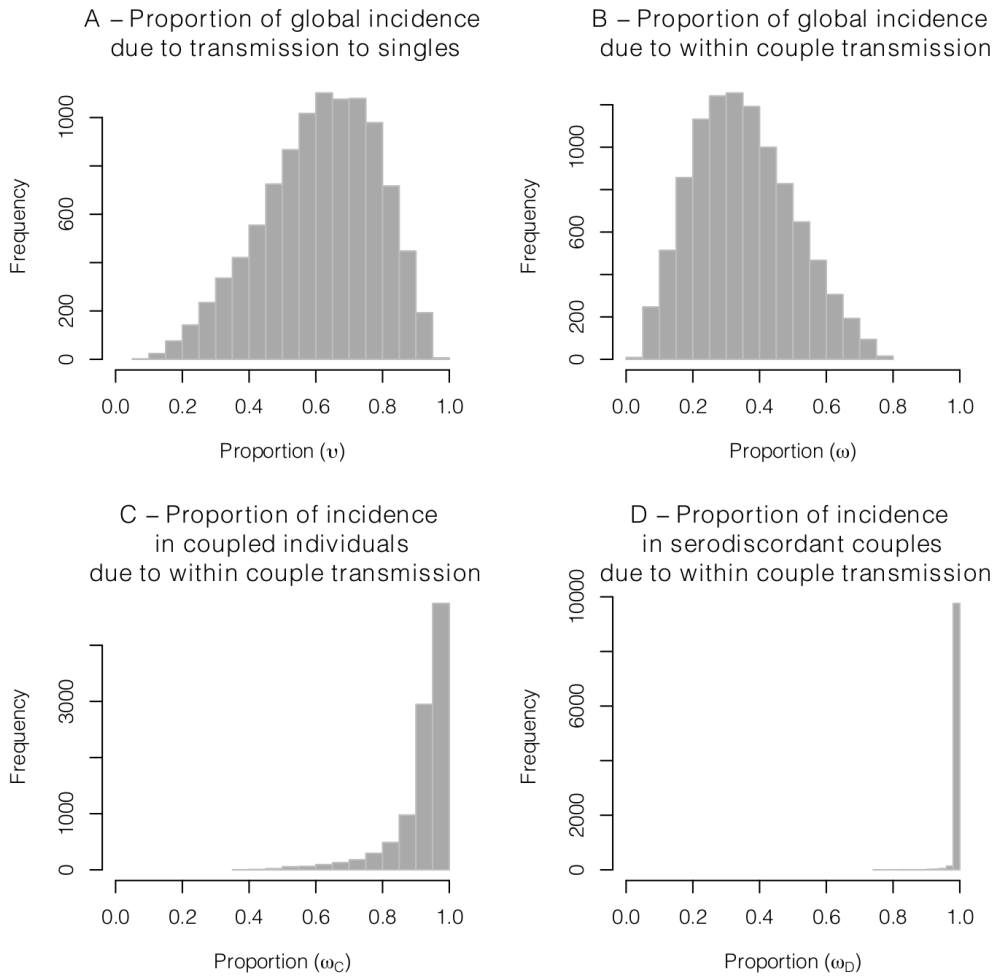

Figure 2.3. Simulated incidence proportions. *Histograms of the transmissions proportions occurring in uncoupled and serodiscordant couples at maturity from 10,000 latin hypercube samplings. Ranges are specified in Table 2.1. When compared to the total incidence at the whole population level, transmission to singles accounts for a large proportion of all cases (panel A) whereas within-couple transmission accounts for a low to moderate proportion (panel B). But when compared to the incidence occurring only among all coupled individuals (discordant or not), the share of within-couple transmissions is much higher (panels C and D). Hence a low importance of within-couple transmission at the whole population level is consistent with high importance of this route of transmission limited to the coupled population.*

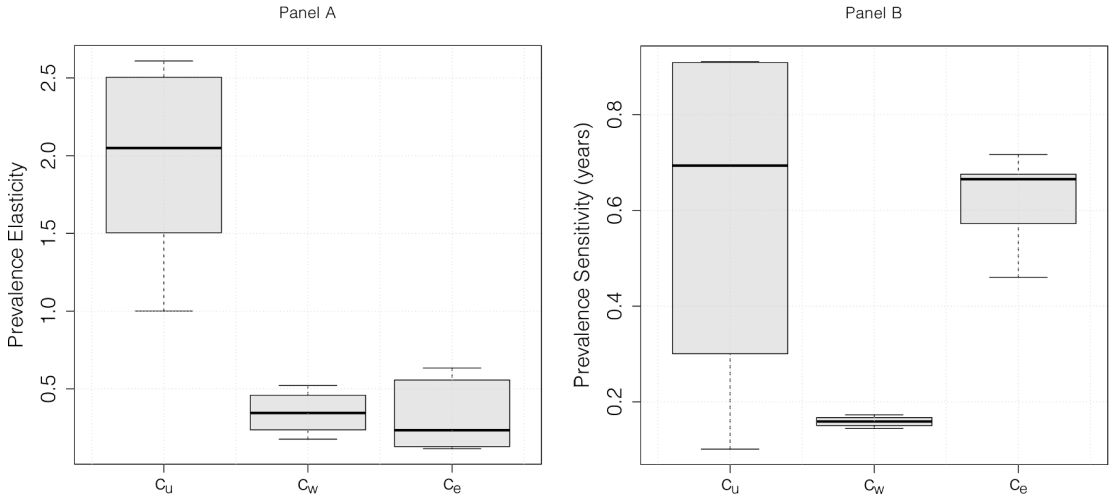

Figure 2.4. Prevalence sensitivities *Left panel shows the elasticities (unitless) of overall HIV prevalence to the three effective mixing rates (proportional change of prevalence for a given proportional change of* c*, that is* $(dPr/Pr)/(dc/c)$*, with* Pr *the prevalence). Right panel shows the sensitivities (absolute change of prevalence for a given absolute change of* c*, that is* dPr/dc*. Units in years). See main text for interpretations.*

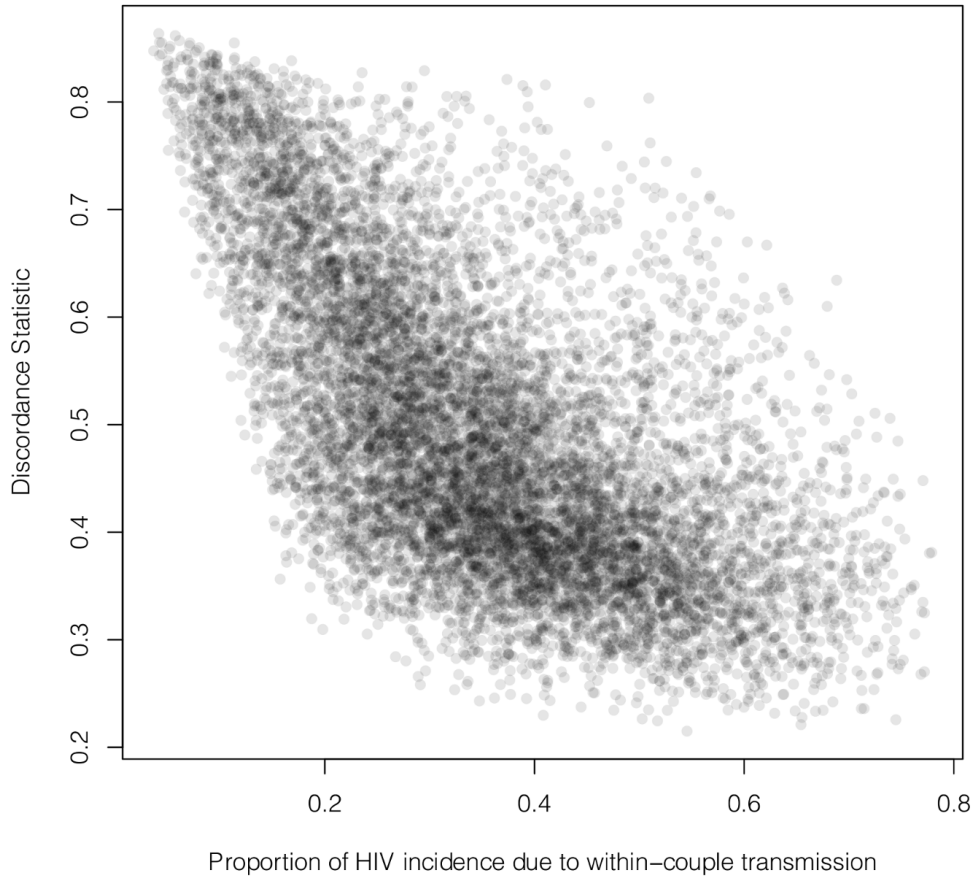

Figure 2.5. Discordant statistic and within-couple transmission contribution. *The discordance statistic $\mathcal{D}$ as a function of the contribution of within-couple transmission to the global incidence (ω). Our 10,000 simulations run with parameters sampled from realistic ranges (Table 1) show a negative relationship, suggesting that for a given HIV prevalence in the whole population, the observed discordance (measured with $\mathcal{D}$) may be a signature of the importance of within-couple transmission.*

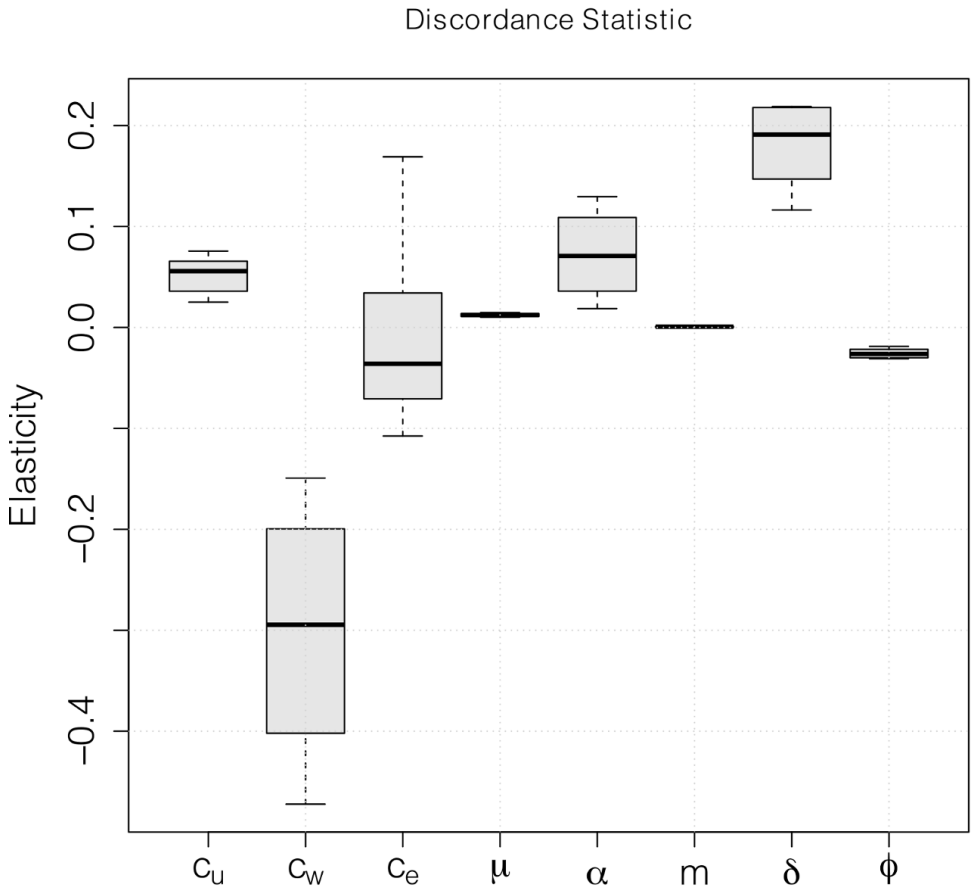

Figure 2.6. Discordant statistic elasticities. *Elasticities of the discordance statistic $\mathcal{D}$ to all model parameters. The relatively large negative elasticity of the mixing rate within discordant couples, c_w, shows its negative relationship with $\mathcal{D}$.*

Appendix A

A.1 Couple formation

The way couples form is assumed to follow a binomial distribution. If $z \in \{0, 1, 2\}$ is the number of susceptible individual(s) just before a couple formation, then we assume $z \sim \text{Binom}(2, p_s)$ with $p_s = X/(X + Y)$ the probability that an uncoupled individual is susceptible. Thus

$$p(z = k) = \binom{2}{k} p_s^k (1 - p_s)^{2-k} \tag{A.1}$$

Hence, we have the following proportions:

- Proportion of couple formation within X is $\frac{X^2}{(X+Y)^2}$
- Proportion of couple formation within Y is $\frac{Y^2}{(X+Y)^2}$
- Proportion of couple formation between X and Y is $\frac{2XY}{(X+Y)^2}$

A.2 Equilibrium in simulations

In order to check that our simulations are reasonably close to the equilibrium, we monitor the derivative of prevalence at the horizon of the simulation (set at 40 years). As shown in Figure A.1, for 10,000 simulations where the parameters have the same constraints as the LHS, the mean value of the normalized derivatives ($dX/X/dt$) for all group is small, comforting we are close to an equilibrium in most of our simulations.

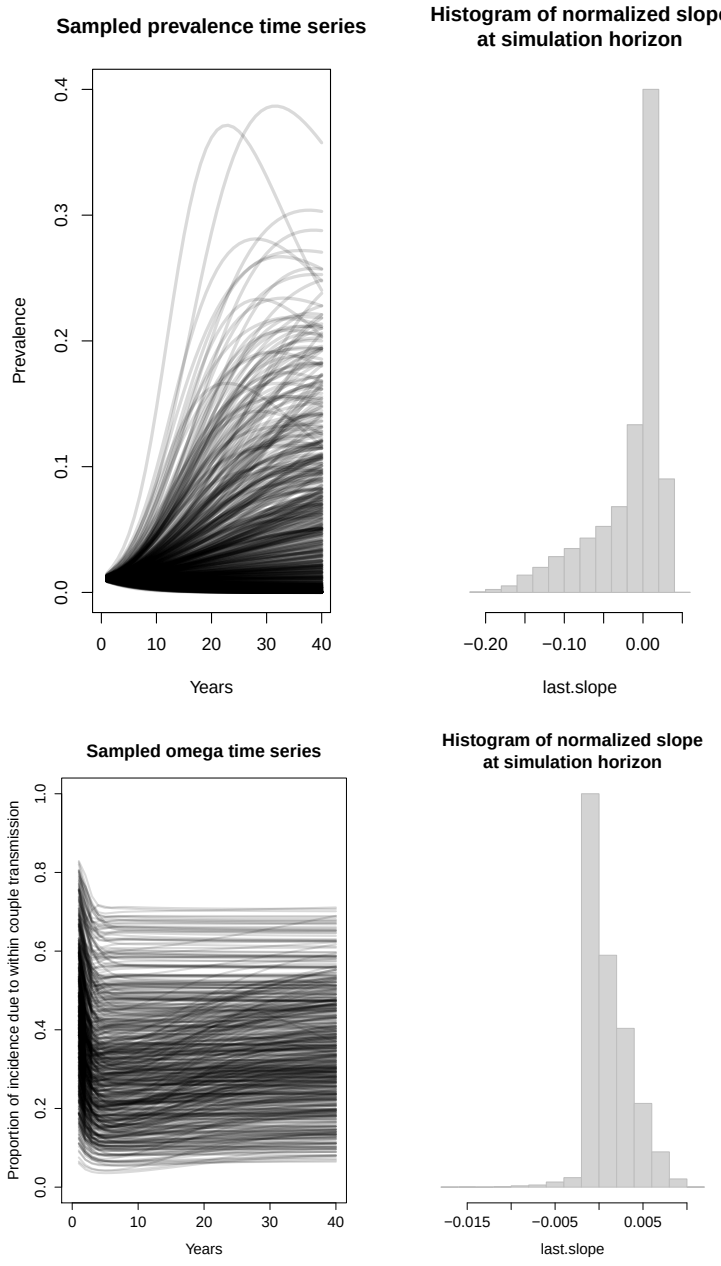

Figure A.1. Prevalence and incidence proportion at time horizon. *Sampled prevalence time series and its normalized derivatives at time horizon (year^{-1}) from 10,000 simulations. For both total prevalence and the proportion of global incidence due to within-couple transmission (ω), most of the simulated values at time horizon have reached an equilibrium.*

A.3 Disease free equilibrium

At the disease free equilibrium we have $Y = D = P = 0$ and $X' = N' = 0$. The system (2.3) becomes

$$\begin{cases} X' = \mu T^* - (2m + \mu)X + 2(\mu + 2\delta)N \\ N' = mX - 2(\delta + \mu)N \end{cases} \tag{A.2}$$

which can easily be solved, giving the proportion of uncoupled and coupled individuals

$$2N^* = \mu T^* \left[(2m + \mu)(\delta + \mu)/m - (\mu + 2\delta)\right]^{-1}$$

$$X^* = \frac{(\delta + \mu)}{m} 2N^*$$

Because $T^* = X^* + 2N^*$ we can substitute,

$$X^* = \sigma T^* \tag{A.3}$$

$$2N^* = (1 - \sigma)T^* \tag{A.4}$$

with

$$\sigma = \frac{\mu + \delta}{\mu + \delta + m} \tag{A.5}$$

being the proportion of single at DFE when the recruitment rate balances the death rate.

A.4 Initial infectious individuals

If U_0 (resp. C_0) is the initial uncoupled (resp. coupled) population, we introduce a small amount ϵ of infectious individuals such that $Y_0 = \epsilon U$ and $X_0 = (1 - \epsilon)U_0$. Similarly, $P_0 = \epsilon^2 C_0$, $N_0 = (1 - \epsilon)^2 C_0$ and $D_0 = 2\epsilon(1 - \epsilon)C_0$. The value for ϵ does not affect significantly our results as long as it is sufficiently small. We chose $\epsilon = 0.01$.

A.5 Latin hypercube sampling

Every parameter z was attributed a range between z_{min} and z_{max}. Then, this range is partitioned log-proportionally

$$z_i = \exp\left(\log(z_{min}) + [\log(z_{max}) - \log(z_{min})]\frac{i-1}{n-1}\right) \tag{A.6}$$

with n the total number of samplings and $i = 1, .., n$. The (ordered) partition $[z_1, ..., z_n]$ is then randomly shuffled, independently for each parameter, leading to a permuted vector of values $[\zeta_0, \zeta_1, ..., \zeta_n]$. Assuming there are K model parameters to be sampled, we have a $n \times K$ sampling matrix, noted $(\zeta_i^k)_{i=1..n,\, k=1..K}$. The i^{th} row ζ_i of this matrix represents the i^{th} simulation run with the set of K parameters randomly assigned from the partitions.

A.6 Discordance Statistic

Figure A.2 shows the distribution of the discordance statistic $\mathcal{D}$ from the 10,000 samples of the LHS.

A.7 Sensitivity Analysis

The methodology to calculate the *elasticity* of a response variable (e.g. prevalence) Z to the model parameters is the following. Let p be a parameter on which the elasticities will be calculated. The latin hypercube sampling (LHS) range for p is partitioned in n values: $p_1, p_2, ..., p_n$. For the first LHS run, p will be fixed at p_1 and all other parameters will be sampled in their respective predefined ranges. For the first LHS run, the average of all Z (defined as $\langle Z \rangle_1$) is calculated. The LHS run is repeated n times and we calculate $e_{p,i}$, the elasticity of parameter p between values p_{i-1} and p_i, as

$$e_{p,i} = \frac{\log\langle Z \rangle_i - \log\langle Z \rangle_{i-1}}{\log(p_i) - \log(p_{i-1})} \tag{A.7}$$

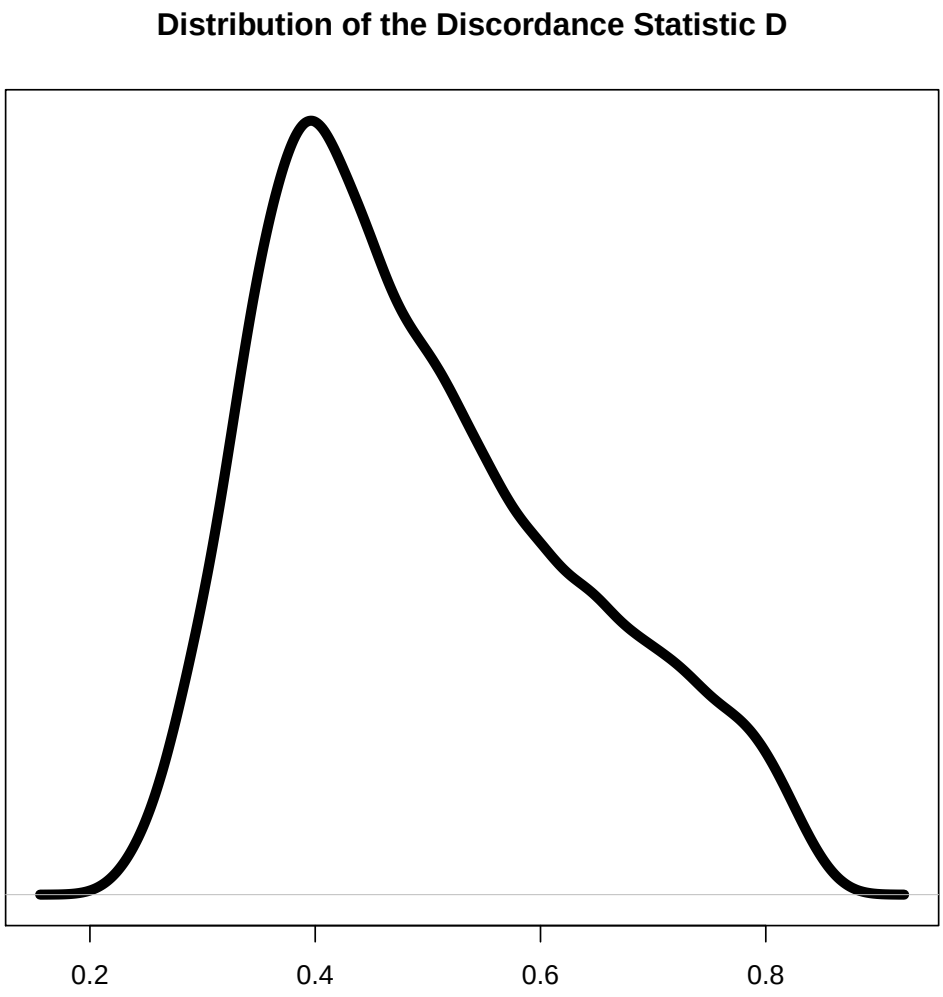

Figure A.2. Distribution of the discordance statistic. *Distribution of the discordance statistic $\mathcal{D}$ from the 10,000 simulations with parameters sampled in the range of Table 1 (main text).*

For a given parameter p, there are $(n-1)$ such sensitivities. Then, we define $e_p = (\sum_i e_{p,i})/(n-1)$, the averaged value of these elasticities. This is this quantity that is reported in the main text. A positive (resp. negative) elasticity on Z means increasing the parameter moves the distribution of Z to larger (resp. smaller) values.

For the *sensitivities*, we apply the same methodology, except that now, the sensi-

tivity formula for the parameter p between values p_{i-1} and p_i is

$$s_{p,i} = \frac{\langle Z \rangle_i - \langle Z \rangle_{i-1}}{p_i - p_{i-1}} \tag{A.8}$$

Elasticity of prevalence with respect to all parameters

Figure A.3 shows the elasticity of the overall HIV prevalence with respect to all model parameters.

Sensitivity of ω_C and ω_D

Before calculating the sensitivity, let us recall the formula defining the proportion of incidence due to within couple transmission:

$$\omega_C = \frac{c_w}{c_w + \lambda c_e(1 + 2N/D)} \text{ and } \omega_D = \frac{c_w}{c_w + \lambda c_e}$$

Note also that increasing c_w decreases D and increases P (the discordant state is more transient) and prevalence –in particular the one in the mixing pool λ – increases too. So we can expect two offsetting effects on ω when increasing c_w, and this is what we can observe in Figure A.4 where the sensitivities ($d\omega/dc$) to the effective contact rates are plotted. These plots are comparable with the plot in Figure 4 in the main text, right panel.

A.8 Vital rates

Life expectancies at birth from all countries in sub-Saharan Africa were downloaded from the UN website (http://esa.un.org/unpd/wpp/Excel-Data/mortality.htm accessed Nov 1st, 2012). French territories, Mayotte and Reunion, were not taken into account. Figure A.5 illustrates this data set.

A.9 HIV induced mortality rate

The HIV induced mortality rate range used in our study was based on mainly two previous studies [3, 96] before ART introduction. The latest [96] studied low and middle income countries, which are more similar to our sub-Saharan countries. than those in the older study [3], which focused on high-income countries. The findings of these two studies are summarized in Figure A.6 where the 95% confidence intervals of the median survival time are shown for different cohorts.

A.10 Coupled population

We used the DHS data to assess the proportion of the population coupled. We gathered in the coupled category the individuals answering they were living as "Married" or "Living together". The remaining answers ("Never married", "Divorced", "Widowed", "Not living together" and "Missing") were categorized as uncoupled. We looked at all countries from sub-Saharan Africa over all the years the DHS surveys were available as of November 1st, 2012. Results are plotted in Figure A.7.

The values from the disease free equilibrium (DFE) formulas (see section A.3 below) were compared to actual data from sub-Saharan Africa countries in the DHS database. We sampled 1,000 values using the latin hypercube method and chose values for δ, m to fit reasonably well the distribution of $2N^*$ with the distribution of DHS data. As shown in Figure A.8, we obtained a fair match.

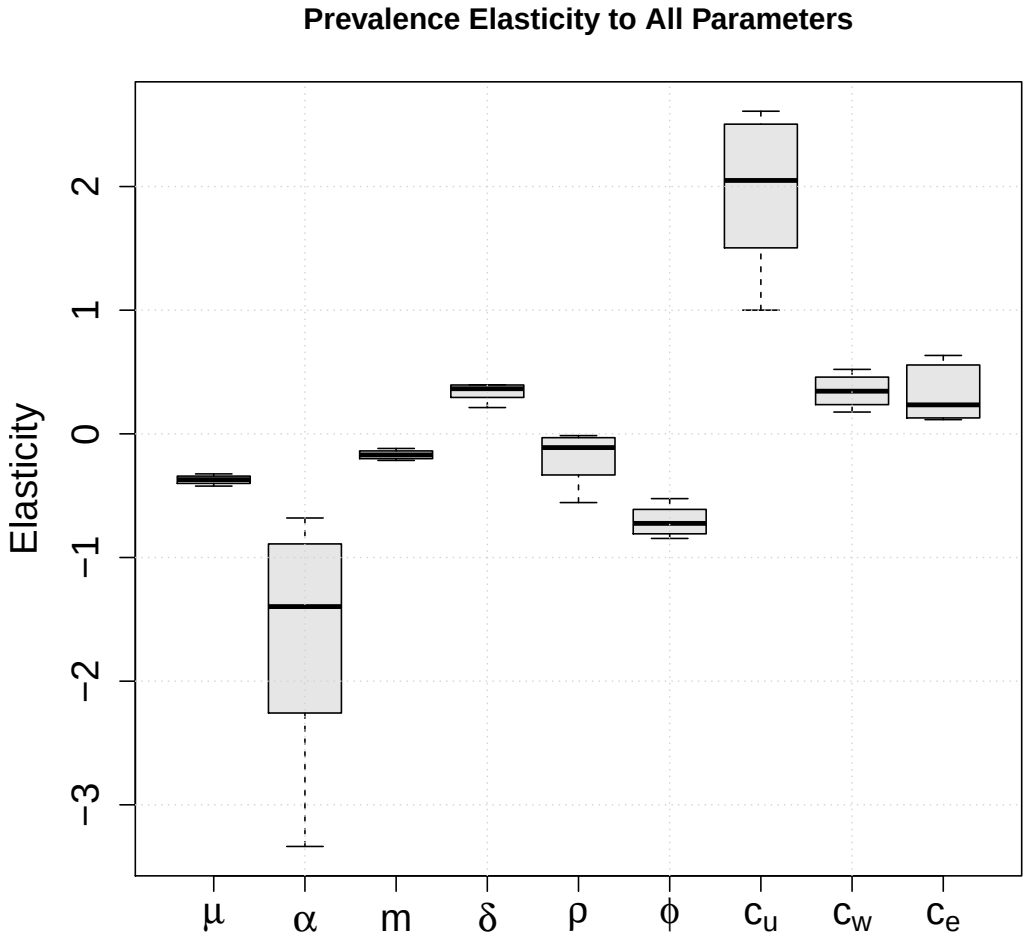

Figure A.3. Prevalence elasticities. *Elasticity of prevalence with respect to all parameters*

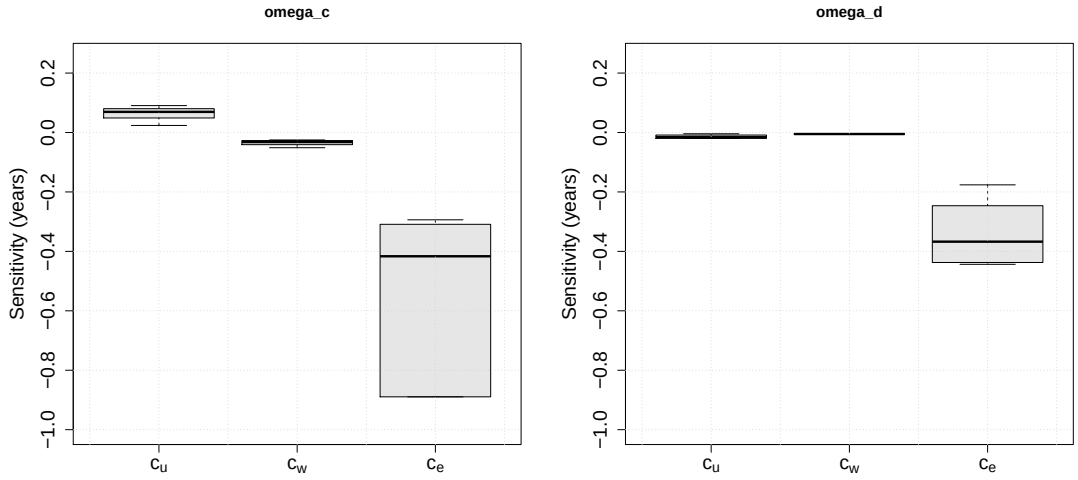

Figure A.4. Incidence proportion sensitivities. *Sensitivities of ω_C and ω_D with respect to the effective contact rates*

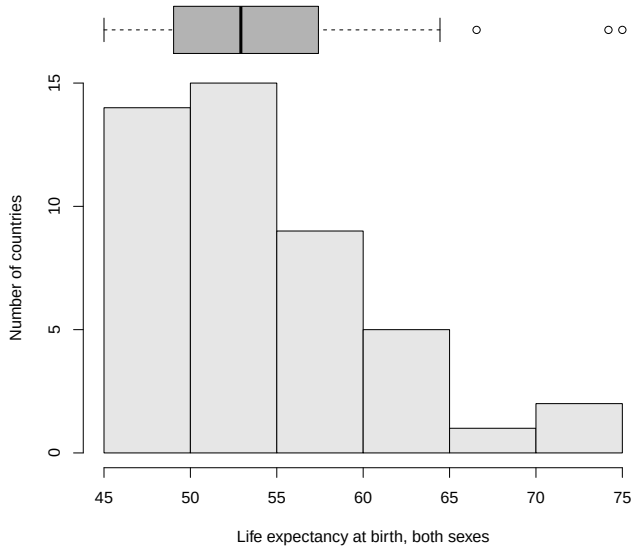

Figure A.5. Life expectancies. *Histogram of life expectancies at birth for both sexes from countries in sub-Saharan Africa. Source: UN.*

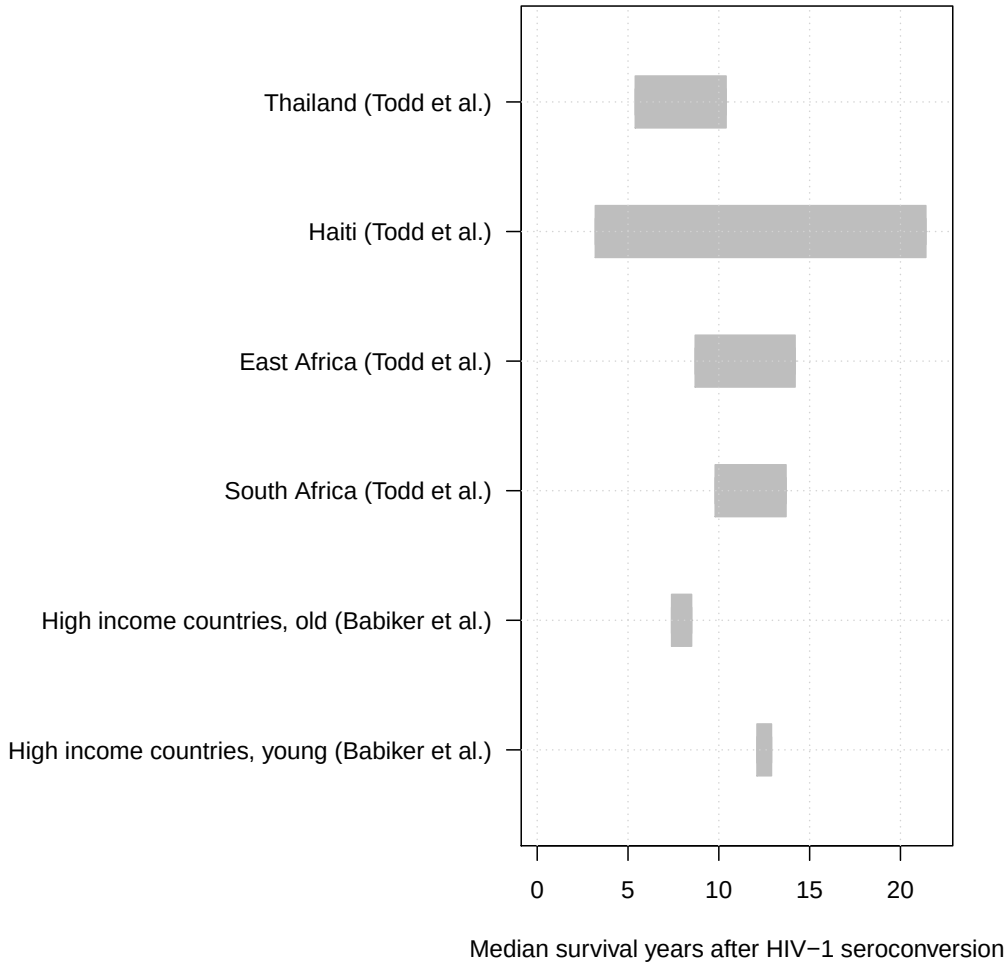

Figure A.6. HIV survival. *Survival times after HIV infection from [3, 96]. See text in section A.9 for more details.*

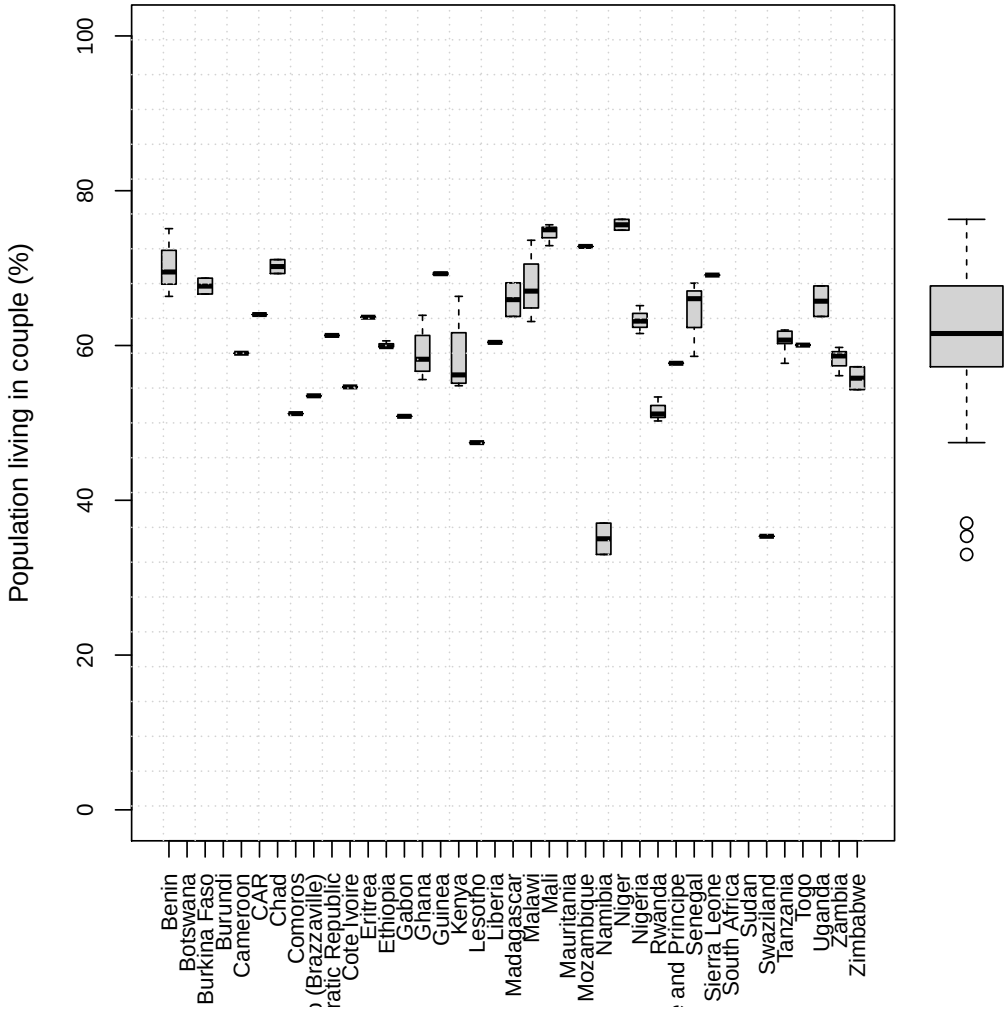

Figure A.7. Coupled population. *Percentage of the population living in coupled (source: DHS - http://www.measuredhs.com). If there is only one DHS survey for a given country, then the box plot is reduced a point. The large box plot on the right hand side agglomerates all values.*

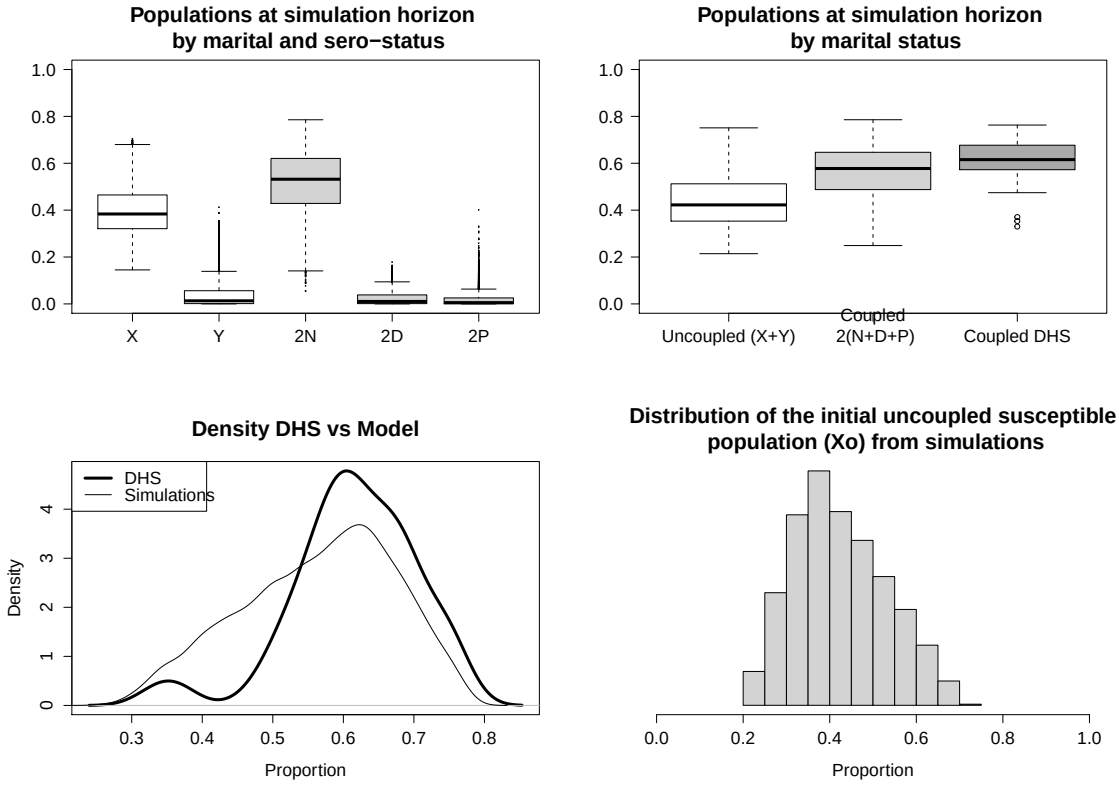

Figure A.8. Simulated demographics. *Top left panel: Proportions of populations at the time horizon of our 10,000 simulations by couple status and HIV serostatus. Top right panel: Proportions of population at the time horizon of our 10,000 simulations by couple status only and compared with DHS data of coupled individuals. Bottom left panel: Comparison of densities of coupled individuals between DHS data and the model simulations. Parameters range for couple dissolution and formation (δ and $\mathfrak{m}$) were chosen such that the model distribution of coupled individuals is similar to DHS data. Bottom right panel: initial distribution (from our 10,000 simulations) of the proportion of uncoupled individuals (X_0).*

Chapter 3

Epidemiological impact of a syphilis vaccine: a simulation study

David Champredon , Caroline Cameron, Marek Smieja, Jonathan Dushoff

3.1 Abstract

Despite the availability of inexpensive antimicrobial treatment, syphilis remains prevalent worldwide, affecting millions of individuals. Furthermore, syphilis infection is suspected of increasing both susceptibility to, and tendency to transmit, HIV. Development of a syphilis vaccine would be a potentially promising step towards control, but the value of dedicating resources to vaccine development should be evaluated in the context of the anticipated benefits. Here, we use a realistic mathematical model to explore the potential impact of rolling out a hypothetical syphilis vaccine on morbidity from both syphilis and HIV and compare it to the impact of expanded "screen and treat" programs using existing treatments. Our results suggest that an efficacious vaccine has the potential to sharply reduce syphilis prevalence under a wide range of scenarios, while expanded treatment interventions are likely to be substantially less effective. Our modeled interventions in our simulated study populations are expected to have little effect on HIV, and in some scenarios lead to small increases in HIV incidence, suggesting that interventions against syphilis should be accompanied with interventions against other sexually transmitted infections to prevent the possibility

that lower morbidity or lower perceived risk from syphilis could lead to increases in other diseases.

3.2 Introduction

Syphilis is a sexually transmitted infection (STI) caused by the bacterium *Treponema pallidum*, which affects 36 million individuals worldwide. Every year, it is estimated that 11 million new syphilis infections occur worldwide and 1.5 million pregnancies are affected, putting their children at risk of congenital syphilis; in 2008, congenital syphilis caused about 500,000 birth-related adverse outcomes, more than half of them fatal [106]. The vast majority of syphilis cases occur in developing countries where the disease is either widespread in the general population or concentrated in high-risk groups (including sex workers, and men who have sex with men (MSM)). After being relatively well controlled in higher-resource countries, syphilis infections have been rebounding since the early 2000s, mostly in high-risk groups.

The primary stage of syphilis manifests as a chancre at the infection site. This typically occurs at the site of sexual contact and is highly infectious. Weeks to months later, secondary syphilis causes fevers, swollen lymph nodes, and rash; this is the stage when most people present for treatment. Left untreated, or inadequately treated, syphilis can progress to tertiary disease, which can involve the brain, heart, or other organs. Although the incidence of tertiary syphilis has been sharply reduced by treatment, cases of tertiary syphilis are still observed worldwide. Co-infections involving syphilis and other sexually transmitted pathogens are frequent [63]. Moreover, it has been reported that infection with most STIs (including syphilis) increases the risks of both acquiring and transmitting HIV [12, 24, 62, 86, 87]. Given its worldwide prevalence and its shared transmission routes with HIV, syphilis infections may increase HIV incidence [45, 83] either because of an increased susceptibility to HIV or increased HIV-infectiousness, although a recent study concluded that the effects of syphilis on incidence via the latter route were small [4]. Although there is little data for the interaction between syphilis and STIs other than HIV, it is plausible that there also exists a similar epidemiological synergy. Penicillin has been the main antibiotic used to treat syphilis over the last 70 years. It is inexpensive, readily available in most regions of the world, effective when administered as a single dose during pri-

mary, secondary and early latent infection, and *Treponema pallidum* has thus far not developed resistance against this antibiotic [72]. In contrast, no vaccine is yet available for syphilis [16]. The technical challenges associated with *T. pallidum* experimentation, including an unusual, fragile membrane structure which makes genetic manipulation difficult, combined with the relative dearth of *T. pallidum* basic science researchers, has impeded the field of *T. pallidum* vaccine research [16,72]. Sterile protection against challenge with a homologous *T. pallidum* strain has been achieved [77], demonstrating proof-of-concept, but the impractical vaccination regimen used in this study precluded further development as a viable vaccine candidate. Further factors hindering syphilis vaccine development include the high costs associated with bench-to-bedside vaccine development studies (between $200 and $900 million), the prolonged timeline associated with vaccine development (typically more than 10 years) and, particular to syphilis, the unresolved issues of the target populations, marketability and profitability of a vaccine [16]. However, intensive syphilis-targeted public health control initiatives, including the CDC's National Plan to Eliminate Syphilis from the US [20,21] and the WHO's Initiative for the Global Elimination of Congenital Syphilis [104], have not achieved the goal of syphilis elimination, suggesting symptomatic antibiotic treatment alone will not successfully eradicate the disease.

Several factors contribute to the difficulty of eliminating syphilis using antibiotic treatment: early infection is difficult to diagnose; varied clinical symptoms lead to mis-diagnoses; diagnostic assays are technically difficult to perform and interpret; an effective and prolonged patient follow-up is required between diagnosis and treatment; and antenatal care may not be available in some settings. These factors lead to missed syphilis diagnoses during the early stage of infection, the highest risk period for transmission and acquisition of additional STIs and congenital syphilis [16]. The continuing high rates of syphilis worldwide, despite the low cost, effectiveness and availability of penicillin treatment, combined with the dire consequences associated with *T. pallidum* infection, especially mother-to-child transmission (MTCT), suggest that alternative means must be used to combat this infection.

The worldwide morbidity caused by syphilis is high, but because eradication through vaccine development will take time and a significant investment of financial and human resources, a careful assessment of the costs and benefits of this option is needed. Indeed, the World Health Organization's 2013 Workshop on "Global Action Plan and Roadmap for STI Vaccine Development and Intro-

duction" highlighted the necessity of mathematical modeling studies to thoroughly compare the costs and benefits of syphilis vaccine development to those of enhanced, targeted screening and treatment programs [14]. Thus, the primary question that we address in this study is the epidemiological impact of a potential syphilis vaccine on sexual and vertical transmission of both syphilis and HIV and compare it against a "screen and treat" program. We consider heterosexual populations in resource-poor settings using simulations from a realistic epidemiological model.

3.3 Methods

Epidemiological dynamics of STIs are challenging to fathom: they involve demographics (birth and death rates), sexual behaviour (partnership formation and dissolutions), natural history of disease and potential interactions with other diseases, and population stratification (risk groups, gender). We developed an agent-based model for this purpose. We hypothesized that syphilis vaccination may have indirect effects on the epidemiology of other STIs, so we chose to model HIV spread along with syphilis because of its high morbidity and co-infection data availability compared to other STIs. In this section, we highlight the main features of the agent-based model. The full technical description of the agent-based model is available in appendix B. Our agent-based model simulates the partnerships and disease-transmission dynamics of a heterosexual population, along with the natural history of both syphilis and HIV, and their interactions. Individuals enter the modelled population at age 12. The general population is stratified, for life, into three sexual risk groups (low, medium and high risk); additionally, females can move in and out of a commercial sex work (CSW) group. The contact pattern for STI transmission is driven by partnership formation and dissolution and a rate of sex acts. Individuals can have multiple concurrent partners, and some partnerships are identified as "spousal" (more stable). The decision to form or dissolve any partnership is based on age, age gap with the partner, current number of partners, symptomatic status of potential STI infections and risk group. Partnerships and sex acts rates can change at each time step. The number and type (with or without condom, low or high transmission risk) of sex acts are distributed randomly, with rates based on age, spousal status, number of concurrent partners, symptomatic status and risk group.

Probabilities of transmission per sex act are specified for both syphilis and HIV, and depend on the age of infection in the infected partner. Individuals with one STI may be more susceptible to acquiring the other, and co-infected individuals may have increased infectiousness of one or both diseases. Infected individuals can be treated; their adherence to treatment depends on their risk group and probability of success is pre-specified for each STI.

We construct, in our agent-based model, three synthetic populations intended to match representative scenarios of syphilis and HIV prevalence in sub-Saharan Africa (Figure 3.1); we do not attempt to represent any specific country. The synthetic populations are exclusively heterosexual and the female-to-male ratio is close to one.

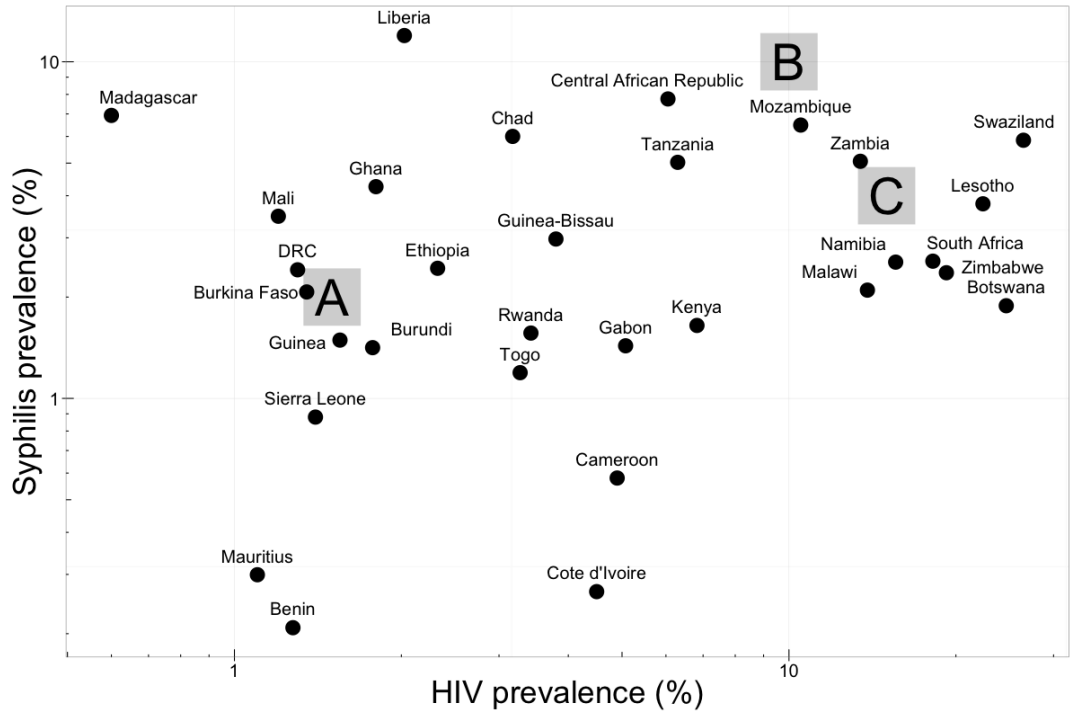

Figure 3.1. *Solid circles are HIV and syphilis prevalence for various countries in sub-Saharan Africa. (Source: WHO; prevalence was averaged over available reports ranging between 2001 and 2013). Grey squares are the prevalence chosen for synthetic populations A, B and C.*

Demographic and behavioural characteristics of synthetic populations are based on data from the Demographic Health Surveys across sub-Saharan Africa. STI prevalence and incidence at the population level are fitted by adjusting the baseline treatment rate for each STI, partnership rates and risk-group proportions.

For each synthetic population, we run 30 Monte Carlo iterations to evaluate the epidemiological impact of a hypothetical syphilis vaccination program compared to symptomatic treatment only. Starting from an initial population of 1250 individuals, the model is run without any STI for 50 years with a coarse time step of 30 days in order to reach equilibrium with the partnerships dynamics. By the end of this "partnership calibration" phase, the synthetic population has a size of 3000 individuals. Then, both syphilis and HIV are introduced at a different level for each risk group, and the model is run for 30 more years with a time step of 5 days (the "disease calibration" phase).

After the calibration phases, the model is run for an additional 20 years with no changes to provide a "baseline" scenario. We check the calibration steps by confirming that prevalence of syphilis and HIV remain relatively stable throughout this time period. Intervention scenarios are run in exactly the same way as the baseline scenario, except that interventions (increased treatment and/or vaccination programs) are introduced after 30 years. Hence, intervention scenarios and baseline only differ between year 30 and 50 (Figure 3.2).

We assume that susceptibility to HIV is increased about 2.5 times during syphilis infection [45, 87, 91]. To our knowledge, there is little evidence regarding the epidemiological effect of HIV infection on syphilis susceptibility [87]; we assume a 1.5 times increase in our main simulations (sensitivity analysis explored values of 1.0 and 2.5). We assume that HIV infectiousness increases up to 50% of its maximum possible level (reached during the acute phase) during a syphilis co-infection [15, 62]. Since evidence that HIV can increase syphilis infectiousness is weak, our model does not change syphilis infectiousness when there is a HIV co-infection. Mother-to-child transmission of syphilis depends on the timing of pregnancy during syphilis infection, highest when pregnancy occurs early post-infection. We model syphilis MTCT probability with a logistic shape starting at 90% and decreasing to 0 as the duration of syphilis infection increases (appendix B). The probability of vertical HIV transmission is assumed constant throughout HIV infection and is set at 25%. Baseline treatment intervention for both HIV and syphilis in simulated population A (respectively B; C) is defined by treating HIV infections at a rate of 25% (respectively 15%, 10%) per year and symptomatic syphilis infections at a rate 25% (respectively 1%, 60%) per year. We consider four syphilis intervention scenarios (Table 3.1). The first (labelled "TrMass") increases the baseline treatment level: every year, on top of the baseline value, an additional 30% proportion of individuals infected with syphilis, symptomatic or not,

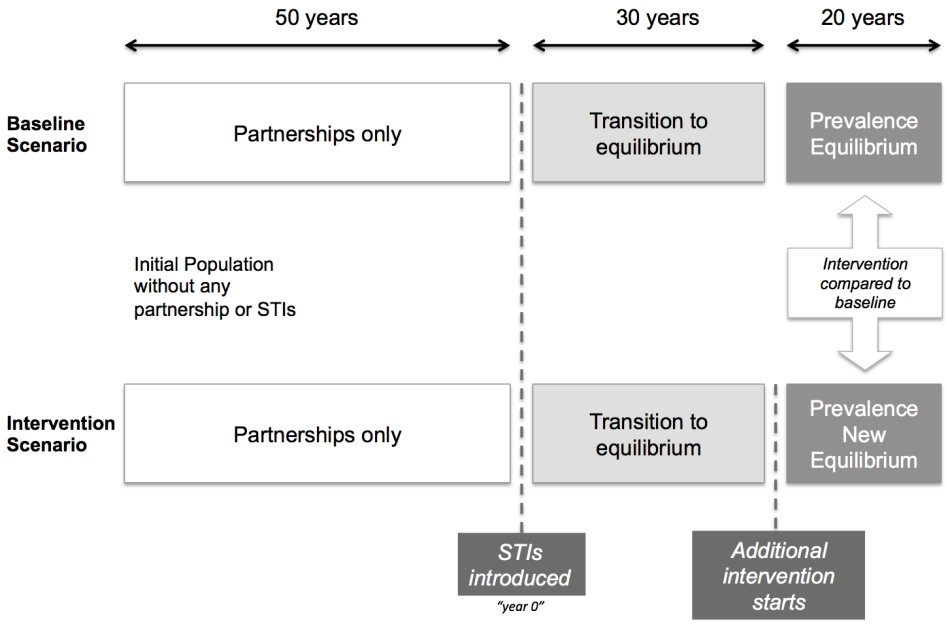

Figure 3.2. Simulation steps. *The model is first run with no STI for 50 years in order to reach a steady state in partnership dynamics. Then STIs are introduced and prevalences reach stable values after running the simulation for 30 years. Finally, interventions are introduced and evaluated over a 20-year period.*

are treated. The three other interventions involve a vaccine that is provided to: i) the whole population at a coverage rate of 10% per annum ("VaxMass"), ii) high-risk group individuals and sex worker only at a coverage of 20% per annum ("VaxHiRisk") and iii) women younger than 18 years-old only, at a coverage rate of 80% per annum ("VaxYoung").

Table 3.1. *Modelled syphilis intervention*

Intervention	**Label**	**Description**
Increased Mass Treatment	TrMass	Increase baseline mass treatment for syphilis by an additional 30% per annum
Vaccination Mass	VaxMass	All sexually active individuals are vaccinated at a rate of 10% per annum
Vaccination High-Risk Group	VaxHiRisk	Individuals in the highest risk group are vaccinated at a rate of 20% per annum
Vaccination Young Women	VaxYoung	Women 18 years old and younger are vaccinated at a rate of 80% per annum

We assume that the failure probability of our hypothetical vaccine is 20% (so that 80% of the population is perfectly protected right after vaccination); values of 0% and 50% were considered in a sensitivity analysis. Vaccine efficacy can wane over time [100], so we assume the modelled syphilis vaccine effectiveness wanes exponentially at a rate of 5% per year (corresponding to 50% loss of effectiveness after 14 years). A sensitivity analysis explored a non-waning vaccine and a rapidly waning one (rate at 70% per year). In the baseline scenario, the vaccine does not provide any infectiousness reduction, but a sensitivity analysis was performed assuming a 50% infectiousness reduction when vaccinated.

We measure the impact of the intervention scenarios described above on both prevalence and the vertical transmission of HIV and syphilis, during the 20 years of intervention.

3.4 Results

Within each of the three synthetic populations (A, B and C), the five scenarios (baseline and four additional interventions) were run and compared. The results for final STI prevalences and MTCT rates are summarized in Figure 3.3.

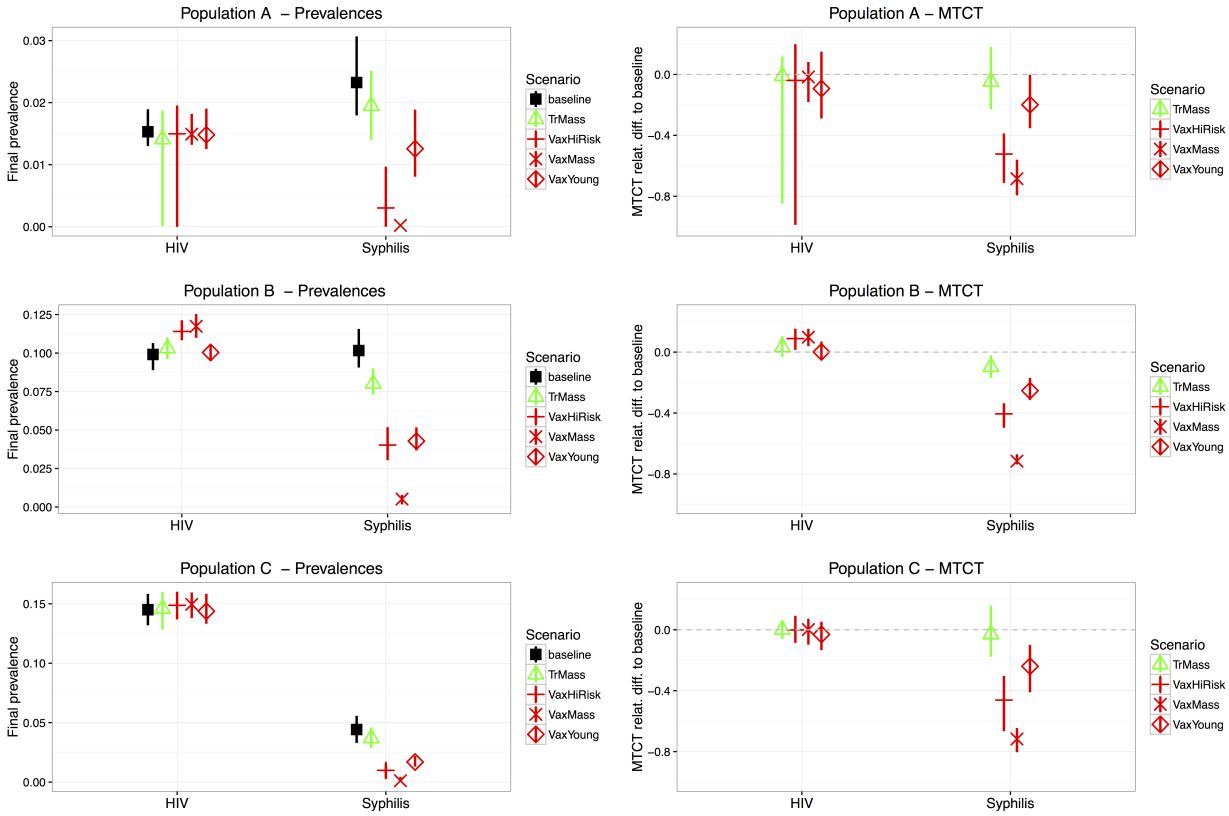

Figure 3.3. Comparing intervention scenarios. *The solid shape represents the median value and the vertical segment the 10-90% quantile range. Panels on the left-hand side show final prevalence of HIV and syphilis for all modeled interventions in the three synthetic populations. Prevalence is calculated after 20 years of intervention. Right-hand side panels show the relative difference of cumulative mother-to-child syphilis transmission compared to the baseline scenario (horizontal dashed line at 0).*

Overall, for all synthetic populations, the most successful intervention to reduce syphilis prevalence is mass vaccination ("VaxMass"): all simulations show extremely low levels of prevalence after 20 years. Indeed, in this intervention scenario, the median syphilis prevalence is reduced to less than 0.01% in all three synthetic populations. Vaccinating the high-risk population ("VaxHiRisk") and

targeting young females only ("VaxYoung") also leads to significant reduction in overall syphilis prevalence. Increasing coverage for syphilis treatment ("Tr-Mass") reduces overall syphilis prevalence much less (Figure 3.3 and appendix C). MTCT of syphilis is also reduced significantly over the 20 years intervention period especially with the mass and high-risk vaccination strategies (Figure 3.3 and appendix C).

HIV prevalence is not affected in populations A and C, and slightly increases in population B during the vaccination interventions targeting the general population ("VaxMass") and high risk groups ("HiRisk"). The changes in HIV vertical transmission mirror the ones observed for the prevalence (Figure 3.3 and appendix C).

The results from the sensitivity analysis (described in the Methods section) do not substantially change the qualitative conclusion drawn from the central scenarios (see suppl. file 3).

3.5 Discussion

The effect of a hypothetical syphilis vaccine on the burden of syphilis disease, in particular its congenital form, is expected to be large. The potential effect on HIV is less straightforward. We used an agent-based model to simulate the horizontal and vertical spread of both syphilis and HIV in various syphilis vaccination scenarios 20 years after their introduction. We modelled synthetic populations representative of settings found in sub-Saharan Africa. As expected, we found that a hypothetical syphilis vaccine could eliminate or dramatically reduce incidence of congenital and sexually acquired syphilis when vaccination strategies target the whole population (mass vaccination) or focused on high-risk groups. We found that targeting young females was much less effective over the studied time horizon of 20 years, because the older cohorts that are not eligible for vaccination continue to spread infections over many years. Given that both syphilis and HIV are suspected to increase the transmission of the other through various mechanisms, we hypothesized that a syphilis vaccine might indirectly reduce HIV incidence. However, in our modelling framework, we found that HIV was largely unaffected by syphilis vaccination, except that in the high syphilis-prevalence population (B) experienced a small increase in HIV transmission. This is because symptomatic syphilis infections in our model are associated with reduced sexual

activity: thus, reducing syphilis will lead to an increase in sexual activity, particularly among high-risk groups. This effect is noticeable when a large proportion of individuals are involved in risky sexual behaviour and syphilis prevalence is high.

This predicted effect from our simulations is similar to an observed phenomenon, with syphilis and HIV exchanging roles. Syphilis and other STIs have increased in many populations since an effective HIV antiretroviral therapy became available early 2000s (documented especially among MSM in western countries, see [22] for example). A possible cause for this increase could be a lower perceived risk of HIV leading to increased sexual exposure. Hence, if a syphilis vaccine is developed, vaccination programs should be accompanied with intensified interventions on transmission of other STIs.

Another real life example that can relate to our simulation results is the impact of the HIV epidemic on various large clinical trials targeting curable STIs. Most of these trials did not show a significant reduction in HIV incidence in the treated arm. General and trial-specific interpretations to these unexpected outcomes have been proposed [51]. Here, our study suggests another possible mechanism: if intensity of sexual activity is affected by (symptomatic) STI episodes, curing some STIs could increase sexual activity, and thus increase incidence of non-treated STIs.

Our simulations also suggest that high HIV prevalence does not hamper syphilis vaccination programs at the population level. This result is robust to vaccine failure at 50% (see sensitivity analysis in suppl. file 3). Because of a lack of data quantifying a potential effect, we did not explicitly model the possibility that HIV infection increases syphilis vaccine failure. Our study has several limitations. Our results are based on synthetic populations, so their practical translation to real communities may not be straightforward. However, we chose the demographic and behavioural characteristics of the three synthetic populations to be similar to what can be found across sub-Saharan Africa, so we expect some relevance when applied to real communities in resource-limited countries. Our model does not account for birth control or abortion, which may not be realistic especially in high-risk groups. This can have the effect of skewing overall STI vertical transmission to larger values. We therefore chose to present vertical transmission in relative rather than absolute terms in Figure 3.3. In summary, our results suggest that a syphilis vaccine has the potential, over a 20 years horizon, to eradicate horizontal and vertical transmission of this disease in populations with various lev-

els of baseline syphilis and HIV prevalence and risk behaviours, while expanded treatment interventions are likely to be substantially less effective. Vaccination programs targeting the whole population and/or high-risk groups achieve significantly better incidence reduction than when targeted at young women only. Our results also highlight that syphilis vaccination programs should be accompanied with intensified interventions on other STIs in order to prevent possible incidence rebounds caused by decreased symptoms, or lower perceived risk, following syphilis vaccination.

Appendix B

B.1 Introduction and Summary

This documentation describes the implementation of a stochastic individual based epidemiological model that studies specifically sexually transmitted infections (STIs). A particular aim of this model is its ability to simulate epidemics of several concomitant STIs. This section gives an overview of the main features of the model, without giving any technical details.

This model attempts to represent fairly realistically three dynamics:

- **Demography:** Some sexually transmitted infections (e.g., HIV, HSV2, Syphilis) have an infectious period that lasts years if not decades. So, unlike other diseases (e.g., influenza) where the demographic changes over the epidemic period could be neglected, here it is important to have a good representation of the ageing processes of the population (growth rates but also age distribution). Individuals are simulated from the age of sexual debut (for example 12 years old) to an age where sexual activity is very unlikely ('maximum age', for example 80 years old). The 'birth' process is a consequence of sexual activity. Death can occur naturally or can be disease induced (both distributed as Weibull). When an individual reaches the maximum age (80 years), death is provoked.
- **Sexual activity:** The contact pattern for STI transmission is driven by partnership formation/dissolution and the rate of sex acts. Individuals can have multiple concurrent partners. Spousal partnerships are also modelled: they are a non-negligible fraction of all partnerships and their formation/dissolution process is distinctive from casual ones. The decision

to form or dissolve any partnership is based on stochastic events following rules based on age, current number of partners, symptomatic status of potential STI infections and risk group. There are three risk groups for the general population: low, medium and high-risk. Individuals belonging to a given risk group will be assigned representative parameter values associated with their risk behavior (e.g., use of condom, number of concurrent partners, partner switch rates, etc.). High activity commercial sex workers (engaging with multiple partners in a very short period of time) form a fourth distinct risk group with a specific partnership formation process. The rate and type of sex acts are distributed randomly based on several variables (*e.g.*,, age, spousal status, number of concurrent partners, symptomatic status, etc.).

- **Disease transmission:** Once the network of partnership is built following the demographic and partnerships processes, diseases can spread through the population. STIs have very different infectious features: probability of transmission per sex act, infectious period and recurrence frequency can vary of orders of magnitudes. Hence, each STI is represented with its own infectivity curve (probability of transmission with respect to time). There are adjusting coefficients on the level of the infectivity curve simulating a potential increase in infectiousness from an individual infected with another STIs. Likewise, susceptibility to STIs varies with potential co-infections.

The simulations are run in three steps. First, a simulation starts from an initial population with no partnerships and the model runs for a long enough time (typically 50 years with a coarse time step of a month) to match target levels on demography (for example growth rate and age distribution) and partnerships (fraction of single individuals, fraction of spousal partnerships). This is the pre-epidemic era where the model should reach its equilibrium values.

The second step introduces STIs in the population. The model is run for a long enough with a fine time step (typically of the order of a day), in order to have a good fit with target prevalences of the epidemic era.

The third step is the analysis and/or prediction. Simulations are run with intervention strategies and/or introduction of a new STI.

There is no migration in or out the population (apart from recruitment of commercial sex workers).

The model is implemented in C++ and wrapped in a R library. Computing power is critical when the population is large and the time horizon long (typically more than 10,000 individuals for more than 10 years with a time step shorter than a week), so a basic parallel implementation is used.

For the reader interested in looking into the C++ and R computer codes, it is available here: `https://github.com/davidchampredon/stiagent`.

B.2 Individuals, Population and STI objects

It is important to note there are three main classes of C++ objects: `Individual`, `Population` and `STI`. In this individual-based model, a distinction is made between attributes at the 'atomic' individual (i.e., age) and the ones that belong to the population (i.e., maximum partnership formation rate).

An individual is mainly characterized by biological and social features (this is *not* an exhaustive list):

- biological: gender, age, STI infections, ...
- social: risk group, number of partnerships, marital status, ...

A population is characterized by a vector of individuals, a vector of STIs and other scalar parameters (like, for example, the maximum rate of partnership formation).

STIs objects describe the key features of the natural history of the infection. It is independent of individuals or populations.

B.3 Demographics

B.3.1 Birth

After every sexual contact, the chance a female gets pregnant is determined by a Bernoulli random variable and its probability (becoming pregnant per sex act) is a model parameter. All new borns and their potential acquired infection are

recorded (so that we can keep track of MTCT incidence in a simulation). Children between birth and minimum age of sexual activity are not modelled. Young individuals just turning the minimum age of sexual activity enter randomly the population. The expected rate of arrival is

$$\alpha = \text{birthRate} \times (1 - m_{\text{infant}})(1 - m_{\text{child}})^4 (1 - m_{\text{child}}/2)^{n_{min}-5}$$

with m_{infant} the mortality rate of infant (< 1 year-old), m_{child} the mortality rate of children < 5 years-old and n_{min} the minimum age of sexual activity (it is assumed the mortality rate for children between 5 and n_{min} is half).

Then, the number N of youth (aged n_{min} years-old) arrivals during a given period of time dt, for a population of size T, is:

$$N \sim \text{Poisson}(\alpha\, T\, dt)$$

B.3.2 Death

The classical methodology of survival analysis is applied here. The probability of dying between this time step and the previous one is assessed for every individual, at every time step. The probability driving this process is based on

$$\Pr(t < T_{\text{death}} < t + dt \mid T_{\text{death}} \geq t) = \frac{F(t + dt) - F(t)}{1 - F(t)}$$

where T_{death} is the time of death and F its cumulative distribution function. It is assumed that the survival time is Weibull distributed, so the associated hazard function h is given by

$$\begin{aligned} h(t) &= \lim_{dt \to 0} \Pr(t < T_{\text{death}} < t + dt \mid T_{\text{death}} \geq t)/dt & \text{(B.1)} \\ &= k\lambda(\lambda t)^{k-1} & \text{(B.2)} \end{aligned}$$

for $k > 0$ and $\lambda > 0$ the standard Weibull shape and scale parameters, and t the age of the individual.

If t_{HIV} is the time when the individual was infected with HIV, the hazard function changes and is now parameterized with new shape and scale parameters, and

duration since infection instead of age:

$$h_{HIV}(t) = k'\lambda'(\lambda'(t - t_{HIV}))^{k'-1}$$

This probability has to be evaluated at every time step, for every individuals (for example, if HIV treatment is initiated, the associated hazard will decrease). An example of a plot of this hazard function is illustrated in Figure B.1.

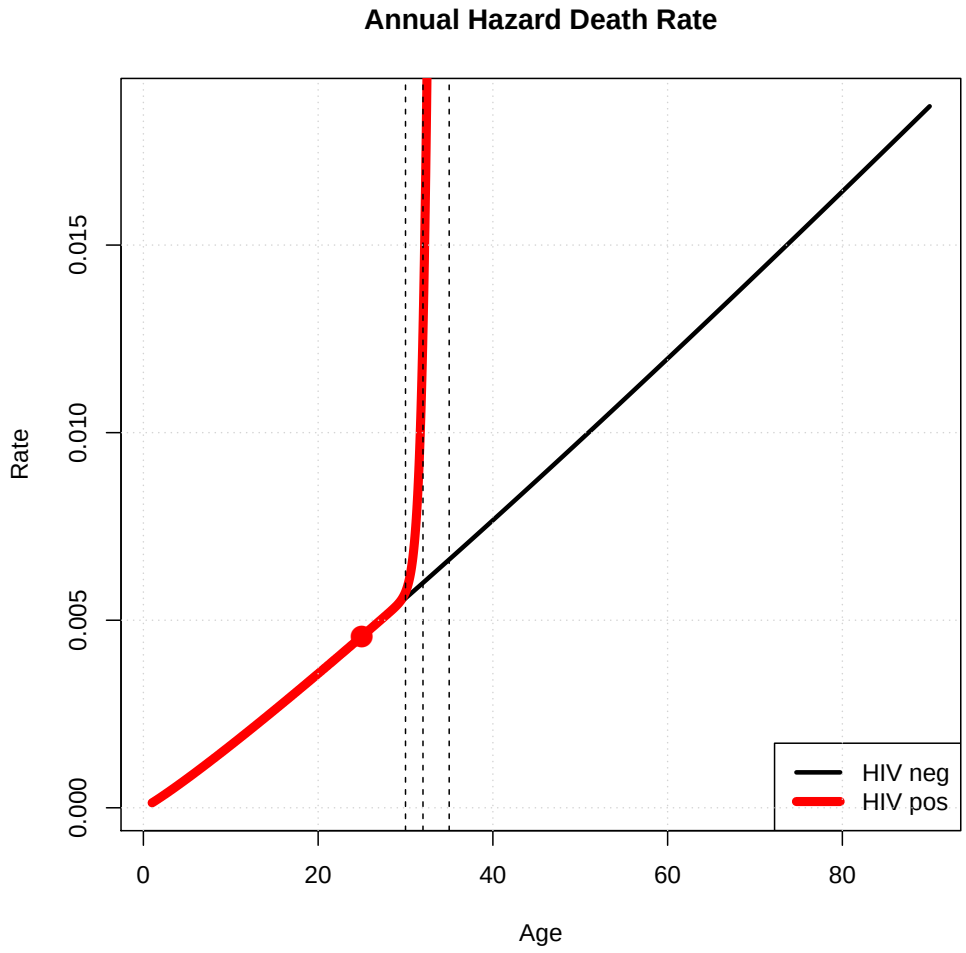

Figure B.1. *Death hazard. The red dot represents the age of HIV acquisition. Vertical dashed lines are set at 5, 7 and 10 years after HIV acquisition.*

B.4 Partnerships

B.4.1 Partnerships formation

Let's define r^* the maximum annual rate of consideration to form partnership and F (resp. M) the population size of females (resp. males) with a partnership deficit. A partnership deficit is defined, for a given individual, as the maximum possible partnerships minus the number of concurrent partnerships. The unit of r^* is time^{-1}.

Females and males who do not have a partnership deficit are - by definition - not available to form new partnerships, hence are ignored right from the start of the formation process.

It is assumed that the maximum number of partnership formations during a unit time period is given by [37]

$$P^* = r^* \frac{FM}{F+M}$$

For sake of clarity, if we assume that every consideration will lead to a partnership formation and note P the total number of partnerships, we have:

$$\begin{aligned}
\frac{dF}{dt} &= -r^* \frac{FM}{F+M} = -\left(r^* \frac{M}{F+M}\right) F = -r_f^* F \\
\frac{dM}{dt} &= -r^* \frac{FM}{F+M} = -\left(r^* \frac{F}{F+M}\right) M = -r_m^* M \\
\frac{dP}{dt} &= \frac{1}{2} 2r^* \frac{FM}{F+M} = r^* \frac{FM}{F+M}
\end{aligned}$$

Hence, r_f^* is interpreted as the rate of partnership formation when female dominance is assumed. The formulation is symmetrical if male dominance is assumed, so we'll assume female dominance.

Formation algorithm

The partnership formation process is stochastic and driven by the algorithm below.

1. Calculate $F^* \sim \text{Binomial}(r_f^* \, dt, F)$, the maximum number of females candidate for partnership formation during the period dt
2. Pick randomly F^* females among the F available females. Collect and store their positions in the population in the set $\mathcal{S}_f$.
3. For each female in $\mathcal{S}_f$, pick randomly an available male
4. Draw the binary random variable Φ that determines if this pair will form a partnership ($\Phi = 1$ means formation success). See B.4.1 for the distribution of Φ.
5. If formation success on this pair ($\Phi = 1$), then form partnership[1]. Else, do nothing.
6. This female is removed from the pool of partnership candidates (whether formation was successful or not): update $\mathcal{S}_f$ accordingly by deleting her position.
7. If $|\mathcal{S}_f| > 0$, go to step 3; else stop.

Formation success random variable (Φ)

Given two candidate individuals, I_m (male) and I_f (female), the success of formation is determined by the binary random variable $\Phi \sim \text{Bernoulli}(p)$. When $\Phi = 1$, the two candidates do form a partnership.

The probability of success to form the partnership depends on several tests on variables from both individuals (age, risk group, etc). Hence, it is assumed the probability of a successful partnership formation between the two candidates is given by

$$\Pr(\Phi = 1) = f_{age} \, f_{risk} \, f_{deficit} \, f_{STI} \tag{B.3}$$

where all functions f are valued in the interval $[0; 1]$ and are defined hereafter.

- **Age.** The age A of an individual determines its attractiveness to the opposite sex. The age gap between the candidate male and female is defined as $G = A_m - A_f$. Then, the age component of the rate of couple formation is assumed to depend on the age and marital status of the female, and the age gap with the candidate male:

[1] `Population.formPartnership(i,j)` is called

$$f_{age} = \varphi(A_f, G)$$

The function φ describes the joint distribution of the female age (a) and age gap (g):

$$\varphi(a, g) = e^{-s_{age} X^T M^{-1} X}$$

with $X = (a - \bar{a}, g - \bar{g})^T$ the (centred) vector for female age and age gap, $\bar{a}$ (resp. $\bar{g}$) the average age (resp. age gap) at partnership formation, s_{age} a shape parameter, and M the covariance matrix

$$M = \begin{pmatrix} \sigma_a^2 & \rho\sigma_a\sigma_g \\ \rho\sigma_a\sigma_g & \sigma_g^2 \end{pmatrix}$$

Parameters σ represents the variance of the ad-hoc variable and ρ the correlation between female age and age gap, and can be calibrated on DHS data.

- **Risk group.** Both candidate individuals belong to a risk group, r_m and $r_f \in \{0, 1, ..., r^*\}$, where r^* is the highest risk group. The candidate couple's risk score is $r_f + r_m$. The probability component regarding the risk group is

$$f_{risk}(r_f, r_m) = e^{-s_0^{risk}(2r^* - (r_f + r_m)) - s_1^{risk}(r_f - r_m)^2}$$

where s_0^{risk} and s_1^{risk} are shape parameters that should be fitted globally (no specific data). Note that when both partner belong to highest risk group ($r_f = r_m = r^*$), then $f_{risk} = 1$ and when both belong to the lowest $f_{risk} = e^{-2r^* s_0^{risk}}$.

- **Partnerships deficit.** Define n_f as the number of concurrent partnerships for the candidate female considered, n_f^* her maximum number of partnerships, $d_f = n_f^* - n_f$ the deficit number of partnerships and deficit ratio $D_f = d_f / n_f^*$. Same notations for males. The probability component regarding the partnership deficit is

$$f_{deficit}(n_f, n_f^*, n_m, n_m^*) = (D_f D_m)^q$$

with $q \geq 1$ a parameter to calibrate globally.

- **STI infection.** If an individual has a symptomatic STI infection, the likeli-

hood to form a partnership is reduced. Symptoms can be painful, reducing the willingness to engage in a sexual contact. Symptoms can be visible (especially in males), reducing the attractiveness of a sexual contact. Define $s_f \in \{0, 1\}$ the variable signalling a symptomatic infection with *any* STI within the candidate female partner, and $\alpha_{sympt,f}$ the relative reduction of the probability that a partnership can be formed in the presence of these symptoms. Same notations for males. Values for parameters α_{sympt} will have to be assumed (not calibrated).

Note: Repulsion of STI symptoms may not be the same for all STIs in reality. This feature can be considered for a future development.

The probability component regarding the STI infection is

$$f_{STI}(s_f, s_m) = \left(\alpha_{sympt,f}\mathbf{1}_{s_f=1} + \mathbf{1}_{s_f=0}\right)\left(\alpha_{sympt,m}\mathbf{1}_{s_m=1} + \mathbf{1}_{s_m=0}\right)$$

where the product is over all STIs modelled.

B.4.2 Spousal union

A spousal union is defined as a partnership that has been celebrated under the civil or religious law. The reason to model this special partnership is to reflect the facts that such a relationship is likely to have a higher sexual intercourses frequency and is more difficult to dissolve because of social pressures.

Determinants

It is assumed that all partnerships starts as casual relationships that can evolve as a spousal union. At every time steps, based on several parameters (described hereafter) all the partnerships a male has are re-assessed to become a spousal union[2].

The spousal progression rate is assumed to be driven by the age of the female (A_f), her age gap G with the potential husband, her current marital status m, the number n of existing wives the male already has, the difference between the age

[2]This can be a limitation in the context of arranged marriage where the partnership starts as a spousal one right from the start (no prenuptial period). To mitigate this limitation, the rate of spousal union can be very high such that spousal determination occurs almost instantaneously.

gap G and the ones of existing wives (if any), and finally the duration of this casual partnership.

The rate of spousal union formation, noted S, is assumed to have the following functional form:

$$S(A_f, G, \tau, m) = B.\left[\mathbf{1}_{n=0} + K\,\mathbf{1}_{1\leq n<n_{max}}\right].d(\tau).sp^* \tag{B.4}$$

With sp^* the maximum rate of spousal progression. Functions B, K and τ are define hereafter.

Age and age gap
Function B represents the probability the spousal transition is successful based on the female's age, age gap and her current marital status m:

$$B = s(A_f, G)$$

$$s(A_f, G) = \mathcal{N}(A_f, \bar{A}_f, \sigma_{A_f})\,\mathcal{N}(G, \bar{G}, \sigma_G)$$

where $\bar{A}_f$ (resp. $\bar{G}$) is the average age (resp. age gap) of a female entering her first union, and $\mathcal{N}(x, m, \sigma) = \exp(-(x-m)^2/2\sigma^2)$ If the female is already in a spousal union, then she cannot be considered to be a spouse of another man (polygynous population).

Note: Future development will consider other shapes for $\mathcal{N}$, as DHS data do not fully support the one chosen.

Gaps with other spouses
Function K reflects the fact that if a female enters an existing polygynous union, the age gap with the new comer (G) is more likely to be larger than with existing wives ($G_1, ..., G_n$):

$$K = K(G_1, ..., G_n, G) = e^{-(\Delta-\bar{\Delta})^2/2\sigma_\Delta^2}$$

$$\Delta = \min(G_1, ..., G_n) - G$$

Duration of partnership
It is assumed the rate of progression to a spousal union changes with the duration

of this partnership τ, and is represented by the function d:

$$d(\tau) = \mathcal{N}(\tau, k_1, k_2)$$

with k_1 (average partnership duration when spousal progression occurs) and k_2 (variance) constants to be fitted globally.

Summary of all spousal progression parameters:

- n the number of existing spouse(s) this male currently has, and n_{max} the maximum number of spouses this male can ever have
- τ the duration of this partnership
- $d(\tau)$ represents the probability of spousal conversion with respect to duration of this partnership
- m the current marital status ("never coupled (nc)", "uncoupled separated (us)") of the *female*
- $\Delta = \min(G_1, ..., G_n) - G$ the difference of age gaps between the youngest existing wife and the candidate wife; its mean is noted $\bar{\Delta}$ and its variance σ_Δ. Both can be calibrated on DHS data

Algorithm

At each time steps:

1. Select one male with at least one casual partnership
2. Loop on all casual partnerships
3. Calculate S_i, the rate of spousal progression of the i^{th} casual partnership, using Equation (B.4)
4. Draw the Bernoulli random variable $\mathcal{S}$ with rate S_i. If $\mathcal{S} = 1$, then upgrade this casual partnership to a spousal union; else do nothing
5. Go to step 1 until all males with at least one casual partnership have been scanned

B.4.3 Partnerships dissolution

Dissolutions of partnerships follows the same idea as their formation. A maximum annual rate of dissolution per partnership, δ^* (unit is time^{-1}), is assumed for the whole population. The total number of partnerships is noted P. This gives a maximum number of candidate partnerships for dissolution. If all dissolution considered would actually dissolve the partnerships, the evolution of the number of partnerships would be given by $P' = -\delta^* P$. However, the success of dissolution will be determined by the characteristics of both individuals forming this partnership.

Dissolution algorithm

The dissolution process is described by the following stochastic algorithm.

1. Calculate $P^* \sim \text{Binom}(\delta^* dt, P)$ the maximum number of partnerships considered for dissolution during the period dt
2. For each partnership, draw the binary random variable Ψ that determines if this partnership will be successfully terminated. See B.4.3 for the distribution of Ψ.
3. If dissolution is successful ($\Psi = 1$), then dissolve this partnership. Else do nothing.
4. If at least one partnership candidate for dissolution remains, go to step 2; else stop.

Dissolution success random variable (Ψ)

Given a candidate partnership composed of two individuals, I_m (male) and I_f (female), the success of dissolution is determined by the binary random variable $\Psi \in \{0, 1\}$. When $\Psi = 1$, this candidate partnership is dissolved. The Bernoulli probability for Ψ is function of several variables, described below.

- **Spouse.** Dissolving a spousal partnership is less likely because of social pressures. Define the binary variable s indicating if this partnership is a

spousal one. The probability component regarding spousal relationship is

$$g_{spouse}(s) = \epsilon \mathbf{1}_{s=1} + \mathbf{1}_{s=0}$$

with $0 < \epsilon < 1$ a parameter to calibrate globally.

- **Relationship duration.** Define d the duration of the candidate partnership. It is assumed that short partnerships are more likely to dissolve than the ones that have survived for a longer time. The probability component regarding relationship duration is

$$g_{duration}(d) = dur_1 + dur_2\, e^{-dur_3\, d}$$

with $0 < dur_1, dur_2 < 1$ and $dur_3 > 0$ parameters to be fitted globally.
Note $dur_1 + dur_2$ is the probability of dissolution just after a time unit (e.g. one day), hence this models a "one-off" contact.

- **Partnerships deficit** The probability this partnership dissolves is assumed to be decreasing as the partnership deficit of both members increases. Define n_f as the number of concurrent partnerships for the female, n_f^* her maximum number of partnerships, $d_f = n_f^* - n_f$ the deficit number of partnerships and deficit ratio $D_f = d_f/n_f^*$. Same notations for males. The probability component regarding the partnership deficit is

$$g_{deficit}(n_f, n_f^*, n_m, n_m^*) = q_{min} + (1 - q_{min})((1 - D_f)(1 - D_m))^q$$

with $q \geq 1$ a shape parameter and q_{min} the minimum contribution of this component.

- **Risk group.** Both candidate individuals belong to a risk group, r_m and $r_f \in \{0, 1, ..., r^*\}$, where r^* is the highest risk group. The candidate couple's risk score is $r_f + r_m$. The probability component regarding the risk group is

$$g_{risk}(r_f, r_m) = e^{(r_m + r_f - 2r^*)drsk_1}$$

with $drsk_1$. This parameter should be fitted globally (no specific data).

- **Age.** Define A_f and A_m the age of the female and male in the partnership candidate for dissolution. The probability to dissolve the couple is assumed to decrease with the "couple age" $A_f + A_m$ and also depends on the age gap.

The probability component regarding ages in this relationship is

$$g_{age}(A_f, A_m) = e^{-(A_f + A_m - \text{dage}_1)^2/\text{dage}_2}$$

with dage_1 is the average couple age where dissolution risk is maximum and dage_2 its variation. These parameters are fitted globally.

- **STI symptoms.** If one of the member of the candidate partnership has a symptomatic STI, this can increase the risk of terminating this partnership. Define $s \in \{0, 1\}$ the variable signalling a symptomatic infection in a given partnership and $0 < d_{sympt} < 1$ the relative reduction of the probability to dissolve in the abscence of these symptoms. The probability component regarding the STI infection is

$$g_{STI}(s) = \mathbf{1}_{s=1} + d_{sympt}\mathbf{1}_{s=0}$$

Note: Some STIs may exhibit more 'repulsive' symptoms, but for now treat all STIs the same way.

Similarly as with the formation process, putting everything together, the probability of a successful partnership dissolution is

$$\Pr(\Psi = 1) = g_{spouse}\, g_{age}\, g_{risk}\, g_{duration}\, g_{deficit}\, g_{STI} \tag{B.5}$$

B.4.4 Number of concurrent partners

The maximum number of concurrent partners, n, is determined for each individual, based on its risk group. It is assumed to have a geometric distribution:

$$n \sim \text{Geom}(p)$$

$$p = c_1 e^{-c_2 r}$$

with c_1 and c_2 gender-dependant shape parameters, and r the risk group of the individual.

B.5 Sexual intercourses

The rate of sexual intercourses in a partnership is assumed to be driven by the male. Although females can have some negotiating power regarding partnership formation and continuation, they seem less able to control sexual practices once in a partnership [74].

Following how partnerships are modelled, there are three categories of sex partners:

- Spouses
- Casual partners
- Sex workers

Three types of sex acts are modelled here:

- sex act with condom
- sex act without condom, "low risk" practices (i.e. vaginal) that do not increase the risk of HIV or STI transmission
- sex act without condom, "high risk" practices (i.e. anal, dry-sex) that increase the risk of HIV or STI transmission

A male will have a specified number of sex acts during a period of time. The model will distribute these sex acts between all different partners and assign them the type of sex act, based on binomial distributions. This is described hereafter.

B.5.1 Total number of sex acts

A male has a rate of sexual intercourses with *any* partners (spousal, casual or sex worker) noted R_{sex} and the actual total number of intercourses performed by this male, N, during a period dt is distributed with a Poisson distribution:

$$N \sim \text{Poisson}(R_{sex}\, dt)$$

The rate R_{sex} is set at a starting value, R_{sex}^{max}, the maximum rate of sexual intercourses for any male (think of it as a biological limit). Then, this rate is reduced

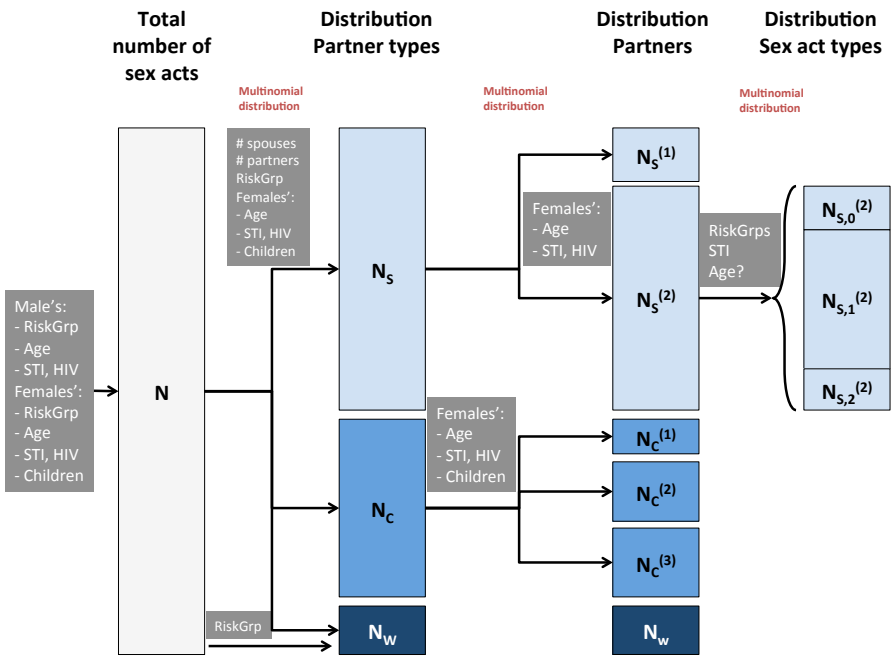

Figure B.2. *Distribution of number and type of sex acts among partners*

by a factor R_M depending on the male's features and another factor R_F depending on his partners' features:

$$R_{sex} = R_{sex}^{max} \times R_M \times R_F$$

Factor R_M depends on the male's age A_m, his risk group r, if he has symptoms of any STI (binary variable $s = 0$ if no symptoms), the total number of partners n. The functional form is defined as:

$$R_M = h_{age}(A_m)\, h_{risk}(r)\, h_{STI}(s)\, h_{nPartn}(n)$$

Similarly, R_F is defined as

$$R_F = h_{age}(\bar{A}_f)\, h_{risk}(\bar{r})\, h_{STI}(\bar{s})$$

where $\bar{A}_f$ is the average age of all male's partners, and similar notation for other variables.

Then, we define each function h corresponding to the associated determinant.

$$h_{age}(a) = \exp\left(-\left(\frac{a - a_{peak}}{\sigma_{age}}\right)^q\right)$$

with a_{peak} the mean age of peak sexual activity (at the population level) and σ_{age} and q shape parameters. These parameter may have to be assumed if no relevant data set found.

$$h_{risk}(r) = (1 - \epsilon_{risk})\frac{r}{r^*} + \epsilon_{risk}$$

with r^* the maximum risk group and ϵ_{risk} representing the fraction of sex acts a male in the lowest risk group has compared to the highest one.

$$h_{STI}(s) = \begin{cases} \epsilon_{STI} & \text{if } s = 1 \\ 1 & \text{if } s = 0 \end{cases}$$

with ϵ_{STI} representing the fraction of sex acts performed when individuals have STI symptoms. To reflect the unbalanced bargaining power between male and female in a relationship (males tend to dictate), this function is segregated by gender, with $\epsilon_{STI,female} > \epsilon_{STI,male}$.

We also model a saturation of sexual acts based on the number of concurrent partners. This is to avoid that an individual with many concurrent partners has an unrealistic rate of sex acts.

$$h_{nPartn}(n) = \frac{2}{1 + e^{-c\,n}} - 1$$

with c a saturation parameter.

B.5.2 Distribution of sex acts among partner types

Among these N sex acts, N_s, N_c and N_w were made with the male's spouse(s), casual partner(s) and sex worker ($N = N_s + N_c + N_w$). The distribution between these three categories is assumed to follow a multinomial law:

$$(N_s, N_c, N_w) \sim \text{Multinom}(N, \mathbf{p})$$

with $\mathbf{p} = (p_s, p_c, p_w)$ the probability vector defining the probabilities that a sex act will be with a spouse, a casual partner or a sex worker. The constraint is: $p_s + p_c + p_w = 1$.

The probability to engage with sex worker, it is based on the male's risk group r:

$$p_w = w_1 e^{-w_2(r^* - r)}$$

with r^* the highest risk group, w_1 and w_2 shape parameters.

The probability to have a sex act with a spouse is set to:

$$p_s = \alpha_s \frac{n_s}{n_s + n_c} \mathbf{1}_{n_c > 0} + (1 - p_w)\mathbf{1}_{n_c = 0}$$

with n_s (resp. n_c) the total number of spouses (resp. casual partners); parameter α a weighting factor depending on the average ages, average STI/HIV infections and average number of children among spouses and casual partnerships.

A constraint on α_s is $0 < \alpha_s <$ (# spouses/total # partnerships) such that $0 \leq p_s \leq 1$.

Finally, we have implicitly

$$p_c = 1 - p_s - p_w$$

The parameters of these probabilities will be calibrated on published data and surveys (DHS).

B.5.3 Distributing the number of sex acts between partners

Assume the male has k_s spouses. We distribute N_s acts between k_s females recursively with a binomial law. If $N_s^{(i)}$ is the number of sex acts allocated to the i^{th} spouse, for $i \in \{1, ..., k_s\}$:

$$\left(N_s^{(1)}, ..., N_s^{(k_s)}\right) \sim \text{Multinom}\left(N_s, \frac{1}{k_s}\right)$$

Hence, there is no preference among spouses.

Similarly, the N_c sex acts with k_c casual partners are distributed with the same

recursive formula, for $i \in \{1, ..., k_c\}$:

$$\left(N_c^{(1)}, ..., N_c^{(k_c)}\right) \sim \text{Multinom}\left(N_c, \frac{1}{k_c}\right)$$

B.5.4 Distributing sex acts types

Once the number of sex acts are allocated to each partner, the type of sex act must be specified. Sex act types allocation is first described for spouses, casual partners and sex workers will have the same methodology.

The $N_s^{(i)}$ sexual intercourses with his i^{th} spouse are distributed among the three sex act types (with condom, no condom low risk, no condom high risk). The number of sex acts performed with a condom is $N_{s,0}^{(i)}$, without condom and low risk practices $N_{s,1}^{(i)}$ and without condom and high risk practices $N_{s,2}^{(i)}$

$$\left(N_{s,0}^{(i)}, N_{s,1}^{(i)}, N_{s,2}^{(i)}\right) \sim \text{Multinom}(N_s^{(i)}; \mathbf{p_s})$$

with $\mathbf{p_s} = (p_{s,0}, p_{s,1}, p_{s,2})$ the vector of probabilities to engage in the respective sex act types.

The following functional forms are assumed for the probabilities:

$$p_{s,0} = p_{s,0}(r_m, r_f) = t_1 e^{-t_2(r_m + r_f)/r^*}$$

with t_1, t_2 shape parameters, r_f (resp. r_m) the risk group of the female (resp. male) and r^* the maximum risk group.

It is assumed that among those sex acts that are not performed with a condom, a fixed proportion β_s of the remaining will engage in medium-risk practices without condoms:

$$p_{s,1} = \beta_s(1 - p_{s,0})$$

Finally, implicitly we have:

$$p_{s,2} = 1 - p_{s,0} - p_{s,1}$$

Similarly, we have for casual partners:

$$\left(N_{c,0}^{(i)}, N_{c,1}^{(i)}, N_{c,2}^{(i)}\right) \sim \text{Multinom}(N_c^{(i)}; \mathbf{p_c})$$

with $\mathbf{p_c}$ calculated the same way as $\mathbf{p_s}$.

B.5.5 Limits on the number of sex acts for females

Because the number of sex acts (within partnerships) is driven by males, there is a risk a female has a total number of sex acts, noted N_f here, unrealistically high if she has several partnerships.

Hence, a maximum rate of sexual intercourses for females is assumed, and noted $R_{sex}^{max,f}$. For a given period dt, if the number of sex acts allocated to a female is higher than $R_{sex}^{max,f} dt$, then the following corrective algorithm is applied to the number of sex acts for *both* female and male (noted N_m here) in this partnership:

If $N_f > R_{sex}^{max,f} dt$ then :

1. $N_f \leftarrow \min\left(N_f\,; \text{int}[R_{sex}^{max,f} dt]\right)$
2. $N_m \leftarrow \max\left(N_m - (N_f^{old} - N_f^{new}); 0\right)$

where int[x] denotes the integer part of any real number x.

Note: This algorithm will be improved in a future version.

B.5.6 Sex acts of males with no partnership

Males with no partnership are simulated with a slightly different process as their sexual acts can only be with sexual workers, hence the distribution of sex acts between different partners is not relevant.

The number of sex acts is still assumed to follow a Poisson distribution

$$N \sim \text{Poisson}(R_{sex}^{single}\, dt)$$

But, the factors determining the effective rate from the maximum rate are different.

$$R_{sex}^{single} = R_{sex}^{max} \times R_M^{single} \times R_{cost}$$

with

$$R_M^{single} = h_{age}(A_m)\, h_{risk}(r)\, h_{STI}(s)\, h_{HIV}(\tau)$$

Compared to R_M for males in partnerships, the factor related to the number of partners is removed, as the male is assumed to have access to an ever-sufficient services from sex workers (economic costs aside).

A new factor representing the transaction cost of sex work services is introduced, R_{cost}. For simplicity, it is set to a constant. Its aim is to limit the number of visits to CSW.

B.6 Commercial sex workers

B.6.1 Recruitment

It is assumed commercial sex workers (CSW) are recruited in the population at a rate proportional to the population size. If $R^{\star}_{csw}$ is the maximum rate of recruitment and N the total population size, the number of CSW recruited during the period of time dt is distributed with a Poisson distribution:

$$N^{new}_{csw} \sim \text{Poisson}\left(R_{csw}\, N\, dt\right)$$

with

$$R_{csw} = \frac{1 + e^{-ab}}{1 + e^{a(x-b)}} R^{\star}_{csw}$$

where x is the proportion of the number of CSW to the total population and a and b two constants. The multiplicative logistic term is introduced to translate a saturation of the demand for CSW: recruitment tends to 0 as the proportion of CSW in the population grows.

The age of the newly recruited CSW is uniformly distributed between a pre-specified age range (e.g. 15 to 40 years old).

The infection status with respect to each STI is also set stochastically. We denote A_s the number of a newly recruited CSW infected with STI s. We assume that

$$A_s \sim \text{Binomial}(N^{new}_{csw}, p_s)$$

where p_s is the current population prevalence of the associated STI (s). The A_s individuals are picked randomly among the new N^{new}_{csw} CSWs. A new CSWs who has been (stochastically) infected, is assumed to have just contracted the infection

(STI duration is set to 1 day).

Previous number of partner is arbitrarily set to Poisson((age-minsexage)/2) and the widow prevalence is set at the same level as the general population.

B.6.2 Cessation

Among all the current CSW in the population (N_{csw}), we assume the rate of individuals dropping out of commercial sex (q_{csw}) is proportional to their number.

$$N_{csw}^{quit} \sim \text{Binomial}\,(q_{csw}\,dt, N_{csw})$$

The risk group of the quitting CSWs is assigned randomly (multinomial among all risk groups). Note that only the risk group (set at a distinctive high value) identifies a CSW from the rest of the population.

B.7 Disease transmission

The transmission of STI will be determined by the probability of transmission per sex act. This probability is calculated from an infectivity curve associated to the infected partner and a susceptibility factor associated to the susceptible partner.

B.7.1 Infectivity curve and susceptibility factor

Infectivity curve

Individuals infected with an STI have an infectivity curve associated to this infection, noted IC. The infectivity curve is normalized such that the peak(s) of infectiousness is 1. At time $t = 0$, the pathogen invade the individual and by definition $IC(0) = 0$.

The shape of this curve depends on the disease. A proxy for the shape of the infectivity curve is the viral load in genital secretions. Other features from the infected

individual (age, co-infections, etc) can impact the shape of this curve. Detailed formulation of the infectivity curves for each STI is described in B.7.3.

Susceptibility factor

The susceptible individual who is at risk of transmission during the sex act considered, has a specific susceptibility factor to a given STI, noted SF. Susceptibility is maximal when $SF = 1$. Let's assume the STI considered is the i^{th} in the list of all STIs modelled. This factor is reduced with respect to circumcision status (for male only):

$$SF_i = SF_i^{circum}$$

where $SF_i^{circum} \leq 1$ are estimated from the literature.

Note: Other features than circumcision may be added in future developments.

B.7.2 Probability of transmission

For one given sexual intercourse, the probability of transmission, PT, is calculated from both the infectivity curve and the susceptibility factor of the pair of individuals considered.

The type of sex act (with or without condom, low or high risk) also impacts the probability and is represented in a functional form with a range between 0 and 1, noted $SAT(type)$ for Sex Act Type. Because only 3 sex act types are considered, the domain of this function is $\{0, 1, 2\}$ with 2 representing high-risk sex (anal, dry-sex), 1 standard sex act and 0 sex act with condom. We have $SAT(2) = 1$ as no risk reduction is allowed when the riskiest sex act is performed, and $SAT(0)$ should be a tiny number to reflect the dramatic reduction of transmission risk when a condom is used. Because of the difference between STIs, the value of $SAT(1)$ is STI-specific.

It is also assumed there is a maximum probability of transmission per sex act for a given STI s, and is noted $PT_{0,s}^*$. This probability assumes no other STI co-infection.

Hence, the formula defining the probability of transmission for a given STI s,

without any other STI co-infections is:

$$PT_{0,s}(t, I_1, I_2, type) = IC_s(t, I_1) \times SF_s(I_2) \times SAT_s(type) \times PT^*_{0,s}$$

with t the duration since infection of the infected partner, I_1 (resp. I_2) vector of relevant features (e.g. age, circumcision status, etc) of the infectious (resp. susceptible) individual, and $type$ the sex act type.

If the susceptible partner is already infected with another STI, then the transmission probability is increased. Given an odds-ratio C_{ij} for increased susceptibility to STI i when already infected with STI j, we assume the overall odds-ratio is

$$R_i = \max_j(C_{ij})$$

The susceptibility factor due to STI co-infections is assumed constant for a given pair of STIs and represented by a matrix C, where the columns represent the STI already infecting the individual (j) and the row the STI the individual is still susceptible to. Entries of the matrix C can be calibrated on published literature (as it is likely that co-infection increases susceptibility we have $1 \leq C_{ij}$).

Hence, the transmission probability taking into account any other STI co-infection is:

$$PT_s(t, I_1, I_2, type) = \frac{R_s\, PT_{0,s}}{1 + (R_s - 1)PT_{0,s}}$$

(formula implied from the odds-ratio definition $OR = \frac{p/(1-p)}{p'/(1-p')}$)

For a pair of individuals who has n_y sex acts of type y during a given period, the probability of transmission of a given STI s after these multiple sex acts is noted MPT and is given by the following formula:

$$MPT_s(t, I_1, I_2) = 1 - \prod_{y=0}^{2}[1 - PT_s(t, I_1, I_2, y)]^{n_y}$$

B.7.3 Probabilities of transmission for every STI

Here, the infectivity curves and susceptible factors are defined for every STI modelled.

HIV

The infectivity curve of HIV is defined by pieces to represent the different stages of the natural history of HIV. The parameters used for its definition are summarized in Table B.1

Table B.1. *Parameters for the infectivity curve of HIV*

Notation	Interpretation
$T_{vl^*_{HIV}}$	Time after initial infection when viral load peaks
q_{HIV}	Shape parameter of acute infection
σ_{HIV}	Dispersion of the duration of acute phase
$VL_{chronic}$	Fraction of peak viral load when chronic stage starts
$D_{chronic}$	Duration (in years) of the chronic infectious stage
$r_{chronic}$	Rate of viral load progression during the chronic stage
D_{AIDS}	Duration (in years) of AIDS (death as end-point)

The infectiousness during the acute period following initial infection is represented by (the subscript HIV is dropped for readability):

$$IC_{HIV,acute}(t) = \exp\left(-\frac{(t - Tvl^*)^{2q}}{\sigma^{2q}}\right)$$

with $0 < t < T_c$ the time since initial infection and $T_c = \sigma(-\ln(VL_{chronic}))^{1/2q} + Tvl^*$, the time after initial infection when the chronic stage starts.

For the chronic phase for $T_c \leq t < T_c + D_{chronic}$

$$IC_{HIV,chronic}(t) = VL_{chronic}\, e^{(t-T_c)r_{chronic}}$$

And finally for the AIDS stage, for $t \geq T_{AIDS} = T_c + D_{chronic}$

$$IC_{HIV,AIDS}(t) = IC_{HIV,chronic}(T_{AIDS}) e^{-(t-T_{AIDS})\ln(VL_{chronic})/D_{AIDS}}$$

The end-point being death, and it is assumed the infectivity level is back at its peak value at this time.

The infectivity curve of HIV *without any other co-infections* is given by putting together the three stages:

$$IC_{HIVonly}(t) = IC_{HIV,acute}(t) + IC_{HIV,chronic}(t) + IC_{HIV,AIDS}(t)$$

When the infected individual is co-infected with another STI, the HIV infectiousness is assumed to increase and mirror the other STI infectiousness, up to a given ratio.

$$IC_{HIV,coSTI}(t) = \left(\sum_s RI_{coSTI}(s) IC_s(t) \right) IC_{HIVonly}(t)$$

with s summing on all STI modelled and $RI_{coSTI}(s)$ is the rebound of HIV infectivity due to co-infection with STI s.

Finally, the full infectivity curve for HIV is

$$IC_{HIV}(t) = IC_{HIVonly}(t) + IC_{HIV,coSTI}(t)$$

Practically, the value is capped at one, that is $IC_{HIV}(t) = \min(1, IC_{HIVonly}(t) + IC_{HIV,coSTI}(t))$.

It is implicitly assumed that co-infections cannot increase HIV infectivity beyond the peak infectivity when only infected with HIV. It is also assumed that the increase of HIV infectivity mirrors the pattern of infectivity of the co-occurring STI.

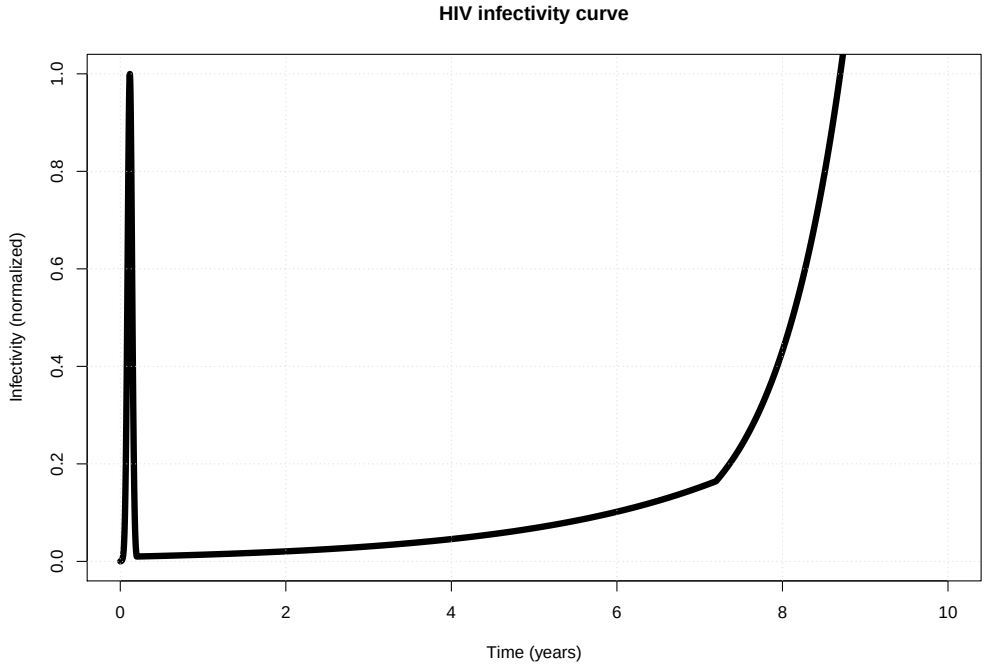

Figure B.3. *Infectivity curves for HIV.*

Syphilis (*Treponema pallidum*, Tp)

Primary syphilis: After initial exposure, a primary chancre develops at the site of entry (usually genital) after 3-90 days (average 3 weeks) [56, 68]. It takes about 4-6 weeks for spontaneous resolution (without treatment) of the primary chancre.

Secondary syphilis: Up to 85% of cases will progress to generalized lesions [56], within 4-10 weeks after the appearance of the initial chancre [56, 68]. A small proportion of cases, 10% [56] 5-22% [68], will develop highly infectious chancres (condylomata lata). Spontaneaous resolution occurs within less than 3 months [56] or several weeks [68].

Early latent syphilis: About 25% of cases experiences a recurrence of secondary syphilis symptoms during a window period of about 6 months

Syphilis (untreated) is expected to be sexually transmissible during 2 years after initial infection [56]. Late latent and tertiary phases are not infectious. Tertiary phase occurs 15-30 years later and is associated with increased mortality in some cases.

Co-infection with HIV might be associated with a higher Tp virulence, but syphilis treatment is the same as HIV-uninfected patients [68]. The infectivity curve is defined with respect to the syphilitic stages.

Primary syphilis infectivity curve is represented with the pseudo-beta function defined in appendix B.11.1:

$$\mathrm{IC}_{\mathrm{Tp.1}}(t) = \nu_{\mathrm{Tp.1}} \times \mathcal{B}\left(\frac{(t - L_{\mathrm{Tp.1}})^+}{D_{\mathrm{Tp.1}}}, a_{\mathrm{Tp.1}}, b_{\mathrm{Tp.1}}\right)$$

with $a_{\mathrm{Tp.1}}$ and $b_{\mathrm{Tp.1}}$ shape parameters, $L_{\mathrm{Tp.1}}$ the latent period before being infectious (suggested 30 days), $D_{\mathrm{Tp.1}}$ the infectiousness duration of primary syphilis (suggested 5 weeks) and $\nu_{\mathrm{Tp.1}}$ the relative virulence of this primary stage (suggested 0.7) compared to peak infectivity (when the value of the infectivity curve is 1).

Secondary syphilis is defined similarly, but with two possibilities for the infectivity curve reflecting the fact that some cases will develop highly infectious condylomata lata.

In the absence of condylomata:

$$IC_{Tp.2}^{no\,condy}(t) = \nu_{Tp.2} \times \mathcal{B}\left(\frac{(t - L_{Tp.2})^+}{D_{Tp.2}}, a_2, b_2\right)$$

when condylomata develop:

$$IC_{Tp.2}^{condy}(t) = \nu_{Tp.2}^{condy} \times \mathcal{B}\left(\frac{(t - L_{Tp.2})^+}{D_{Tp.2}^{condy}}, a_2^{condy}, b_2^{condy}\right)$$

with a_2 and b_2 shape parameters, $L_{Tp.2}$ the latent period from infection before secondary syphilis is triggered(suggested L_{Tp} plus 7 weeks), $D_{Tp.2}$ the infectiousness duration of secondary syphilis (suggested 8 weeks) and $\nu_{Tp.2}$ the relative virulence of this secondary stage (suggested 0.7) compared to peak infectivity.

The parameters with the superscript $condy$ apply to the case when condylomata develop. In this case, the parameters are assumed to be different.

The probability that condolymata develop is represented by the binary random variable κ_{condy} that takes value 1 with probability p_{condy} (suggested 0.15), else is 0.

Hence, for secondary syphilis we have:

$$IC_{Tp.2}(t) = \kappa_{condy} IC_{Tp.2}^{condy}(t) + (1 - \kappa_{condy}) IC_{Tp.2}^{no\,condy}(t)$$

Early latent syphilis is considered as a repeat of symptoms that occurred during secondary syphilis, hence it is defined similarly:

$$IC_{Tp.el}(t) = \nu_{Tp.el} \times \mathcal{B}\left(\frac{(t - L_{Tp.el})^+}{D_{Tp.el}}, a_{el}, b_1 el\right)$$

with a_{el} and b_{el} shape parameters, $L_{Tp.el}$ the latent period before earl latent stage is triggered (suggested L_{Tp} plus 12 months), $D_{Tp.1}$ the infectiousness duration of primary syphilis (suggested 5 weeks) and $\nu_{Tp.el}$ the relative virulence of this primary stage compared to peak infectivity.

Finally, the total infectivity curve for syphilis is:

$$IC_{Tp.el}(t) = IC_{Tp.1}(t) + \kappa_{Tp.2} IC_{Tp.2}(t) + \kappa_{Tp.el} IC_{Tp.el}(t)$$

with $\kappa_{Tp.2}$ (resp. $\kappa_{Tp.el}$) the binary random variable taking value 1 with probability $p_{Tp.2}$ (resp. $\kappa_{Tp.el)}$ representing the probability to develop secondary (resp. early latent) syphilis. (suggested: $p_{Tp.2} = 0.85$ and $\kappa_{Tp.el} = 0.20$)

A graphical representation is given in Figure B.4

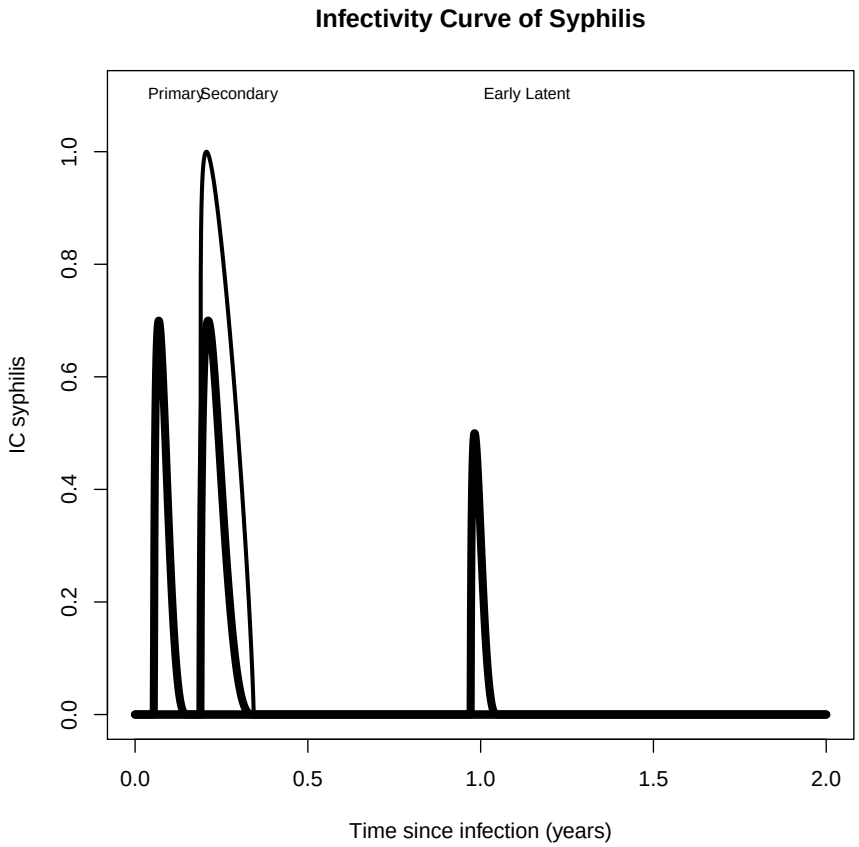

Figure B.4. *Infectivity curve for Syphilis. The thin curve in the secondary syphilis stage represents the case when highly infectious condolymata develop.*

B.7.4 Mother-to-child (vertical) transmission

When a female is both pregnant and infected with a STI, transmission of the pathogen to the children is modeled as a stochastic event. For all STI except syphilis, the probability of mother-to-child transmission is assumed constant (it

does not depend on pregnancy stage and duration of infection):

$$p_{MTCT} = \textbf{constant}$$

For syphilis, there is some evidence [64, 65] that risk of vertical transmission is higher during the early stages of syphilis infection. Hence, a decreasing logistic shape is assumed for the probability of syphilis mother-to-child transmission:

$$p_{MTCT}^{Tp} = \frac{a}{1 + e^{b(\tau - c)}}$$

with τ the duration of syphilis infection and a, b, c shape parameters.

For every pregnant female infected with an STI, the vertical transmission to the new born is decided by drawing a random variable from a Bernoulli distribution with probability p_{MTCT}.

B.8 Treatment and vaccination

B.8.1 Treatment implementation

When an individual is infected with an STI, receiving a treatment will affect (most likely reduce) her/his infectiousness, symptomatic status and increase the chances of being cleared from the pathogen, if the STI is curable.

An individual starting a treatment will go through several steps before potentially having a positive outcome.

Treatment microbiological failure

There is a risk of failure with any treatment. An individual may poorly respond to prescribed drugs, or be infected with a drug-resistant strain of the pathogen (adherence is treated separately hereafter).

For a given STI, let TMS be the random variable representing microbiological treatment success (conditional on full adherence) and p_{fail} the probability of treatment failure. It is assumed that TMS has a Bernoulli distribution ($TMS = 1$ is

successful treatment):

$$TMS \sim \text{Bern}(1 - p_{fail})$$

Adherence

Right from treatment inception, adherence is determined based on the individual's risk group and symptomatic status. A non-adherent behaviour will reduce the amount of drug intake. If adherence A is measured as the fraction of the optimal drug intake ($0 \leq A \leq 1$, with $A = 1$ being full adherence), then it is assumed

$$A = a_0 e^{-a_1 r} a_2$$

with r the risk group of the individual, a_0 the maximum adherence, a_2 a reducing factor when the infection is asymptomatic (it is assumed that a symptomatic infection motivates more to adhere to treatment).

Treatment reduction effect

Treatment is affecting the infectivity curve, with the aim of reducing it to either 0 for curable STI or a very small value for non-curable STIs (e.g. HIV).

We assume there is an hypothetical treatment reduction effect (TRE^*) conditional on microbiological success and full adherence. Duration of treatment has an optimal length note TD^*. TRE is a function of treatment duration τ and we have $TRE^*(0) = 1$ (no reduction of infectiousness at the very start of treatment) and $TRE^*(TD^*) = 0$ or ϵ (treatment has cured [when STI is curable] or heavily suppressed [when non-curable] the pathogen). The actual treatment reduction effect TRE is given by

$$TRE(A, TMS, \tau) = [A \times TRE^*(\tau) + (1 - A)]\, TMS + (1 - TMS)$$

Function TRE^* will be defined specifically for each STI.

The infectivity curve before treatment (IC) is thus modified into an infectivity curve during treatment (IC^{treat}):

$$IC^{treat}(t, \tau) = IC(t) \times TRE(A, TMS, \tau)$$

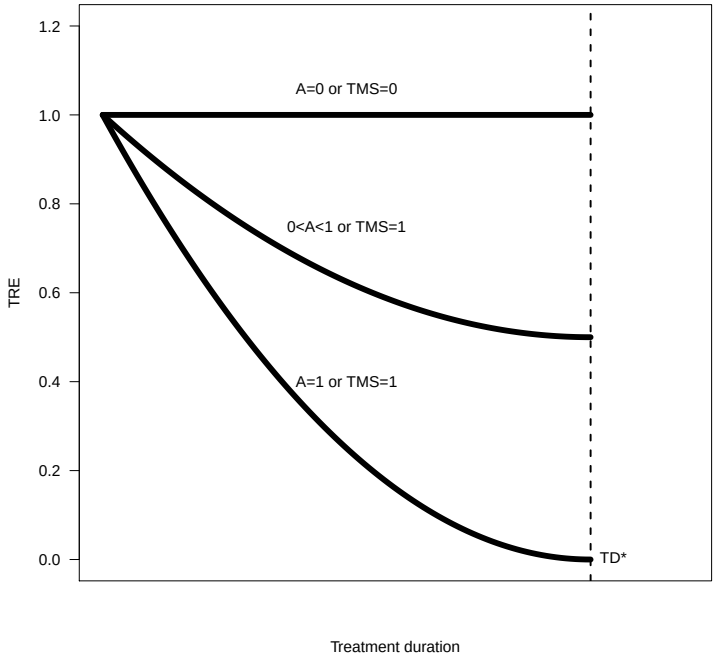

Figure B.5. *Treatment reduction effect.*

For curable STIs, cure is achieved by assessing the value of a random variable with a Bernoulli distribution

$$\mathrm{Cure} \sim \mathrm{Bern}(\mathrm{TRE}(\mathrm{TD}^*))$$

If $\mathrm{Cure} = 1$, the STI is cured. If $\mathrm{Cure} = 0$ the infectivity curve is set back, as if $\mathrm{TRE} = 1$.

B.8.2 Vaccine implementation

The individuals eligible for vaccination are selected according to pre-defined criteria defined at the simulation level (for example age). Given an individual receives a vaccine injection, his/her immunity to the STI is instantaneously set to 100% with probability $1 - p_{fail}$, with p_{fail} the failure probability of the vaccine. The immunity decreases at the exponential rate w, such that immunity t time

units after (successful) vaccination is:

$$\text{immunity}(t) = e^{-wt}$$

The susceptibility factor to that STI at time t, $SF(t)$, is updated every time step:

$$SF(t) = SF(t-1)(1 - \text{immunity}(t))$$

A vaccinated individual can acquire the associated STI if the vaccine effectiveness has waned sufficiently. In that cases, the model gives the possibility to simulate a reduction of infectiousness provided by the previous vaccination. Put simply, the vaccine is not strong enough to protect the individual from infection, but if infection happens, the individual will be less infectious. The vaccine reduction effect (VRE) on infectiousness is simply modelled as a constant multiplicative factor applied to the infectivity curve.

B.9 Calibration

This agent-based model has many model parameters, that are all summarized in Tables B.2, B.5, B.6, B.7, B.8 and B.9. They can be classified in groups that specifically affect:

- demographics
- partnerships dynamics
- sexual behaviour
- diseases natural history
- treatments

Only the parameters in the "diseases natural history" and "treatments" were not calibrated to data. Fixed values were assumed either based on the literature or arbitrarily set (Tables B.7, B.8, B.9).

The fitting procedure consist in fitting groups of parameters sequentially. Many "feedback loops" exist: for example, demographics can affect indirectly STI prevalence (for example, a lack of young individuals could force disease transmission to stay in older cohorts, limiting te prevalence), but STI prevalence can also af-

fect demographics (e.g. HIV-induced deaths). Hence, given the large number of parameters, a practical way to identify parameters is to fit them sequentially by groups. The order of this sequence is arbitrary and justified as follows. Demographic processes are considered the most fundamental, hence they should be fitted first. Then partnership dynamics and sexual behaviour are fitted to relevant data.

Demographic parameters were first fitted. Not all parameters were fitted: crude birth rate and children mortalities were directly inputed from the literature. Only the deaths hazard were fitted and the fitting procedure was relatively straightforward (simply matching a pre-specified life expectancy with or without HIV). These demographic parameters remained unchanged during the next fitting steps. See Table B.2.

The partnerships parameters were i) set to a fixed value taken either from the literature or arbitrarily, ii) fitted to the DHS database, or iii) fitted to prespecified STI prevalences (Table B.5). Similarly, sexual behaviour parameters were i) set to a fixed value or ii) fitted to prespecified STI prevalences (Table B.6).

The calibration method used is an Approximate Bayesian Approximation (ABC). The summary statistic F is simply the sum of squared differences to the target data. STI prevalences are fitted by risk groups and ages. We have:

$$\begin{aligned} F(X) &= (\mathtt{PartnerRatio}(X)/\mathtt{target}_{PR} - 1)^2 \\ &\quad +(\mathtt{MedAgeMar}(X)/\mathtt{target}_{MAM} - 1)^2 \\ &\quad + \sum_s (\mathtt{STIRiskGrpPrev}_s(X)/\mathtt{target}_{RGP,s} - 1)^2 \\ &\quad + \sum_{a,s} (\mathtt{STIAgePrev}_{a,s}(X)/\mathtt{target}_{AP,a,s} - 1)^2 \end{aligned}$$

with $\mathtt{target}_x$ the target values from the data, $\mathtt{PartnerRatio}$ the proportion of individuals in partnerships from the simulation (fitted on DHS), $\mathtt{MedAgeMar}$ the median age at marriage for women (fitted on DHS), $\mathtt{STIRiskGrpPrev}_s$ the prevalence of each STI by risk group (no data, scenario assumptions) and $\mathtt{STIAgePrev}_s$ the STI prevalence by age (shape for HIV fitted on DHS, levels are scenario assumptions).

B.10 Simulations

Below is the high-level algorithm used to perform epidemiological analyses.

1. start with initial population, no partnerships, no STI
2. run simulation long enough such that the partnership dynamics are in a steady state. Fit of equilibrium values to target demographic and partnership data should be performed at that step
3. introduce STIs into the population and run long enough such that prevalence and incidence of all STIs reach their steady state
4. determine a date after the prevalence and incidence steady states are reached to implement an intervention (e.g., vaccine)
5. set a horizon where the baseline (i.e. no intervention) and intervention simulations are compared

B.11 Appendix

B.11.1 Pseudo-beta shape function

For infectivity curves associated with STIs of limited duration, the shape function was inspired from the beta distribution density (because it has a bounded support).

$$\mathcal{B}(x, a, b) = x^{a-1}(1-x)^{b-1}/C$$

where C is the normalizing constant such that the maximum value of $\mathcal{B}$ is 1 on the interval [0;1]:

$$C = \left(\frac{a-1}{a+b-2}\right)^{a-1}\left(\frac{b-1}{a+b-2}\right)^{b-1}$$

It is assumed that for any $a, b > 1$ and $x < 0$ and $x > 1$ we have $\mathcal{B}(x, a, b) = 0$. The maximum of $\mathcal{B}$ is reached at $x_{max} = (a-1)/(a+b-2)$.

B.11.2 Tables of all parameters

Parameter	Description	Value	Source
`birthRate`	Annual crude birth rate for the whole population	0.037	The World Bank (SSA only)
m_{infant}	Annual infant(< 1 year-old) mortality rate	0.06	CIA World Fact Book (data averaged and rounded to the nearest percentage for SSA)
m_{child}	Annual children(between 1 and 5 year-old) mortality rate	0.04	The World Bank (SSA only)
k	shape parameter for Weibull distribution of death hazard	2.5	fitted to average life expectancy of 70 years
λ	scale parameter for Weibull distribution of death hazard	0.01	fitted to average life expectancy of 70 years
k'	shape parameter for Weibull distribution of death hazard after acquiring HIV	12.98	fitted to maximum survival of 10 years after HIV acquisition
λ'	scale parameter for Weibull distribution of death hazard after acquiring HIV	0.05	fitted to maximum survival of 10 years after HIV acquisition
`minSexAge`	Minimum age (in years) for sexual contact	12	assumption
`maxSexAge`	Maximum age (in years) for sexual contact	60	assumption
`minCSWAge`	Minimum age (in years) for a female to practice commercial sex work	15	assumption
`maxCSWAge`	Maximum age (in years) for a female to practice commercial sex work	45	assumption

Table B.2. *Exhaustive list of all model parameters related to demographics. These parameters are the same across all synthetic populations A, B and C. SSA: Sub-Saharan African countries*

Parameter	Description	Value(s)	Source
Formation			
r_f^*	maximum formation rate (female dominance)	2.0 ; 3.1 ; 3.1	fitted to target STIs prevalence
s_{age}	shape parameter for age component of partnership formation	0.27	fitted to target STIs prevalence
a^*	location parameter for the age component of partnership formation	43 years	assumption
g_{min}	minimum age gap (male age minus female age) for partnership formation	-7 years	assumption
$\bar{g}$	mean age gap at partnership formation	10.1 years	fitted to target STIs prevalence
s_{gap_1}	shape parameter for age gap component in partnership formation	5	assumption
s_{gap_2}	shape parameter for age gap component in partnership formation	2	assumption
s_0^{risk}	shape parameter for risk group component in partnership formation	0.3	fitted to target STIs prevalence
s_1^{risk}	shape parameter for risk group component in partnership formation	1.0	fitted to target STIs prevalence
q	shape parameter for partner deficit component in partnership formation	0.40	fitted to target STIs prevalence
$a_{sympt,f}$	probability component of partnership formation if female is symptomatic from any STI	0.82	fitted to target STIs prevalence
$a_{sympt,m}$	probability component of partnership formation if male is symptomatic from any STI	$a_{sympt,f}$	n/a

Table B.3. *Exhaustive list of all model parameters related to partnerships. A single value means it is shared for all synthetic populations. Several values indicates the one associated to each synthetic populations A, B and C respectively. DHS data were averaged across the following sub-Sahara African countries (DHS recode version in parentheses): Burkina-Faso (4), Cameroon (4), Ethiopia (6), Kenya (5), Lesotho (5), Malawi (5), Rwanda (6), Senegal (6), Swaziland (5), Zambia (5), Zimbabwe (6).*

Parameter	Description	Value(s)	Source
Spousal progress			
sp^*	maximum annual rate of spousal progression	0.05	based on DHS (proportion living in spousal union)
$\bar{A}_f$	mean female age progressing to spousal union	18 years	based on DHS (Women's median age at first marriage)
σ_{A_f}	standard deviation of female age progressing to spousal union	9.25 years	assumption
$\bar{G}$	mean age gap for a partnership progressing to spousal union	4.75 years	assumption based on [6]
σ_G	standard deviation of age gap for a partnership progressing to spousal union	14.2 years	assumption based on [6]
k_1	mean partnership duration when progression to spousal union occurs	5 years	assumption
k_2	variance of partnership duration when progression to spousal union occurs	3 years	assumption
$\bar{\Delta}$	mean age gap difference b/w youngest existing wife and candidate wife	12 years	assumption
σ_Δ	standard deviation of age gap difference b/w youngest existing wife and candidate wife	5 years	assumption

Table B.4. *Exhaustive list of all model parameters related to partnerships. A single value means it is shared for all synthetic populations. Several values indicates the one associated to each synthetic populations A, B and C respectively. DHS data were averaged across the following sub-Sahara African countries (DHS recode version in parentheses): Burkina-Faso (4), Cameroon (4), Ethiopia (6), Kenya (5), Lesotho (5), Malawi (5), Rwanda (6), Senegal (6), Swaziland (5), Zambia (5), Zimbabwe (6).*

Parameter	Description	Value(s)	Source
Dissolution			
δ^*	maximum annual dissolution rate	0.1 ; 0.4 ; 0.4	fitted to target STIs prevalence
ϵ	probability component for dissolution of a spousal partnership	0.06	based on DHS (proportion living in spousal union)
dur_1	shape parameter (duration) of probability component for dissolution	0.324	fitted to target STIs prevalence
dur_2	shape parameter (duration) of probability component for dissolution	0.69	fitted to target STIs prevalence
dur_3	shape parameter (duration) of probability component for dissolution	0.15	fitted to target STIs prevalence
$drisk_1$	shape parameter (risk group) of probability component for dissolution	0.7	fitted to target STIs prevalence
$dage_1$	shape parameter (partners' age) of probability component for dissolution	75.9 years	fitted to target STIs prevalence
$dage_2$	shape parameter (partners' age) of probability component for dissolution	0.1	fitted to target STIs prevalence
$dage_{min}$	shape parameter (partners' age) of probability component for dissolution	0.7	fitted to target STIs prevalence
q	shape parameter for partner deficit component in partnership dissolution	2.1	fitted to target STIs prevalence
q_{min}	shape parameter for partner deficit component in partnership dissolution	0.3	fitted to target STIs prevalence
$d_{symptom}$	dissolution probability relative reduction for asymptomatic case in partnership	0.55	fitted to target STIs prevalence

Table B.5. *Exhaustive list of all model parameters related to partnerships. A single value means it is shared for all synthetic populations. Several values indicates the one associated to each synthetic populations A, B and C respectively. DHS data were averaged across the following sub-Sahara African countries (DHS recode version in parentheses): Burkina-Faso (4), Cameroon (4), Ethiopia (6), Kenya (5), Lesotho (5), Malawi (5), Rwanda (6), Senegal (6), Swaziland (5), Zambia (5), Zimbabwe (6).*

Parameter	Description	Value(s)	Source
$\texttt{propRisk0}$	proportion of the population in risk group 0 (safest)	0.60 ; 0.25 ; 0.35	fitted to target STIs prevalence
$\texttt{propRisk1}$	proportion of the population in risk group 1	0.35 ; 0.55 ; 0.50	fitted to target STIs prevalence
$\texttt{propRisk2}$	proportion of the population in risk group 2 (riskiest)	0.05 ; 0.20 ; 0.15	fitted to target STIs prevalence
c_1	parameter for the geometric distribution for concurrency (female and male)	0.35	fitted to target STIs prevalence
$c_{2,f}$	parameter for the geometric distribution for concurrency (female)	0.6	fitted to target STIs prevalence
$c_{2,m}$	parameter for the geometric distribution for concurrency (male)	0.7	fitted to target STIs prevalence
R_{sex}^{max}	maximum annual sex acts rate for males	360	assumption
$R_{sex}^{max,f}$	maximum annual sex acts rate for females (non CSW)	500	assumption
a_{peak}	shape parameter related to sexual activity peak age	20 years	assumption
σ_{age}	shape parameter related to standard deviation of sexual activity peak age	30 years	assumption
q	shape parameter related to frequency of age-dependant sexual activity	5.0	assumption
ϵ_{risk}	parameter related to frequency of risk-dependant sexual activity	0.4	assumption
ϵ_{STI}	frequency reduction of STI symptoms-dependant sexual activity	0.8	assumption
c	saturation parameter of sexual activity in concurrent partnerships	2.0	assumption
α_s	spouse preference parameter in multinomial distribution	2.0	assumption
w_1	shape parameter for the probability of risk-dependent sex acts with CSW	0.5	assumption
w_2	shape parameter for the probability of risk-dependent sex acts with CSW	8.0	assumption
R_{cost}	factor to limit the overall number of visits to CSW	0.1	assumption
t_1	shape parameter for the distribution of sex act types	0.2	assumption
t_2	shape parameter for the distribution of sex act types	0.7	assumption
β_s	proportion low versus high risk sex act types	0.76	fitted to target STIs prevalence
R_{csw}^*	maximum CSW annual recruitment rate	0.005	fitted to target STIs prevalence
a	shape parameter for CSW recruitment saturation	800	assumption
b	shape parameter for CSW recruitment saturation	0.0005	assumption
q_{csw}	CSW annual cessation rate	0.049	fitted to target STIs prevalence

Table B.6. *Exhaustive list of all model parameters related to sexual behaviour. A single value means it is shared for all synthetic populations. Several values indicates the one associated to each synthetic populations A, B and C respectively. CSW: commercial sex worker.*

Parameter	Description	Value	Source
HIV			
$\text{Tvl}^*_{\text{HIV}}$	Time after initial infection when viral load peaks	6 weeks	assumption based on [19]
q_{HIV}	Shape parameter of acute infection	2	assumption based on [19]
σ_{HIV}	Dispersion of the duration of acute phase	2 weeks	assumption based on [19]
$\text{VL}_{\text{chronic}}$	Fraction of peak viral load when chronic stage starts	10^{-2}	assumption based on [19]
$\text{D}_{\text{chronic}}$	Duration (in years) of the chronic infectious stage	7 years	assumption based on [19]
r_{chronic}	Rate of viral load progression during the chronic stage	0.4	assumption based on [19]
D_{AIDS}	Duration (in years) of AIDS (death as end-point)	1 year	assumption based on [19]
$\text{PT}^*_{0,\text{HIV}}$	maximum probability of HIV transmission per sex act	0.06	assumption based on [12]
$\text{SAT}_{\text{HIV}}(1)$	multiplicative factor reducing transmission probability for low risk sex type	0.1	assumption based on [58]
$\text{p}^{\text{HIV}}_{\text{MTCT}}$	HIV mother to child transmission probability	0.3	assumption based on [33]
Syphilis			
$\nu_{\text{Tp.1}}$	primary syphilis virulence (relative to peak)	0.7	assumption based on [56, 68]
$a_{\text{Tp.1}}$	shape parameter primary syphilis	1.05	assumption based on [56, 68]
$b_{\text{Tp.1}}$	shape parameter primary syphilis	2	assumption based on [56, 68]
$\text{L}_{\text{Tp.1}}$	latent period primary syphilis	4 weeks	assumption based on [56, 68]
$\text{D}_{\text{Tp.1}}$	infectiousness duration primary syphilis	6 weeks	assumption based on [56, 68]
$\nu_{\text{Tp.2}}$	secondary syphilis virulence (relative to peak)	0.7	assumption based on [56, 68]
$a_{\text{Tp.2}}$	shape parameter secondary syphilis	1.5	assumption based on [56, 68]
$b_{\text{Tp.2}}$	shape parameter secondary syphilis	4	assumption based on [56, 68]
$\text{L}_{\text{Tp.2}}$	latent period secondary syphilis	16 weeks	assumption based on [56, 68]
$\text{D}_{\text{Tp.2}}$	infectiousness duration secondary syphilis	10 weeks	assumption based on [56, 68]
p_{condy}	probability that condylomata develop in secondary syphilis	0.15	assumption based on [56, 68]
$\nu^{\text{condy}}_{\text{Tp.2}}$	secondary syphilis w/ condylomata virulence (relative to peak)	1.0	assumption based on [56, 68]
$a^{\text{condy}}_{\text{Tp.2}}$	shape parameter secondary syphilis w/ condylomata	1.1	assumption based on [56, 68]
$b^{\text{condy}}_{\text{Tp.2}}$	shape parameter secondary syphilis w/ condylomata	1.8	assumption based on [56, 68]
$\text{D}^{\text{condy}}_{\text{Tp.2}}$	infectiousness duration secondary syphilis w/ condylomata	10 weeks	assumption based on [56, 68]
$\text{L}_{\text{Tp.el}}$	latent period early latent syphilis	1 year	assumption based on [56, 68]
$\text{D}_{\text{Tp.el}}$	infectiousness duration early latent syphilis	8 weeks	assumption based on [56, 68]
$\nu_{\text{Tp.el}}$	secondary syphilis w/ condylomata virulence (relative to peak)	1.0	assumption based on [56, 68]
$a_{\text{Tp.el}}$	shape parameter early latent syphilis	1.5	assumption based on [56, 68]
$b_{\text{Tp.el}}$	shape parameter early latent syphilis	4	assumption based on [56, 68]
$\text{D}_{\text{Tp.el}}$	infectiousness duration early latent syphilis w/ condylomata	8 weeks	assumption based on [56, 68]
$\text{PT}^*_{0,\text{Tp}}$	maximum probability of syphilis transmission per sex act	0.45	assumption based on [56, 68]
$\text{SAT}_{\text{Tp}}(1)$	multiplicative factor reducing transmission probability for low risk sex type	0.9	assumption based on [56, 68]
$\text{p}^{\text{Tp}}_{\text{MTCT}}$	syphilis mother to child transmission probability	0.9	assumption based on [9]

Table B.7. *Exhaustive list of all model parameters related to HIV and syphilis*

Description	Baseline Value	Source
HIV infectiousness rebound when syphilis co-infection (prop. peak infectivity)	0.5	assumption
Syphilis infectiousness rebound when HIV co-infection	0	assumption
Syphilis susceptibility increase when already infected with HIV	1.5	assumption
HIV susceptibility increase when already infected with syphilis	2.5	[45, 87, 91]

Table B.8. *Exhaustive list of all model parameters related to HIV/syphilis co-infection*

Description	Baseline Value	Source
probability treatment failure for HIV	0.01	assumption
probability treatment failure for syphilis	0.0	assumption
maximum adherence (α_0)	0.98	assumption
adherence reduction factor when asymptomatic (α_2)	0.7	assumption
shape parameter for adherence reduction factorbased on risk group (α_1)	0.1	assumption
maximum adherence (α_0)	0.98	assumption

Table B.9. *Exhaustive list of all model parameters related to STI treatment*

Appendix C

Table C.1. *Mother to child transmission results. Relative to baseline scenario.*

Scenario	STI	median	10% quantile	90% quantile	population
TrMass	HIV	-0.010	-0.848	0.118	A
VaxMass	HIV	-0.017	-0.181	0.082	A
VaxYoung	HIV	-0.093	-0.289	0.150	A
VaxHiRisk	HIV	-0.039	-0.988	0.199	A
TrMass	Tp	-0.047	-0.229	0.181	A
VaxMass	Tp	-0.684	-0.794	-0.560	A
VaxYoung	Tp	-0.199	-0.353	-0.002	A
VaxHiRisk	Tp	-0.523	-0.712	-0.388	A
TrMass	HIV	0.033	-0.031	0.105	B
VaxMass	HIV	0.098	0.039	0.153	B
VaxYoung	HIV	0.001	-0.053	0.069	B
VaxHiRisk	HIV	0.089	0.015	0.154	B
TrMass	Tp	-0.098	-0.169	-0.021	B
VaxMass	Tp	-0.716	-0.737	-0.671	B
VaxYoung	Tp	-0.253	-0.314	-0.170	B
VaxHiRisk	Tp	-0.406	-0.497	-0.335	B
TrMass	HIV	0.001	-0.062	0.064	C
VaxMass	HIV	0.001	-0.098	0.073	C
VaxYoung	HIV	-0.031	-0.134	0.053	C
VaxHiRisk	HIV	-0.001	-0.086	0.092	C
TrMass	Tp	-0.030	-0.176	0.158	C
VaxMass	Tp	-0.717	-0.804	-0.645	C
VaxYoung	Tp	-0.239	-0.411	-0.100	C
VaxHiRisk	Tp	-0.462	-0.666	-0.303	C

Table C.2. *Final prevalences of HIV and syphilis*

Scenario	STI	median	10% quantile	90% quantile	population
baseline	HIV	0.01531	0.013	0.01894	A
TrMass	HIV	0.01411	0.00015	0.01873	A
VaxHiRisk	HIV	0.01498	0	0.01954	A
VaxMass	HIV	0.01492	0.0132	0.0182	A
VaxYoung	HIV	0.01482	0.01252	0.01904	A
baseline	Tp	0.02325	0.01794	0.03069	A
TrMass	Tp	0.01948	0.01397	0.0251	A
VaxHiRisk	Tp	0.00303	0	0.00969	A
VaxMass	Tp	0.00022	0	0.00027	A
VaxYoung	Tp	0.01257	0.00807	0.01887	A
baseline	HIV	0.09907	0.08892	0.10648	B
TrMass	HIV	0.10308	0.09615	0.11017	B
VaxHiRisk	HIV	0.11403	0.1083	0.12132	B
VaxMass	HIV	0.11737	0.10988	0.12534	B
VaxYoung	HIV	0.10038	0.0948	0.10499	B
baseline	Tp	0.10162	0.09061	0.11566	B
TrMass	Tp	0.08011	0.07297	0.0901	B
VaxHiRisk	Tp	0.04022	0.03035	0.0519	B
VaxMass	Tp	0.00517	0.00167	0.00784	B
VaxYoung	Tp	0.04282	0.03673	0.05172	B
baseline	HIV	0.14502	0.13191	0.15833	C
TrMass	HIV	0.14589	0.12835	0.16019	C
VaxHiRisk	HIV	0.14873	0.1369	0.16015	C
VaxMass	HIV	0.14956	0.13791	0.1596	C
VaxYoung	HIV	0.14376	0.13323	0.15845	C
baseline	Tp	0.04423	0.03291	0.05574	C
TrMass	Tp	0.03692	0.02867	0.04589	C
VaxHiRisk	Tp	0.00988	0.0029	0.01587	C
VaxMass	Tp	0.00115	0	0.00437	C
VaxYoung	Tp	0.01689	0.01305	0.02194	C

Chapter 4

Intrinsic and realized generation intervals in infectious-disease transmission

Champredon D, Dushoff J. Proceedings of the Royal Society B: Biological Sciences 2015; 282: 20152026.

DOI: 10.1098/rspb.2015.2026

4.1 Abstract

The generation interval is the interval between the time that an individual is infected by an infector and the time this infector was infected. Its distribution underpins estimates of the reproductive number and hence informs public health strategies. Empirical generation-interval distributions are often derived from contact-tracing data. But linking observed generation intervals to the underlying generation interval required for modeling purposes is surprisingly not straightforward, and misspecifications can lead to incorrect estimates of the reproductive number, with the potential to misguide interventions to stop or slow an epidemic. Here, we clarify the theoretical framework for three conceptually different generation-interval distributions: the "intrinsic" one typically used in mathematical models and the "forward" and "backward" ones typically observed from contact tracing data, looking respectively forward or backward in time. We ex-

plain how the relationship between these distributions changes as an epidemic progresses and discuss how empirical generation-interval data can be used to correctly inform mathematical models.

4.2 Introduction

Much infectious disease modeling focuses on estimating the reproductive number – the number of new cases caused on average by each case. In the specific case where the case is introduced in a fully susceptible population, we talk about the basic reproductive number $\mathcal{R}_0$. The reproductive number provides information about the disease's potential for spread and the difficulty of control. It is often thought of a single number: an average [2] or an appropriate sort of weighted average [35]. But the reproductive number can also be thought of as a distribution across the population of possible infectors: different hosts may have different tendencies to transmit disease.

The reproductive number provides information about how a disease spreads, on the scale of disease generations. It does not, however, contain information about the population-level rate of spread (e.g. how disease incidence increases through time, which can be critical for public health interventions). Hence, another important quantity is the population-level *rate of spread*. In disease outbreaks, the rate of spread is often inferred from case-incidence reports and used to estimate the reproductive number.

The reproductive number and the rate of spread are linked by the *generation interval* – the interval between the time that an individual is infected by an infector, and the time that the infector was infected [95].

Whereas the rate of spread measures the speed of the disease at the population level, the generation interval measures speed at the individual level. It is typically inferred from contact tracing, sometimes in combination with clinical data. Like the reproductive number, the generation interval can be thought of as a single number (typically its mean), or as a distribution.

Several previous studies have investigated aspects of the generation interval. Svensson [95] made one of the earliest attempts to define a mathematical framework for the generation interval. Several authors [66, 95] described a decrease in the generation interval over the course of an epidemic and it was argued this phe-

nomenon could be caused by competition between infectors [66]. Nishiura [81] explained, in the context of a specific epidemiological model (compartmental Susceptible-Infected-Recovered), how observed mean generation intervals are expected to change through time and the bias this can introduce in estimating the basic reproductive number.

Generation intervals and mean generation time have also been studied in other fields, including human demography [71], bacterial population growth [67] and population genetics [43]. To our knowledge, the question of how observed generation intervals change with population dynamics has not been studied outside of epidemiology, however, possibly because other fields are relatively more interested in relatively stable populations, and less interested in outbreaks, where such changes are likely to be important.

Here we develop a new framework to discuss generation-interval distributions and to evaluate how they change as an epidemic develops. We define an *intrinsic* generation interval whose distribution depends only on the average infectiousness of an individual at a given time after infection, and which we assume does not change as the epidemic progresses. We then investigate how this and other factors shape the distribution of *realized* generation distributions – which can either be measured *forward*, by studying who is infected by the cohort that acquires infection at a given time, or *backward*, by studying who infected a given cohort (Figure 4.1).

Our work extends previous approaches by giving a general explanation of the temporal evolution of the full distribution of the generation interval and by confirming our theoretical results with detailed numerical simulations.

4.3 Results

4.3.1 Model formulation

We consider a simple and general model framework that covers a wide range of epidemiological model structures [52]. We define $S(t)$ as the proportion of susceptible individuals in the population at time t, $i(t)$ as the incidence rate – the rate at which new cases occur at time t – and $K(\tau)$ as the rate of secondary infections caused by an individual infected τ time units ago. (Note that the notation $I(t)$

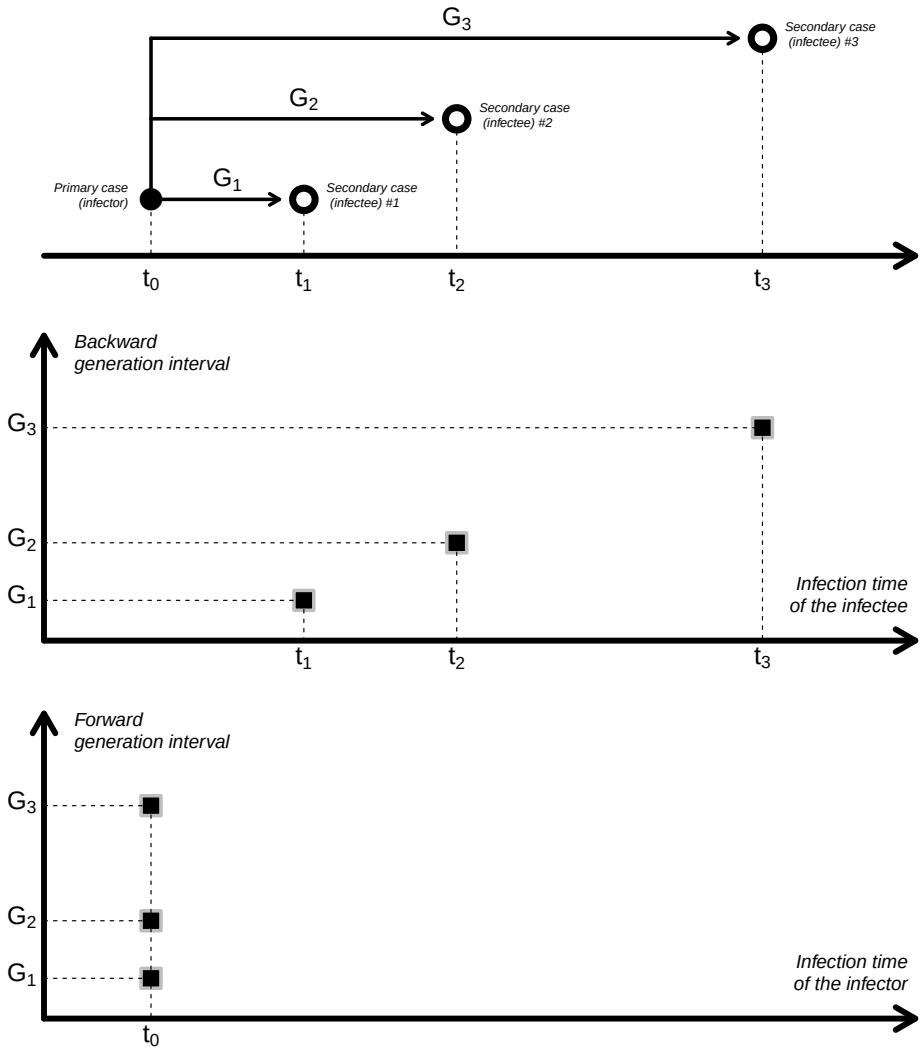

Figure 4.1. *Illustration of backward and forward generation intervals. Top panel illustrates the example of a primary case (solid circle), infected at time* t_0 *then infecting three other individuals (open circle), respectively at times* t_1, t_2 *and* t_3*. The generation intervals are defined as* $G_i = t_i - t_0$ *for* $i = 1, 2, 3$*. The middle panel plots the backward generation intervals (black squares), that is from the infectees' point of view. There is only one backward generation interval per infectee. The bottom panel plots the forward generation intervals (black squares) for the primary case. The x-axis represents the infection time of the infector, hence the three forward generation intervals are all defined at time* t_0*.*

is traditionally used for disease prevalence, hence our use of lower-case i for the incidence rate). We can conceptually separate K into two components and write $K(\tau) = F(\tau)\lambda(\tau)$, where $F(\tau)$ is the probability that an individual is infectious τ time units after being infected and $\lambda(\tau)$ is the mean infectiousness τ time units after an individual was infected, given that the individual is infectious at that time. Most compartmental models effectively assume that $\lambda(\tau)$ is a constant, but many factors could in theory affect mean infectiousness, including disease titers, how the disease spreads through the body and how active individuals are at various stages of the disease.

The number of infections occurring at time t caused by infectors who were themselves infected at time s (before t) is modeled as

$$i_s(t) = K(t-s)i(s)S(t), \tag{4.1}$$

The incidence at time t is then given by integrating over infections caused by infectors infected at different times:

$$i(t) = \int_0^t i_s(t)ds = S(t)\int_0^t K(t-s)i(s)ds \tag{4.2}$$

This formulation is known as the renewal equation.

In this model, the intrinsic infectiousness of a given infector, and thus the intrinsic generation interval, is described by $K(\tau)$. As we explain below, actual generation intervals that are observed (or estimated) as a disease spreads through a population do not necessarily correspond to the intrinsic generation interval.

Like several previous studies [81, 89, 95], we distinguish between taking the infector's point of view (looking forward in time to when secondary infections occur) or taking the infectee's (looking backward in time to when the infector was infected) – we call these *forward* and *backward* generation intervals, respectively (Figure 4.1). Hence, we define $f_s(\tau)$ as the distribution (over τ) of *forward* generation intervals for infections caused *by* individuals infected at time s and transmitting at time $s+\tau$. Similarly, $b_t(\tau)$ is the distribution of *backward* generation intervals for infections *of* individuals infected at time t by an infector infected τ time units ago.

Since every generation interval has an infector and infectee, and thus a forward and backward interpretation, it is not immediately obvious why these distribu-

tions should differ. As we will see below, the distinction is due to the way realized generation intervals change over time.

4.3.2 Intrinsic generation interval

From equation (4.1), we see that the intrinsic infectiousness of a given infector is simply described by $K(\tau)$. The basic reproductive number, which is the expected number infected by a single infectious individual in a totally susceptible population [2], is thus:

$$\mathcal{R}_0 \stackrel{def}{=} \int_0^\infty K(\tau)\,d\tau \tag{4.3}$$

The intrinsic generation-interval *distribution* is then obtained by normalizing the intrinsic infectiousness kernel:

$$g(\tau) \stackrel{def}{=} K(\tau)/\mathcal{R}_0 \tag{4.4}$$

The distribution g is what should be estimated in order to calculate $\mathcal{R}_0$ or to simulate disease spread. It is conceptually equivalent to the "basic" generation time introduced by Nishiura [81].

We can thus rewrite the renewal equation (4.2) in terms of $\mathcal{R}_0$ and $g(t)$:

$$i(t) = \mathcal{R}_0\, S(t) \int_0^t g(t-s)i(s)\,ds \tag{4.5}$$

4.3.3 Forward generation interval

To calculate the forward generation-interval distribution, we start with the instantaneous incidence (4.1) and condition on the time s when the infector became infected. Thus we replace t with $\tau = t - s$:

$$i_s(s+\tau) = \mathcal{R}_0\, i(s)g(\tau)S(s+\tau) \tag{4.6}$$

The expected number of secondary infections that will be generated per infector ($i(s) = 1$) is thus:

$$\int_0^\infty \mathcal{R}_0\, g(\tau)S(s+\tau)\,d\tau \tag{4.7}$$

Since $\mathcal{R}_0\, i(s)$ is assumed to be constant through time ($\mathcal{R}_0$ is a constant and we conditioned on time s), the forward generation-interval distribution for infectors infected at time s, f_s, is proportional to $g(\tau)S(s+\tau)$. So, its definition is simply obtained by normalizing:

$$f_s(\tau) \overset{def}{=} \frac{g(\tau)S(s+\tau)}{\int_0^\infty g(x)S(s+x)dx} \tag{4.8}$$

4.3.4 Backward generation interval

Again, using the instantaneous incidence (4.1) but now conditioning on t, the time when the infectee becomes infected, we have:

$$i_s(t) = \mathcal{R}_0\, i(t-\tau)\, g(\tau)\, S(t) \tag{4.9}$$

The force of infection on each susceptible individual is thus given by:

$$\int_0^\infty \mathcal{R}_0\, i(t-\tau)g(\tau)d\tau \tag{4.10}$$

Similarly to the forward case, we see that backward generation interval is proportional to $g(\tau)\, i(t-\tau)$, so its distribution is simply defined by normalizing:

$$b_t(\tau) \overset{def}{=} \frac{g(\tau)\, i(t-\tau)}{\int_0^\infty g(x)\, i(t-x)dx} \tag{4.11}$$

Finally, in the particular case where mean infectiousness λ is assumed constant over time, $K(\tau)$ is proportional to the probability $F(\tau)$, and we can write the three generation intervals directly in terms of F, the probability that a person is infectious at time τ after becoming infected:

$$g(\tau) = \frac{F(\tau)}{\int_0^\infty F(x)dx} \tag{4.12}$$

$$f_s(\tau) = \frac{F(\tau)S(s+\tau)}{\int_0^\infty F(x)S(s+x)dx} \tag{4.13}$$

$$b_t(\tau) = \frac{F(\tau)\, i(t-\tau)}{\int_0^\infty F(x)\, i(t-x)\, dx} \tag{4.14}$$

4.3.5 Example

In this section, we illustrate the temporal evolution of the three generation-interval (intrinsic, backward and forward) distributions described by equations (4.4), (4.11) and (4.8) with a simple epidemiological model.

In Figures 4.2 and 4.3, we use the well-known SEIR compartmental model (Susceptible-Exposed-Infectious-Recovered) where we include n_E (resp. n_I) exposed (resp. infectious) compartments in order to model realistic duration of latency and infectiousness with Erlang distributions (Gamma distributions with integer shape parameter) [102]. We will refer to this model as an Erlang SEIR and details of this model are given in the Methods section below. This model was run with parameters: $n_E = n_I = 3$, $\mathcal{R}_0 = 4.0$, mean duration of latency and infectiousness both equal to 5 days.

Figure 4.2 shows how temporal variation in force of infection affects the backward generation interval b_t. Left, center and right columns represent calendar time points 20, 48 and 70 days after the start of the epidemic, respectively.

The first row shows g, the intrinsic generation-interval distribution. This does not change over the course of the epidemic, so the three figures on the first row are the same. The vertical dashed line at 8.3 days represents the mean of the distribution.

The second row shows the incidence curve i. The dotted curve is the incidence over the course of the whole epidemic. The open circle shows the current calendar time. The bold curve and the shaded area illustrate that we look backward to multiply the intrinsic generation distribution by the incidence curve shown to obtain the backward distribution (the width of the shaded area matches the width of the curve shown in the first row). The grey arrow shows the direction of integration, here looking backward from the current time. The third row depicts the backward generation-interval distribution (bold curve, with mean shown by a vertical bold line) resulting from Equation (4.11), which is the product of bold curves from the first (intrinsic generation interval) and second row (time-reversed incidence). The intrinsic generation interval (grey curve, mean shown by a ver-

tical grey line) is shown for comparison. Finally, the last row illustrates how the mean backward generation interval changes through time throughout the epidemic. The horizontal dashed line represents the mean intrinsic generation interval. The three circles represent the calendar time points (20, 48 and 70 days) chosen for the illustrations in the second and third rows.

Similarly, Figure 4.3 shows how temporal variation in the susceptible population affects forward generation interval f_s. Just as changes in the backward generation interval are explained by patterns of change in incidence, changes in the forward generation interval are explained by patterns of change in the proportion susceptible. Calendar time points were chosen to be 10, 38 and 50 days in this case. An animated version of Figures 4.2 and 4.3 is provided as file `movie_GI.gif` in http://dx.doi.org/10.5061/dryad.4dd3s.

The backward generation-interval distribution differs significantly from the intrinsic one, its mean increasing monotonically from 0 to values much larger than the mean intrinsic generation interval. The backward generation time is seen from the point of view of a susceptible: who is likely to infect them? Early in the epidemic, when the number of infectious individuals is increasing, the backward generation time tends to be short, because relatively more currently infectious individuals were infected recently. Similarly, when the epidemic is declining, there will be relatively fewer infectious individuals infected recently, tending to increase the backward generation time.

The forward generation interval is seen from the point of view of the infector: when are they likely to infect somebody? Since the number of susceptibles decreases throughout a single epidemic outbreak, there will always be relatively more susceptibles available soon after infection than later, so the mean forward generation time will always be less than the intrinsic generation time. Early and late in the epidemic, however, the number of susceptibles changes slowly, so the forward generation time is approximately the same as the intrinsic generation interval (Figure 4.3). The shorter generation interval in the middle of the epidemic may seem counter-intuitive: why do infections happen faster when susceptibles are being depleted rapidly? The answer is that we calculate the generation-interval distribution *conditional on an infection occurring*. As the number of susceptibles decreases the number of infections per infectious individual goes down, but the infections that do happen tend to happen faster, because the *relative* number of susceptibles is higher in the near future than later on. See middle panel of Figure 4.3.

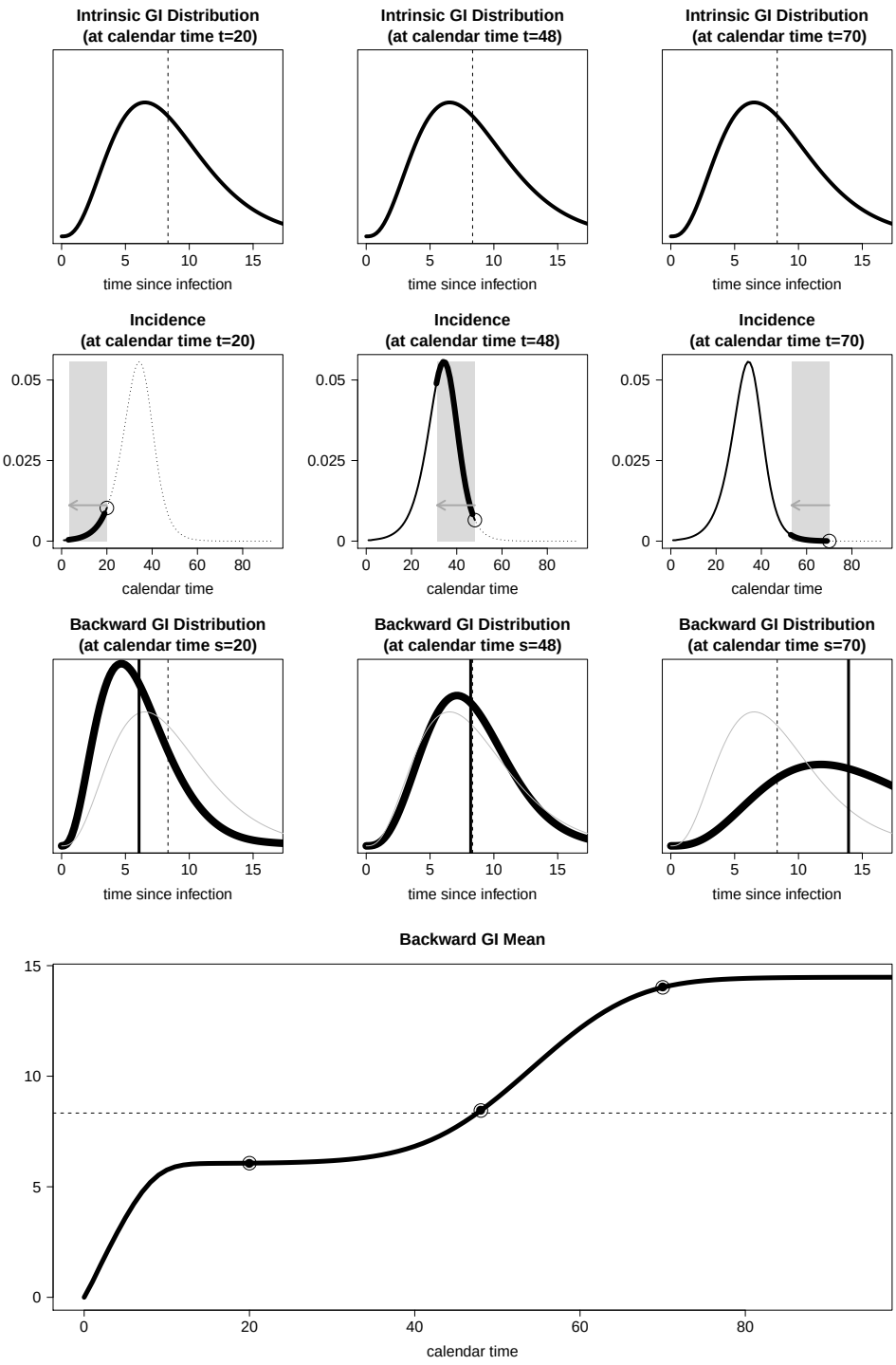

Figure 4.2. *Mean backward generation interval. See main text (section 4.3.5) for explanations.*

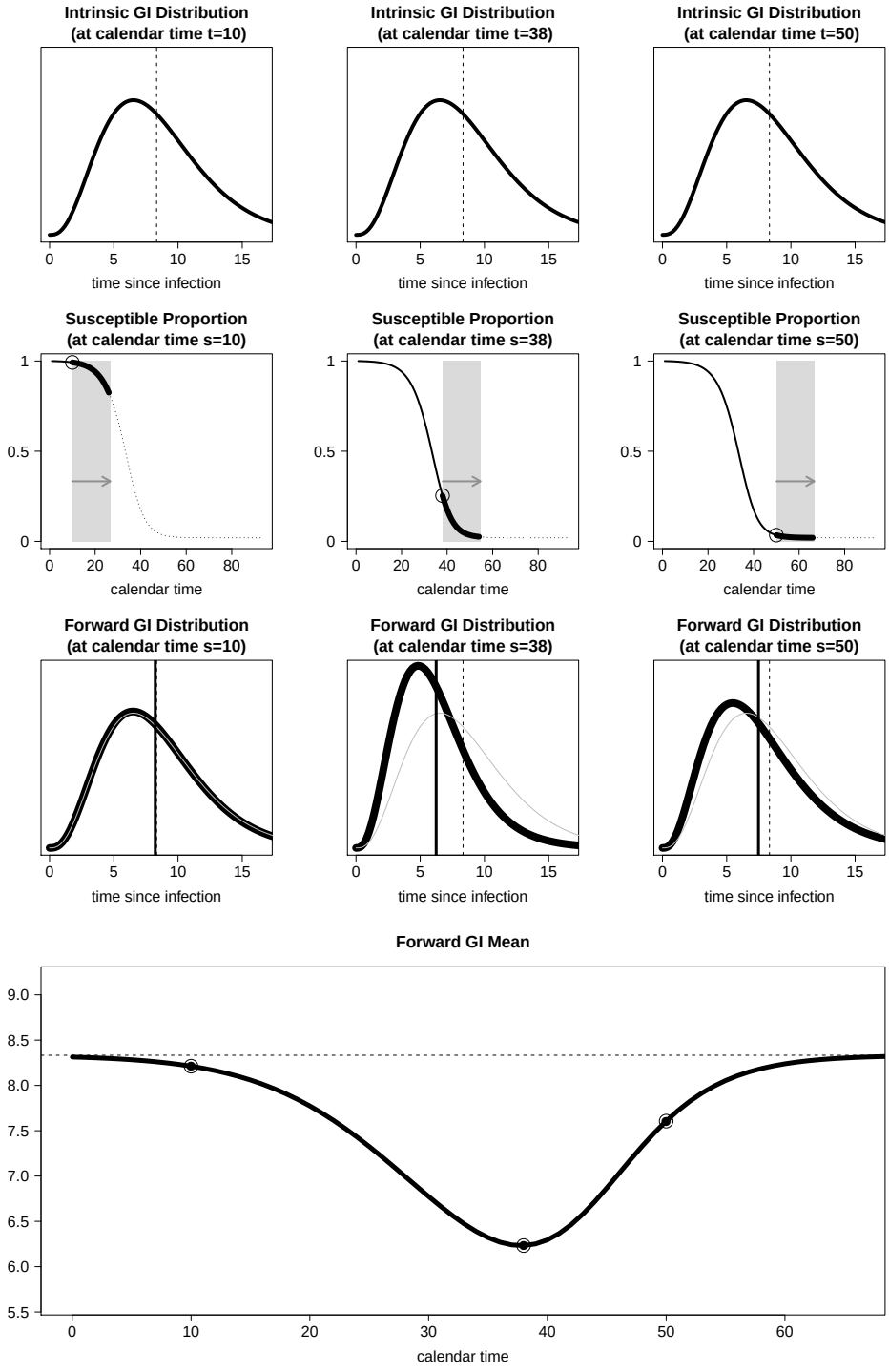

Figure 4.3. *Mean forward generation interval. See main text (section 4.3.5) for explanations*

Our example above is constructed with a particular value of $\mathcal{R}_0$. In Figure 4.4, we show how the mean generation intervals change through time for a range of $\mathcal{R}_0$ values. All else being equal, higher $\mathcal{R}_0$ leads to faster epidemics, and sharper deviations of both forward and backward generation intervals from the intrinsic generation-interval distribution g. Note that this figure is very similar to Figure 3 in [81], but with the important difference that here, we explicitly mark the epidemic end-points (solid circles in Figure 4.4) to illustrate the actual deviations that can be experienced in practice.

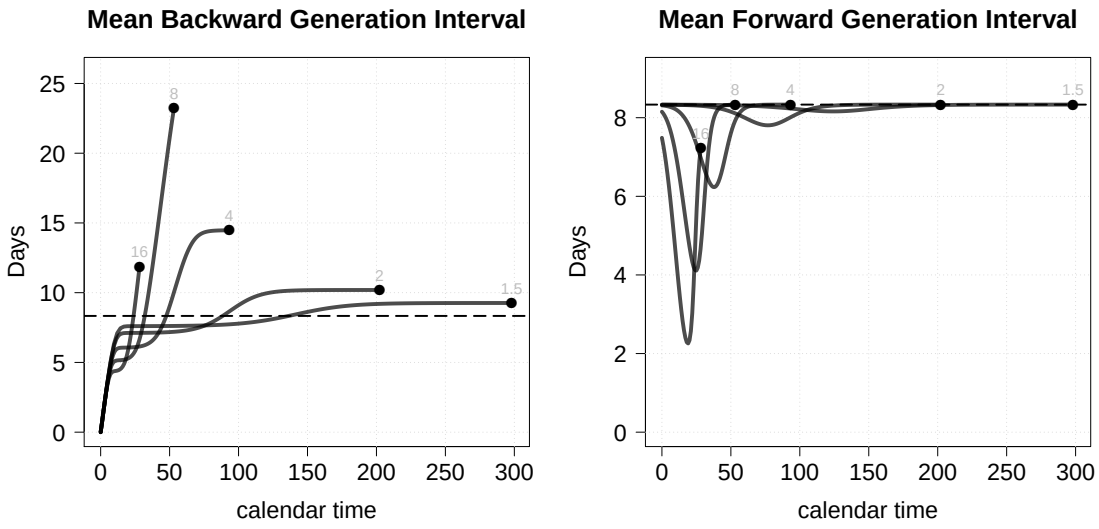

Figure 4.4. *Temporal evolution of mean backward and forward generation intervals for different values of $\mathcal{R}_0$. Curves were integrated until the time of last incident case (solid circle) and the value of $\mathcal{R}_0$ is indicated at this end-point (grey numbers). The horizontal dashed line is the mean intrinsic generation interval.*

4.3.6 Comparison with simulations

We compare the analytical formulations of both forward (4.13) and backward (4.14) generation intervals with stochastic simulations in the Erlang SEIR framework, assuming a constant infectiousness λ.

Figure 4.5 shows good agreement of the mean generation intervals (both forward and backward) between the stochastic simulations (using a Gillespie algorithm [46], see Methods section) and the numerical solutions of Equations (4.13) and (4.14).

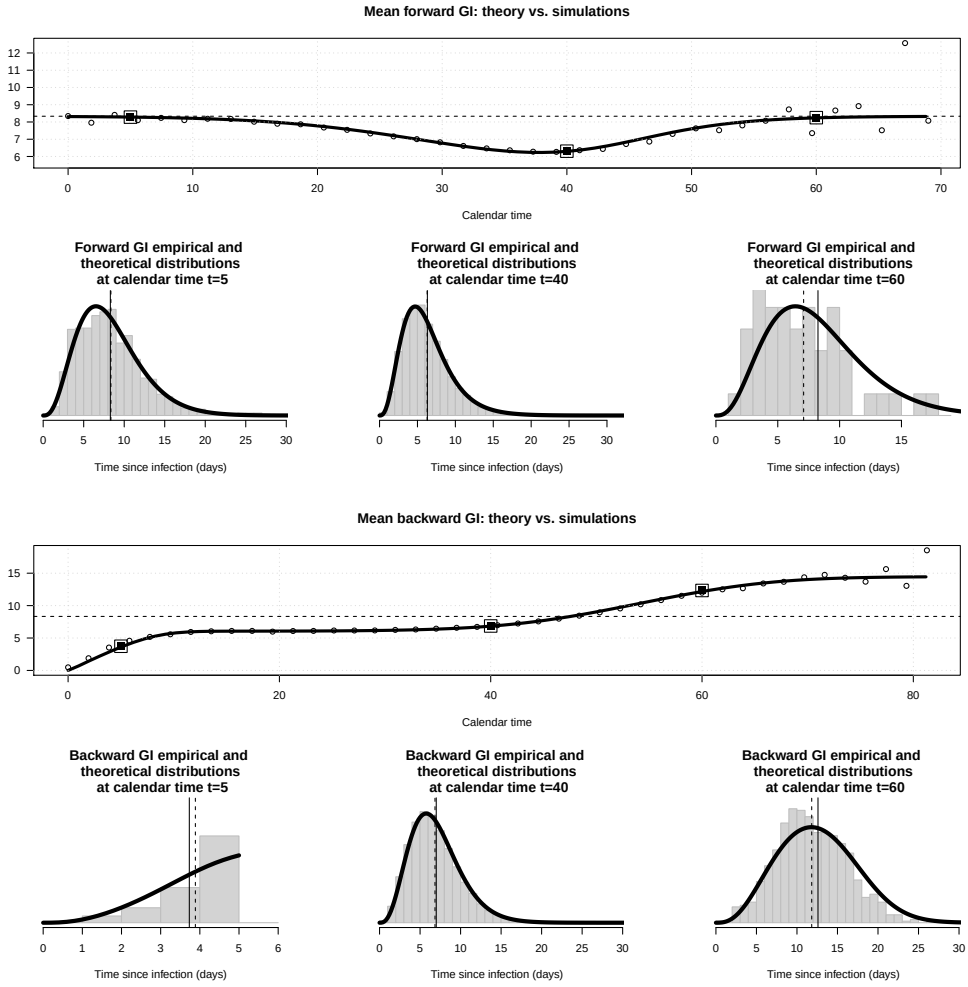

Figure 4.5. Mean generation intervals: theory v.s. simulations. *Numerical validation of forward and backward generation-interval distributions. Top panel: the thick line is the mean of the forward generation interval obtained by integrating equation (4.13). The open circles represent the mean of the forward generation intervals from stochastic simulations. The horizontal dashed line depicts the mean intrinsic generation interval. The three squares show the calendar times chosen for the distribution in the second panel. Second panel: empirical (gray histogram) and theoretical (black line) forward generation-interval distribution at calendar times 5, 40 and 60 days. Third and fourth panels represent the same quantities as the first and second panels, but for the backward generation interval using equation (4.14). Model parameters:* $\mathcal{R}_0 = 4$; $\mathfrak{n}_E = \mathfrak{n}_I = 3$; *mean latency and mean infectious duration both equal 5 days; Monte-Carlo iterations = 30; population size= 25,000.*

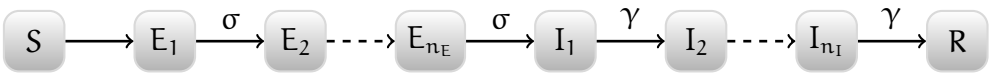

Figure 4.6. *Erlang SEIR model.*

4.4 Methods

4.4.1 Compartmental model

To estimate generation-interval distributions for our examples, we used numerical simulations with a flexible compartmental model: a classical SEIR model (Susceptible-Exposed-Infectious-Recovered) with n_E (resp. n_I) sub-compartments for the exposed (resp. infectious) state [1, 5] (Figure 4.6). This modelling framework implicitly specifies Erlang-distributed (i.e. Gamma distribution with integer shape parameter) duration of latency and infectiousness which can reasonably approximate real epidemiological observations [102]. A deterministic formulation of this model is given by a system of differential equations. Let S be the proportion of susceptible individuals in the whole population; E_k the proportion of individuals in the k^{th} compartment of latency (i.e., infected but not infectious yet); I_k the proportion of individuals in the k^{th} compartment of infectiousness; β the constant effective contact rate; σ the average rate of progression from one latency stage to the next; γ the average rate of progression from one infectious stage to the next. The model is given by the system of equations (4.15):

$$S'(t) = -\beta S(t) \sum_{k=1}^{n_I} I_k(t) \tag{4.15a}$$

$$E_1'(t) = \beta S(t) \sum_{k=1}^{n_I} I_k - \sigma E_1(t) \tag{4.15b}$$

$$E_m'(t) = \sigma(E_{m-1}(t) - E_m(t)) \quad \text{for } m = 2, ..., n_E \tag{4.15c}$$

$$I_1'(t) = \sigma E_{n_E}(t) - \gamma I_1(t) \tag{4.15d}$$

$$I_n'(t) = \gamma(I_{n-1}(t) - I_n(t)) \quad \text{for } n = 2, ..., n_I \tag{4.15e}$$

Similarly, a system of differential equations defines the probability of residency in a given latent or infectious state for individuals infected at a fixed time s. We

define $L_k(\tau)$ as the probability that an individual infected τ time units ago is in the k^{th} latent stage E_k; $F_k(\tau)$ as the probability that an individual infected τ time units ago is in the k^{th} infectious stage I_k. We have:

$$L_1'(\tau) = -\sigma L_1(\tau) \tag{4.16a}$$
$$L_m'(\tau) = \sigma(L_{m-1}(\tau) - L_m(\tau)) \quad \text{for } m = 2, ..., n_E \tag{4.16b}$$
$$F_1'(\tau) = \sigma L_{n_E}(\tau) - \gamma F_1(\tau) \tag{4.16c}$$
$$F_n'(\tau) = \gamma(F_{n-1}(\tau) - F_n(\tau)) \quad \text{for } n = 2, ..., n_I \tag{4.16d}$$

with the initial conditions $L_1(0) = 1$, $L_k(0) = 0$ for all $k = 2, ..., n_E$ and $F_k(0) = 0$ for all $k = 2, ..., n_I$.

We solved both systems (4.15) and (4.16) numerically using the `lsoda` method from the **R** [82] package `deSolve` [94] version 1.11.

4.4.2 Stochastic simulations

We validated the results from our deterministic model (4.15), by implementing a discrete-state stochastic version of this model using an exact Gillespie algorithm [46]. Briefly, this algorithm simulates exponentially distributed event times for progression from one state to the next one (e.g. from susceptible (S) to exposed (E)). Both the intensity and event type frequency depend on the rates defined in (4.15). We extend the classical Gillespie algorithm by identifying every individual in the simulation. Hence we can keep track of the generation intervals at pre-specified times both from the infector (forward) and the infectee (backward) view points. The outputs of interest from a simulation are pairs of generation interval (forward or backward) and calendar time (time elapsed since the start of the epidemic). Simulated generation intervals are aggregated and averaged in one-day time buckets. A detailed description of this algorithm is given in Algorithm 1. The full code to replicate all results and figures of this study is available at http://dx.doi.org/10.5061/dryad.4dd3s.

Algorithm 1: Simplified Gillespie algorithm for the Erlang SEIR model

Input: Time horizon T, contact rate β, number of I (resp. E) compartments n_I (resp. n_E), mean residency time in any I compartments $1/\gamma$, mean residency time in any E compartments $1/\sigma$, initial number of infectious individuals i_0, total population N.

$t \leftarrow 0$
$S[0] \leftarrow N - i_0$
$E_k[0] \leftarrow 0$ for all $k > 0$
$I_1[0] \leftarrow i_0$
$I_k[0] \leftarrow 0$ for all $k > 1$
while $t < T$ **do**
    /* Draw the next event time τ */
    $\lambda_S \leftarrow \beta S[t] \sum_{k=1}^{n_I} I_k[t]/N$
    $\lambda_E \leftarrow \frac{\sigma}{n_E} \sum_{k=1}^{n_E} E_k[t]$
    $\lambda_I \leftarrow \frac{\gamma}{n_I} \sum_{k=1}^{n_I} I_k[t]$
    $\lambda \leftarrow \lambda_S + \lambda_E + \lambda_I$
    $\tau \sim \text{Exp}(\lambda)$
    /* Draw the next event type */
    $u \sim \text{Uniform}(0, \lambda)$
    if $u < \lambda_S$ **then**
        /* event type is new infection */
        Pick randomly a new infectee among $S[t]$: individual a
        Set infection time for individual a at $t + \tau$
        Pick randomly its infector among $I_1[t], ..., I_{n_I}[t]$: individual c
        /* calculate generation interval */
        $G \leftarrow t + \tau - \text{time.acquisition}(c)$
        /* backward generation interval for individual a (infectee) */
        $b(a) \leftarrow G$
        /* forward generation interval for individual c (infector) */
        $f(c) \leftarrow \text{vector}(f(c), G)$
    else
        /* event type is not infection */
        Pick randomly individual in ad hoc compartment (based on u value)
        Move this individual to the next compartment
    end

    $t \leftarrow t + \tau$
end

4.5 Practical implication

During the early phase of a pathogen outbreak, generation interval information is strongly "censored", since a relatively large proportion of infections are still ongoing. This information cannot be used to reliably estimate forward generation intervals, but can estimate backward generation intervals (or it may simply be lumped, which has a similar effect as using backward intervals). A naive – but common – approach is to use the mean (and sometimes the variance) of this data to inform the intrinsic generation interval distribution g of a mathematical model (e.g., used for forecasting). This method will lead to a systematic bias: since shorter generation intervals are more likely to have concluded (and thus be observed), the mean generation interval will be systematically underestimated [81]. An alternative approach is to fit the backward generation interval distribution b of the model (obtained with (4.11)) to the backward contact tracing data at each available calendar time. As an approximation to fitting the whole distribution, one can aim to fit both the mean and variance of the backward generation interval distribution to the data.

The backward generation interval fit to the mean and variance is illustrated in Figure 4.7, where contact tracing data was simulated from an Erlang SEIR model. The potential pitfalls of naively fitting, without recognizing the difference between the intrinsic generation interval distribution g and the observed backward interval b is also shown (dashed lines): the resulting mean and variance of observed intervals are a noticeably poorer match to the data.

Note that, depending on the model complexity, the minimization problem can be high dimensional and there might be identifiability issues between parameters. Also, when the number of data points is small (very first days of the outbreak), fitting may be challenging because the mean of the backward generation interval distribution b is very insensitive to model parameters (see left panel of Figure 4.4).

This example serves as a simple illustration for an important point: data from contact-tracing can provide misleading information about a pathogen's underlying intrinsic generation interval g. The factors that underlie how the realized forward and backward generation intervals change through time should be taken into account when evaluating observed intervals. Future work on constructing a more elaborate and robust statistical framework to perform such fit is warranted.

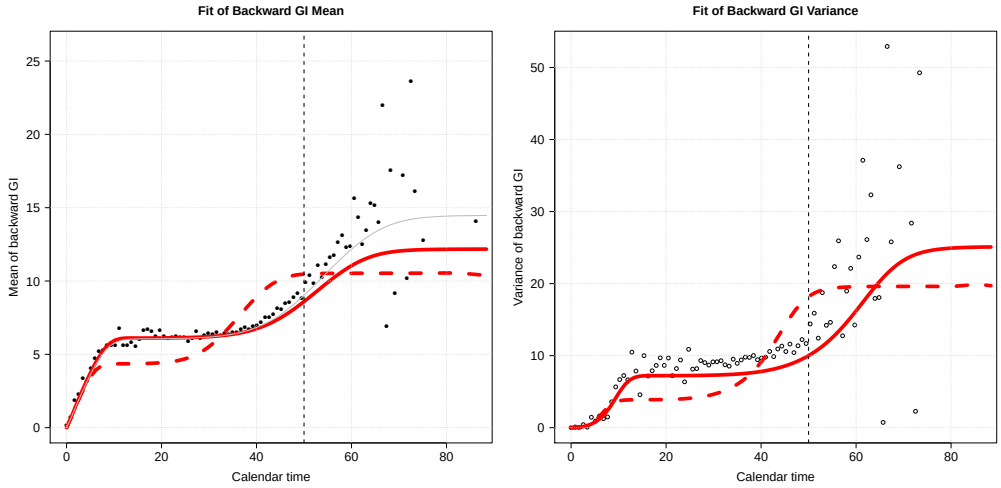

Figure 4.7. *Comparison between fitting the backward (*$\mathfrak{b}$*) or intrinsic (*$\mathfrak{g}$*) generation interval distribution of an Erlang SEIR model to synthetic data. Model parameters used to generate the data were* $\mathcal{R}_0 = 4$*;* $n_E = n_I = 3$*; mean latency and mean infectious duration both equal to 5 days; population size at 25,000.* ***Left panel****: Fit to the mean of the backward generation interval distribution. Solid black circles are the simulated backward generation intervals data. The red solid thick curve is the fitted mean backward generation interval* $\mathfrak{b}$ *from the Erlang SEIR model to the mean backward generation intervals data. The red dashed thick curve is the fitted mean backward generation interval* $\mathfrak{b}$ *when fitting (naively) the* intrinsic *distribution* $\mathfrak{g}$ *from the same Erlang SEIR model to the backward generation intervals data. The thin grey curve is* $\mathfrak{b}$ *when using the "true" parameter values that generated the simulated data.* ***Right panel****: Fit to the variance of the backward generation interval distribution. Open circles represent the simulated data. The red thick solid line is the variance of the fitted distribution* $\mathfrak{b}$ *when fitting* $\mathfrak{b}$ *to the simulated backward generation intervals data. The red thick dashed line represents the variance of the fitted distribution* $\mathfrak{b}$ *when (naively) fitting the intrinsic distribution* $\mathfrak{g}$ *to the simulated backward generation intervals data. Only the points to the left of the vertical dashed line (at calendar time 50) were used in both fits. An approximate Bayesian Computation method with 1000 iterations was performed for both fits.*

4.6 Discussion

Conceptually, there are three generation-interval distributions (Table 4.1). We called the first "intrinsic" generation-interval distribution, which defines theoretically the disease transmission process. This is the distribution typically used in mathematical models, such as in the well-known renewal equation (4.2), and is often assumed invariant with respect to time. Variation in intrinsic generation interval, if it occurs, is driven by changes in the biological or social processes underlying disease transmission, e.g. quarantines or social-distancing practices, but not by the spread of disease *per se*. The other two generation-interval distributions are typically obtained by *observing* the actual infection time differences between the infector and its infectee. If the point of view is from the infectee, then there is only one interval to consider and this defines the so-called "backward" generation interval. If we take the infector's viewpoint, then there are potentially several generation intervals (because the infector could have infected several individuals) and this defines the "forward" generation interval (Figure 4.1). In other words, if we believe generation intervals are drawn from their respective distribution (i.e., b and f with our notations), then the backward generation interval we get in the first place is a single draw, whereas the latter represents several draws.

Table 4.1. *The three generation-interval distributions*

Generation-interval distribution type	**Notation**	**Usage**	**Defining Equation**
Intrinsic	g	Mathematical modelling	(4.4)
Backward	b	Observed when a cohort is investigated by looking backward in time to see who infected each individual.	(4.11)
Forward	f	Observed when a cohort is tracked forward in time to see who individuals infect.	(4.8)

We have developed a theoretical framework that explains the temporal variation of both backward and forward generation-interval distributions. We confirm the findings from Nishiura [81] that were derived for mean generation intervals in the context of exponential growth of incidence. We extend their interpretability to the

whole generation-interval distribution (not the mean only) in a general modelling framework (no exponential growth assumption). In particular, our interpretation does not involve the concept of competition between infectors [66].

Our theoretical results were confirmed with numerical simulations, using an Erlang SEIR compartmental model. Note that other sorts of models should work equally well, as long as it is possible to derive analytically or numerically the proportion of susceptible individuals S, the incidence $\mathfrak{i}$ and the probability F to be infectious τ time units after being infected.

As noted by previous studies [66,81,89,95], the temporal shape of the mean backward generation interval in Figure 4.2 has important modelling consequences. Indeed, the mean backward generation interval can remain significantly below (resp. above) the mean intrinsic generation interval early (resp. late) in the epidemic. So, estimates of the generation intervals obtained by contact tracing can underestimate (when observed too early) or overestimate (when observed too late) the mean intrinsic generation interval. This is related to the problem of "length-biased sampling" [93]. Put simply, generation intervals measured through contact-tracing may be a biased estimate of the intrinsic generation interval. In particular, if estimates of b are used to estimate g early in an epidemic, the length of the generation interval is likely to be underestimated. This effect is more pronounced when the reproductive number of the epidemic considered is large (Figure 4.4).

An important application of generation intervals is the estimation of the basic reproductive number $\mathcal{R}_0$, which is in turn used for various public health decisions. The *intrinsic* generation-interval distribution g is the link between the observed growth rate (incidence data) and $\mathcal{R}_0$ [101]. If g is systematically underestimated, as discussed above, $\mathcal{R}_0$ is likely to be underestimated as well (see [81] for an example illustrating this issue on Dutch influenza data).

Our work suggests a possible methodology to correct for these potential pitfalls: if it is possible to derive (analytically or numerically) from the mathematical model either the intrinsic generation-interval distribution g or the probability F to be infectious after a given duration from the infection time, then modellers can derive the backward (or forward) generation-interval distribution from equations (4.11) and (4.14), and fit this distribution (and not g) to the relevant contact tracing data.

There are some limitations to our work. First, while we consider generation inter-

vals, in practice serial intervals (the interval between *symptom onset* in the infector and symptom onset in the infectee) are easier to observe for many diseases. Serial intervals are less tractable theoretically and in general do not have the same distribution as generation intervals. However, in some settings their distribution can be strongly correlated or even identical [44, 95]. Second, our theoretical framework relies on the assumption of homogeneous mixing. Although this is a common assumption, heterogeneity is often very important in practice (see [73] for example), and could affect the patterns found here. Third, we do not account for the possibility that mixing rates or the course of infection change through time, for example due to seasonality, awareness of the epidemic, or medical intervention. Like earlier authors, we focus on the intrinsic dynamics of the disease system. Fourth, a robust, statistically based method to infer model parameters associated to generation intervals from observable data available early in an epidemic is still needed. Statistical methods have been proposed to estimate intrinsic generation intervals (see for example [18, 32, 54]), but further work is necessary to extend these methods to our framework, for example constructing estimation methods directly using the backward generation interval distribution in the context of missing data. Establishing a link between our framework and the serial interval (the most likely observable quantity) is also warranted.

Informing the generation-interval distribution of a mathematical model from contact tracing data is not straightforward, and a naive approach can lead to spurious epidemiological projections from the model. Extending previous work, our study provides a clear and coherent theoretical framework to understand and assess the differences between three conceptually distinct generation-interval distributions. Future work should consider building statistical tools leveraging our study on real contact tracing data.

Data Availibility

The computer code that was used to generate the numerical results and figures in this study is available on Dryad at http://dx.doi.org/10.5061/dryad.4dd3s.

Chapter 5

Conclusion

PUBLIC health can benefit from mathematical models to inform and support its decisions to control the spread of infectious diseases. Thanks to the growing amount of epidemiological data and computing power available, it is now possible to model epidemics relatively realistically. But data is not a necessary ingredient for a mathematical model to be relevant. Just the activity of modelling can raise questions that would never have been asked otherwise. Moreover, the analysis of complex mechanisms through the lens of mathematical models can bring unique and highly relevant insights. Indeed, non-linear effects resulting from the transmission process and potential interventions are difficult to comprehend without them. This is what this thesis explored: understand various complex epidemiological mechanisms and incorporate existing data in order to inform public health issues.

In chapter 2, we investigated the importance of within-couple transmission compared to other sexual transmission routes. Assessing their respective contribution to the HIV epidemic is critical to design effective intervention strategies. A deterministic compartmental model with an innovative, yet simple, design for partnership dynamics was developed. Using Demographic and Health Surveys from Sub-Sahara African countries to inform model parameters, we found this route rarely represents the majority of transmissions. This study was also the first to carefully define the contribution to each sexual transmission route (Figure 2.2), and shed some light on the correlation between the proportion of serodiscordant couples in a given population and the intensity of within-couple transmission (discordance statistic $\mathcal{D}$, equation (2.6)). This model and the mechanistic

understandings derived are relevant to other sexually transmitted infection epidemics.

The impact of a hypothetical vaccine against syphilis was analyzed in chapter 3. In contrast to the HIV serodiscordant couples study, a relatively complex "agent-based" mathematical model was used. This type of model was a natural candidate because demographic, partnership and biological dynamics had all to be taken into account, in a relatively realistic way (*e.g.,* risk behaviour heterogeneity, gender-specific, co-infections effects, etc.). Our results suggest that an efficacious vaccine has the potential to sharply reduce syphilis under a wide range of scenarios. Because of the epidemiological synergy between HIV and syphilis (it is suspected that they promote transmission and acquisition of each other), the impact of the syphilis vaccine on HIV morbidity was also considered. Surprisingly, even by accounting for the HIV/syphilis co-infection interactions, the decrease in syphilis prevalence following vaccination had little effect on the HIV epidemic. Another unexpected effect was the small increase of HIV incidence in settings with a large proportion of high risk behaviour. This study is the first to investigate the morbidity impact of a hypothetical syphilis vaccine. The modelling framework developed here can readily be used to investigate similar immunization questions regarding other sexually transmitted infections.

Beyond specific pathogens, chapter 4 revisited a fundamental quantity in mathematical models applied to epidemiology: the generation interval distribution. Despite earlier work, there was no satisfactory framework that defined the different forms of generation interval (*i.e.,* intrinsic, forward and backward), explained how their distribution changes as the epidemic unfolds, or linked them to contact-tracing data. Our study clarified these concepts and suggested a new methodology to correctly inform mathematical models from observed generation-interval data.

There are many limitations to the findings presented in this thesis and many of them were discussed in each chapter. The overarching limitation for the STIs studies (chapters 2 and 3), is the limited quantity and quality of data regarding partnerships and sexual behaviours. These studies mostly relied on surveys, the reliability of which have been questioned, for example by [53]. Hence, results from our analyses may be calibrated on data that are not representative of reality.

For the more theoretical investigation about the generation interval (chapter 4),

the limitation is again associated with data. Infection times – which define the generation interval – are rarely observable, whereas symptoms onset are. This limits the practical applications, although it could be argued that these distributions are the same for pathogens for which infectiousness begins only after symptoms appear. Moreover, building the transmission tree that informs our mathematical model may not be fully reliable because the epidemiological field work of contact-tracing is also error-prone.

Although the limitations about behavioural data cannot be overcome at a large scale today, they have already been directly addressed in various studies, thanks to molecular sequencing. Because of the exponentially decreasing cost of sequencing, it is now possible to reconstruct the phylogeny of pathogens infecting a given population and then, infer the most likely transmission tree. The advantage of this method is that it does not rely on individuals' memory or honesty to reconstruct the transmission tree. Such phylogenetic reconstruction with mathematical modelling in mind has already been made ([11]). This is definitely an avenue to explore for transmission trees in general (benefiting the work in chapter 4), but especially for STI models.

As mentioned in the Introduction of this thesis, thanks to increasing computing power, mathematical models are getting more complex in order to include numerous epidemiological mechanisms and/or embrace diverse data sets. This often results in models with a large number of parameters, making the interpretation of results difficult. Sensitivity analyses of model parameters could be a simple way to assess the robustness of interpretations, but they may not be feasible because the computing time needed would be an order of magnitude higher (for example, performing a full sensitivity analysis on the agent-based model in chapter 3 would take months with the computing power available today). Technological breakthroughs, like quantum computers, may allow computational models to reach this next level.

To conclude, as illustrated by the studies presented in this thesis, a broad range of mathematical and computational tools are available to support and inform public health issues. At one end of the spectrum, theoretical studies help define concepts and understand mechanisms. At the other end, computational models help to bridge the theoretical world with observed epidemiological data.

Bibliography

[1] D. ANDERSON AND R. WATSON, *On the spread of a disease with gamma distributed latent and infectious periods*, Biometrika, 67 (1980), pp. 191–198.

[2] R. M. ANDERSON AND R. M. MAY, *Infectious Diseases of Humans - Dynamics and Control*, Oxford University Press, 1991.

[3] A. BABIKER, S. DARBY, D. DE ANGELIS, D. KWART, K. PORTER, V. BERAL, J. DARBYSHIRE, N. DAY, N. GILL, AND R. COUTINHO, *Time from HIV-1 seroconversion to AIDS and death before widespread use of highly-active antiretroviral therapy: a collaborative re-analysis*, The Lancet, 355 (2000), pp. 1131–1137.

[4] R. F. BAGGALEY AND T. D. HOLLINGSWORTH, *Brief Report: HIV-1 Transmissions During Asymptomatic Infection: Exploring the Impact of Changes in HIV-1 Viral Load Due to Coinfections.*, Journal of acquired immune deficiency syndromes (1999), 68 (2015), pp. 594–598.

[5] N. T. J. BAILEY, *Some stochastic models for small epidemics in large populations*, Appl. Statist, 13 (1964), pp. 9–19.

[6] M. BARBIERI, V. HERTRICH, AND M. GRIEVE, *Age difference between spouses and contraceptive practice in sub-Saharan Africa*, Population (english edition), 60 (2005), pp. 617–654.

[7] M. S. BARTLETT, *Measles periodicity and community size*, Journal of the Royal Statistical Society. Series A (General), 120 (1957), pp. 48–70.

[8] S. E. BELLAN, K. J. FIORELLA, D. Y. MELESSE, W. M. GETZ, B. G. WILLIAMS, AND J. DUSHOFF, *Extra-couple HIV transmission in sub-Saharan Africa: a mathematical modelling study of survey data*, The Lancet, 381 (2013), pp. 1561–1569.

[9] S. M. BERMAN, *Maternal syphilis: pathophysiology and treatment.*, BULLETIN-WORLD HEALTH ORGANIZATION, 82 (2004), pp. 433–438.

[10] D. BERNOULLI, Essai d'une nouvelle analyse de la mortalite causee par la petite verole, et des avantages de l'inoculation pour la prevenir, Mémoires de Mathématiques et Physiques de l'Académie Royale des Sciences, (1766).

[11] D. BEZEMER, A. CORI, O. RATMANN, A. VAN SIGHEM, H. S. HERMANIDES, B. E. DUTILH, L. GRAS, N. RODRIGUES FARIA, R. VAN DEN HENGEL, A. J. DUITS, P. REISS, F. DE WOLF, C. FRASER, AND ATHENA OBSERVATIONAL COHORT, *Dispersion of the HIV-1 Epidemic in Men Who Have Sex with Men in the Netherlands: A Combined Mathematical Model and Phylogenetic Analysis*, PLoS Medicine, 12 (2015), p. e1001898.

[12] M.-C. BOILY, R. F. BAGGALEY, L. WANG, B. MASSE, R. G. WHITE, R. J. HAYES, AND M. ALARY, *Heterosexual risk of HIV-1 infection per sexual act: systematic review and meta-analysis of observational studies*, The Lancet Infectious Diseases, 9 (2009), pp. 118–129.

[13] BRANDON L. GUTHRIE, GUY DE BRUYN, AND CAREY FARQUHAR, *HIV-1-Discordant Couples in Sub-Saharan Africa: Explanations and Implications for High Rates of Discordancy*, Current HIV Research, 5 (2007), pp. 416–429.

[14] N. BROUTET, U. FRUTH, C. DEAL, S. L. GOTTLIEB, H. REES, AND O. B. O. P. O. T. . S. V. T. CONSULTATION, *Vaccines against sexually transmitted infections: The way forward*, Vaccine, 32 (2014), pp. 1630–1637.

[15] K. BUCHACZ, P. PATEL, M. TAYLOR, P. R. KERNDT, R. H. BYERS, S. D. HOLMBERG, AND J. D. KLAUSNER, *Syphilis increases HIV viral load and decreases CD4 cell counts in HIV-infected patients with new syphilis infections*, AIDS (London, England), 18 (2004), pp. 2075–2079.

[16] C. E. CAMERON AND S. A. LUKEHART, *Current status of syphilis vaccine development: Need, challenges, prospects*, Vaccine, 32 (2014), pp. 1602–1609.

[17] S. CASSELS, S. CLARK, AND M. MORRIS, *Mathematical models for HIV transmission dynamics: tools for social and behavioral science research*, JAIDS Journal of Acquired Immune Deficiency Syndromes, 47 (2008), p. S34.

[18] S. CAUCHEMEZ, P.-Y. BOËLLE, G. THOMAS, AND A.-J. VALLERON, *Estimating in Real Time the Efficacy of Measures to Control Emerging Communicable Diseases*, American Journal of Epidemiology, 164 (2006), pp. 591–597.

[19] CDC, *Report of the NIH Panel to Define Principles of Therapy of HIV Infection and Guidelines for the Use of Antiretroviral Agents in HIV-Infected Adults and Adolescents*, MMWR. Morbidity and mortality weekly report, 47 (1998), pp. 1–91.

[20] ——, *Syphilis Elimination Communication Plan*, (2001), pp. 1–23.

[21] ——, *The National Plan to Eliminate Sphilis from the United States*, (2006), pp. 1–66.

[22] ——, *Sexually Transmitted Disease Surveillance 2014*, tech. rep., Nov. 2015.

[23] C. CELUM, R. S. WANG, N. MUGO, A. MUJUGIRA, J. M. BAETEN, J. I. MULLINS, J. P. HUGHES, E. A. BUKUSI, C. R. COHEN, E. KATABIRA, A. RONALD, C. FARQUHAR, G. J. STEWART, J. MAKHEMA, M. ESSEX, E. WERE, K. H. FIFE, G. DE BRUYN, G. E. GRAY, J. A. MCINTYRE, R. MANONGI, S. KAPIGA, D. COETZEE, S. ALLEN, M. INAMBAO, K. KAYITENKORE, E. KARITA, W. KANWEKA, S. DELANY, H. REES, B. VWALIKA, W. STEVENS, M. S. CAMPBELL, K. K. THOMAS, R. W. COOMBS, R. MORROW, W. L. H. WHITTINGTON, M. J. MCELRATH, L. BARNES, AND R. RIDZON, *Acyclovir and Transmission of HIV-1 from Persons Infected with HIV-1 and HSV-2*, New England Journal of Medicine, 362 (2010), pp. 427–439.

[24] D. CHAMPREDON, S. E. BELLAN, W. DELVA, S. HUNT, C.-F. SHI, M. SMIEJA, AND J. DUSHOFF, *The effect of sexually transmitted co-infections on HIV viral load amongst individuals on antiretroviral therapy: a systematic review and meta-analysis*, BMC infectious diseases, 15 (2015), pp. 1–11.

[25] D. J. CHAN, L. MCNALLY, M. BATTERHAM, AND D. E. SMITH, *Relationship between HIV-RNA load in blood and semen in antiretroviral-naïve and experienced men and effect of asymptomatic sexually transmissible infections.*, Current HIV Research, 6 (2008), pp. 138–142.

[26] H. CHEMAITELLY AND L. J. ABU-RADDAD, *External infections contribute minimally to HIV incidence among HIV sero-discordant couples in sub-Saharan Africa*, Sexually transmitted infections, 89 (2012), pp. 138–141.

[27] H. CHEMAITELLY, I. CREMIN, J. SHELTON, T. B. HALLETT, AND L. J. ABU-RADDAD, *Distinct HIV discordancy patterns by epidemic size in stable sexual partnerships in sub-Saharan Africa*, Sexually transmitted infections, 88 (2012), pp. 51–57.

[28] H. CHEMAITELLY, J. D. SHELTON, T. B. HALLETT, AND L. J. ABU-RADDAD, *Only a fraction of new HIV infections occur within identifiable stable discordant couples in sub-Saharan Africa*, AIDS (London, England), 27 (2013), pp. 251–260.

[29] B. J. COBURN, D. J. GERBERRY, AND S. BLOWER, *Quantification of the role of discordant couples in driving incidence of HIV in sub-Saharan Africa*, The Lancet Infectious Diseases, 11 (2011), pp. 263–264.

[30] M. S. COHEN, G. M. SHAW, A. J. MCMICHAEL, AND B. F. HAYNES, *Acute HIV-1 infection*, New England Journal of Medicine, 364 (2011), pp. 1943–1954.

[31] K. L. COOKE AND J. A. YORKE, *Some equations modelling growth processes and gonorrhea epidemics*, Mathematical Biosciences, 16 (1973), pp. 75–101.

[32] B. J. COWLING, V. J. FANG, S. RILEY, J. S. MALIK PEIRIS, AND G. M. LEUNG, *Estimation of the Serial Interval of Influenza*, Epidemiology, 20 (2009), pp. 344–347.

[33] K. M. DE COCK, M. G. FOWLER, E. MERCIER, AND I. DE VINCENZI, *Prevention of mother-to-child HIV transmission in resource-poor countries: translating research into policy and practice*, JAMA, (2000).

[34] D. DE WALQUE, *SeroDiscordant Couples in Five African Countries: Implications for Prevention Strategies*, Population and development review, 33 (2007), pp. 501–523.

[35] O. DIEKMANN, K. DIETZ, AND J. HEESTERBEEK, *The basic reproduction ratio for sexually transmitted diseases: I. Theoretical considerations*, Mathematical Biosciences, 107 (1991), pp. 325–339.

[36] O. DIEKMANN, J. HEESTERBEEK, AND J. METZ, *On the definition and the computation of the basic reproduction ratio R 0 in models for infectious diseases in heterogeneous populations*, Journal of Mathematical Biology, 28 (1990), pp. 365–382.

[37] K. DIETZ AND K. HADELER, *Epidemiological models for sexually transmitted diseases*, Journal of Mathematical Biology, 26 (1988), pp. 1–25.

[38] D. DONNELL, J. M. BAETEN, K. K. THOMAS, W. STEVENS, C. R. COHEN, J. MCINTYRE, C. CELUM, AND F. T. P. I. P. H. H. T. S. TEAM, *Heterosexual HIV-1 transmission after initiation of antiretroviral therapy: a prospective cohort analysis*, The Lancet, 375 (2010), pp. 2092–2098.

[39] K. DUNKLE, R. STEPHENSON, E. KARITA, E. CHOMBA, K. KAYITENKORE, C. VWALIKA, L. GREENBERG, AND S. ALLEN, *New heterosexually transmitted HIV infections in married or cohabiting couples in urban Zambia and Rwanda: an analysis of survey and clinical data*, The Lancet, 371 (2008), pp. 2183–2191.

[40] D. J. D. EARN, P. ROHANI, B. BOLKER, AND B. T. GRENFELL, *A simple model for complex dynamical transitions in epidemics*, Science, 287 (2000), pp. 667–670.

[41] S. H. ESHLEMAN, S. E. HUDELSON, A. D. REDD, L. WANG, R. DEBES, Y. Q. CHEN, C. A. MARTENS, S. M. RICKLEFS, E. J. SELIG, S. F. PORCELLA, S. MUNSHAW, S. C. RAY, E. PIWOWAR-MANNING, M. MCCAULEY, M. C. HOSSEINIPOUR, J. KUMWENDA, J. G. HAKIM, S. CHARIYALERTSAK, G. DE BRUYN, B. GRINSZTEJN, N. KUMARASAMY, J. MAKHEMA, K. H. MAYER, J. PILOTTO, B. R. SANTOS, T. C. QUINN, M. S. COHEN, AND J. P. HUGHES, *Analysis of Genetic Linkage of HIV From Couples Enrolled in the HIV Prevention Trials Network 052 Trial*, The Journal of Infectious Diseases, 204 (2011), pp. 1918–1926.

[42] O. EYAWO, D. DE WALQUE, J. W. YEWDELL, G. GAKII, R. T. LESTER, AND E. J. MILLS, *HIV status in discordant couples in sub-Saharan Africa: a systematic review and meta-analysis*, The Lancet Infectious Diseases, 10 (2010), pp. 770–777.

[43] J. N. FENNER, *Cross-cultural estimation of the human generation interval for use in genetics-based population divergence studies*, American Journal of Physical Anthropology, 128 (2005), pp. 415–423.

[44] P. E. M. FINE, *The Interval between Successive Cases of an Infectious Disease*, American Journal of Epidemiology, 158 (2003), pp. 1039–1047.

[45] D. T. FLEMING AND J. N. WASSERHEIT, *From epidemiological synergy to public health policy and practice: the contribution of other sexually transmitted diseases to sexual transmission of HIV infection.*, Sexually transmitted infections, 75 (1999), pp. 3–17.

[46] D. T. GILLESPIE, *Exact stochastic simulation of coupled chemical reactions*, The Journal of Physical Chemistry, 81 (1977), pp. 2340–2361.

[47] J. GLYNN, M. CARAËL, A. BUVÉ, R. MUSONDA, AND M. KAHINDO, *HIV risk in relation to marriage in areas with high prevalence of HIV infection*, JAIDS Journal of Acquired Immune Deficiency Syndromes, 33 (2003), p. 526.

[48] R. H. GRAY, M. J. WAWER, R. BROOKMEYER, N. SEWANKAMBO, D. SERWADDA, F. WABWIRE MANGEN, T. LUTALO, X. LI, T. VANCOTT, AND T. C. QUINN, *Probability of HIV-1 transmission per coital act in monogamous, heterosexual, HIV-1-discordant couples in Rakai, Uganda*, The Lancet, 357 (2001), pp. 1149–1153.

[49] D. T. HALPERIN AND H. EPSTEIN, *Concurrent sexual partnerships help to explain Africa's high HIV prevalence: implications for prevention*, The Lancet, 364 (2004), pp. 4–6.

[50] J. W. HARGROVE, J. H. HUMPHREY, A. MAHOMVA, B. G. WILLIAMS, H. CHIDAWANYIKA, K. MUTASA, E. MARINDA, M. T. MBIZVO, K. J. NATHOO, P. J. ILIFF, O. MUGURUNGI, AND T. Z. S. GROUP, *Declining HIV prevalence and incidence in perinatal women in Harare, Zimbabwe*, Epidemics, 3 (2011), pp. 88–94.

[51] R. J. HAYES, D. WATSON-JONES, C. CELUM, J. VAN DE WIJGERT, AND J. WASSERHEIT, *Treatment of sexually transmitted infections for HIV prevention: end of the road or new beginning?*, AIDS (London, England), 24 (2010), pp. S15–S26.

[52] J. A. P. HEESTERBEEK AND K. DIETZ, *The Concept of R0 in Epidemic Theory*, Statistica Neerlandica, 50 (1996), pp. 89–110.

[53] S. HELLERINGER, H.-P. KOHLER, L. KALILANI-PHIRI, J. MKANDAWIRE, AND B. ARMBRUSTER, *The reliability of sexual partnership histories: implications for the measurement of partnership concurrency during surveys*, AIDS (London, England), 25 (2011), pp. 503–511.

[54] N. HENS, L. CALATAYUD, S. KURKELA, T. TAMME, AND J. WALLINGA, *Robust Reconstruction and Analysis of Outbreak Data: Influenza A(H1N1)v Transmission in a School-based Population*, American Journal of Epidemiology, 176 (2012), pp. 196–203.

[55] J. A. C. HONTELEZ, M. N. LURIE, T. BÄRNIGHAUSEN, R. BAKKER, R. BALTUSSEN, F. TANSER, T. B. HALLETT, M.-L. NEWELL, AND S. J. DE VLAS, *Elimination of HIV in South Africa through Expanded Access to Antiretroviral Therapy: A Model Comparison Study*, PLoS Medicine, 10 (2013), p. e1001534.

[56] A. HORVÁTH, *Biology and Natural History of Syphilis*, in Sexually Transmitted Infections and Sexually Transmitted Diseases, Springer Berlin Heidelberg, Berlin, Heidelberg, Feb. 2011, pp. 129–141.

[57] M. B. HOSHEN AND A. P. MORSE, *A weather-driven model of malaria transmission*, Malaria Journal, 3 (2004).

[58] J. P. HUGHES, J. M. BAETEN, G. DE BRUYN, M. INAMBAO, W. KILEMBE, C. FARQUHAR, C. CELUM, AND THE PARTNERS IN PREVENTION HSV/HIV TRANSMISSION STUDY TEAM, *Determinants of Per-Coital-Act HIV-1 Infectivity Among African HIV-1-Serodiscordant Couples*, The Journal of Infectious Diseases, 205 (2012), pp. 358–365.

[59] S. HUGONNET, F. MOSHA, J. TODD, K. MUGEYE, A. KLOKKE, L. NDEKI, D. A. ROSS, H. GROSSKURTH, AND R. J. HAYES, *Incidence of HIV infection in stable sexual partnerships: a retrospective cohort study of 1802 couples in Mwanza Region, Tanzania*, JAIDS Journal of Acquired Immune Deficiency Syndromes, 30 (2002), p. 73.

[60] E. L. IONIDES, D. NGUYEN, Y. ATCHADÉ, S. STOEV, AND A. A. KING, *Inference for dynamic and latent variable models via iterated, perturbed Bayes maps*, Proceedings of the National Academy of Sciences, 112 (2015), pp. 719–724.

[61] L. F. JOHNSON, R. DORRINGTON, D. BRADSHAW, V. PILLAY-VAN WYK, AND T. REHLE, *Sexual behaviour patterns in South Africa and their association with the spread of HIV: insights from a mathematical model*, Demographic Research, 21 (2009), pp. 289–340.

[62] L. F. JOHNSON AND D. A. LEWIS, *The Effect of Genital Tract Infections on HIV-1 Shedding in the Genital Tract: A Systematic Review and Meta-Analysis*, Sexually transmitted diseases, 35 (2008), pp. 946–959.

[63] S. C. KALICHMAN, J. PELLOWSKI, AND C. TURNER, *Prevalence of sexually transmitted co-infections in people living with HIV/AIDS: systematic review with implications for using HIV treatments for prevention*, Sexually transmitted infections, 87 (2011), pp. 183–190.

[64] G. KARP, F. SCHLAEFFER, A. JOTKOWITZ, AND K. RIESENBERG, *Syphilis and HIV co-infection*, European Journal of Internal Medicine, 20 (2009), pp. 9–13.

[65] U. R. KARUMUDI AND M. AUGENBRAUN, *Syphilis and HIV: a dangerous duo*, Expert Review of Anti-infective Therapy, 3 (2005), pp. 825–831.

[66] E. KENAH, M. LIPSITCH, AND J. M. ROBINS, *Generation interval contraction and epidemic data analysis*, Mathematical Biosciences, 213 (2008), pp. 71–79.

[67] D. G. KENDALL, *On the Role of Variable Generation Time in the Development of a Stochastic Birth Process*, Biometrika, 35 (1948), pp. 316–330.

[68] M. E. KENT AND F. ROMANELLI, *Reexamining Syphilis: An Update on Epidemiology, Clinical Manifestations, and Management*, Annals of Pharmacotherapy, 42 (2008), pp. 226–236.

[69] W. KERMACK AND A. MCKENDRICK, *Contributions to the mathematical theory of epidemics. III. Further studies of the problem of endemicity*, Proceedings of the Royal Society of London. Series A, 141 (1933), pp. 94–122.

[70] W. O. KERMACK AND A. G. MCKENDRICK, *A contribution to the mathematical theory of epidemics*, Proceedings of the Royal Society of London. Series A, 115 (1927), pp. 700–721.

[71] N. KEYFITZ, *Applied Mathematical Demography*, Springer, New York, 2005.

[72] R. E. LAFOND AND S. A. LUKEHART, *Biological Basis for Syphilis*, Clinical Microbiology Reviews, 19 (2006), pp. 29–49.

[73] J. O. LLOYD-SMITH, S. J. SCHREIBER, P. E. KOPP, AND W. M. GETZ, *Superspreading and the effect of individual variation on disease emergence*, Nature, 438 (2005), pp. 355–359.

[74] N. LUKE AND K. M. KURZ, *Cross-generational and transactional sexual relations in sub-Saharan Africa*, Washington, DC: International Center for Research on Women (ICRW), (2002).

[75] M. N. LURIE, B. G. WILLIAMS, K. ZUMA, D. MKAYA-MWAMBURI, G. GARNETT, M. SWEAT, J. GITTELSOHN, AND S. KARIM, *Who infects whom? HIV-1 concordance and discordance among migrant and non-migrant couples in South Africa*, AIDS (London, England), 17 (2003), p. 2245.

[76] N. A. MEDLAND, J. H. MCMAHON, E. P. CHOW, J. H. ELLIOTT, J. F. HOY, AND C. K. FAIRLEY, *The HIV care cascade: a systematic review of data sources, methodology and comparability*, Journal of the International AIDS Society, 18 (2015).

[77] J. N. MILLER, *Immunity in experimental syphilis VI. Successful vaccination of rabbits with Treponema pallidum, Nichols strain, attenuated by γ-irradiation*, The Journal of Immunology, (1973).

[78] M. MORRIS AND M. KRETZSCHMAR, *Concurrent partnerships and the spread of HIV*, AIDS (London, England), 11 (1997), pp. 641–648.

[79] A. NARESH, R. BEIGI, L. WOC-COLBURN, AND R. A. SALATA, *The Bidirectional Interactions of Human Immunodeficiency Virus-1 and Sexually Transmitted Infections: A Review*, Infectious Diseases in Clinical Practice, 17 (2009), pp. 362–373.

[80] P. NDASE, C. CELUM, K. THOMAS, D. DONNELL, K. H. FIFE, E. BUKUSI, S. DELANY-MORETLWE, AND J. M. BAETEN, *Outside sexual partnerships and risk of HIV acquisition for HIV uninfected partners in African HIV serodiscordant partnerships*, Journal of acquired immune deficiency syndromes (1999), 59 (2012), p. 65.

[81] H. NISHIURA, *Time variations in the generation time of an infectious disease: Implications for sampling to appropriately quantify transmission potential*, Mathematical Biosciences and Engineering, 7 (2010), pp. 851–869.

[82] R CORE TEAM, *R: A Language and Environment for Statistical Computing*.

[83] S. J. REYNOLDS, A. R. RISBUD, M. E. SHEPHERD, A. M. ROMPALO, M. V. GHATE, S. V. GODBOLE, S. N. JOSHI, A. D. DIVEKAR, R. R. GANGAKHEDKAR, R. C. BOLLINGER, AND S. M. MEHENDALE, *High rates of syphilis among STI patients are contributing to the spread of HIV-1 in India*, Sexually transmitted infections, 82 (2006), pp. 121–126.

[84] N. J. ROBINSON, D. MULDER, B. AUVERT, J. WHITWORTH, AND R. J. HAYES, *Type of partnership and heterosexual spread of HIV infection in rural Uganda: results from simulation modelling*, International journal of STD & AIDS, 10 (1999), pp. 718–725.

[85] R. ROSS, *The prevention of malaria*, New York, 1910.

[86] K. ROTCHFORD, W. A. STRUM, AND D. WILKINSON, *Effect of Coinfection With STDs and of STD Treatment on HIV Shedding in GenitalTract Secretions: Systematic Review and Data Synthesis*, Sexually transmitted diseases, 27 (2000), pp. 243–248.

[87] J.-A. RØTTINGEN, D. W. CAMERON, AND G. P. GARNETT, *A systematic review of the epidemiologic interactions between classic sexually transmitted diseases and HIV: how much really is known?*, Sexually transmitted diseases, 28 (2001), pp. 579–597.

[88] L. A. RVACHEV AND I. M. LONGINI, JR., *A mathematical model for the global spread of influenza*, Mathematical Biosciences, 75 (1985), pp. 3–22.

[89] G. SCALIA-TOMBA, Å. SVENSSON, T. ASIKAINEN, AND J. GIESECKE, *Some model based considerations on observing generation times for communicable diseases*, Mathematical Biosciences, 223 (2010), pp. 24–31.

[90] D. SERWADDA, R. H. GRAY, M. J. WAWER, AND R. Y. STALLINGS, *The social dynamics of HIV transmission as reflected through discordant couples in rural Uganda.*, AIDS (London, England), 9 (1995), pp. 745–750.

[91] J. SEXTON, G. GARNETT, AND J.-A. R TTINGEN, *Metaanalysis and Metaregression in Interpreting Study Variability in the Impact of Sexually Transmitted Diseases on Susceptibility to HIV Infection*, Sexually transmitted diseases, 32 (2005), pp. 351–357.

[92] J. D. SHELTON, *A tale of two-component generalised HIV epidemics*, The Lancet, 375 (2010), pp. 964–966.

[93] R. SIMON, *Length biased sampling in etiologic studies.*, American Journal of Epidemiology, 111 (1980), pp. 444–452.

[94] K. SOETAERT, T. PETZOLDT, AND R. W. SETZER, *Solving differential equations in R: package deSolve*, Journal of Statistical Software, (2010).

[95] Å. SVENSSON, *A note on generation times in epidemic models*, Mathematical Biosciences, 208 (2007), pp. 300–311.

[96] J. TODD, J. GLYNN, M. MARSTON, T. LUTALO, S. BIRARO, W. MWITA, V. SURIYANON, R. RANGSIN, K. E. NELSON, AND P. SONNENBERG, *Time from HIV seroconversion to death: a collaborative analysis of eight studies in six low and middle-income countries before highly active antiretroviral therapy*, AIDS (London, England), 21 (2007), p. S55.

[97] T. TONI, D. WELCH, N. STRELKOWA, A. IPSEN, AND M. P. H. STUMPF, *Approximate Bayesian computation scheme for parameter inference and model selection in dynamical systems*, Journal of The Royal Society Interface, 6 (2009), pp. 187–202.

[98] S. A. TRASK, C. A. DERDEYN, U. FIDELI, Y. CHEN, S. MELETH, F. KASOLO, R. MUSONDA, E. HUNTER, F. GAO, S. ALLEN, AND B. H. HAHN, *Molecular Epidemiology of Human Immunodeficiency Virus Type 1 Transmission in a Heterosexual Cohort of Discordant Couples in Zambia*, Journal of Virology, 76 (2002), pp. 397–405.

[99] UNAIDS, *THE GAP REPORT*, tech. rep., Aug. 2014.

[100] E. VIDOR, *Evaluation of the Persistence of Vaccine-Induced Protection with Human Vaccines*, Journal of Comparative Pathology, 142 (2010), pp. S96–S101.

[101] J. WALLINGA AND M. LIPSITCH, *How generation intervals shape the relationship between growth rates and reproductive numbers*, Proceedings of the Royal Society B: Biological Sciences, 274 (2007), pp. 599–604.

[102] H. J. WEARING, P. ROHANI, AND M. J. KEELING, *Appropriate models for the management of infectious diseases*, PLoS Medicine, 2 (2005), p. e174.

[103] A. WESOLOWSKI, C. J. E. METCALF, N. EAGLE, J. KOMBICH, B. T. GRENFELL, O. N. BJØRNSTAD, J. LESSLER, A. J. TATEM, AND C. O. BUCKEE, *Quantifying seasonal population fluxes driving rubella transmission dynamics using mobile phone data*, Proceedings of the National Academy of Sciences, (2015), p. 201423542.

[104] WHO, *The global elimination of congenital syphilis: rationale and strategy for action*, WHO, (2007), pp. 1–46.

[105] ——, *Global incidence and prevalence of selected curable sexually transmitted infections*, WHO, (2008), pp. 1–28.

[106] ——, *Investment case for eliminating mother-to-child transmission of syphilis*, tech. rep., Sept. 2012.

[107] A. J. WINTER, S. TAYLOR, J. WORKMAN, D. WHITE, J. D. ROSS, A. V. SWAN, AND D. PILLAY, *Asymptomatic urethritis and detection of HIV-1 RNA in seminal plasma.*, Genitourinary medicine, 75 (1999), pp. 261–263.

[108] S. YANG, M. SANTILLANA, AND S. C. KOU, *Accurate estimation of influenza epidemics using Google search data via ARGO*, Proceedings of the National Academy of Sciences, 112 (2015), pp. 14473–14478.